National Library of Canada
Acquisitions and Bibliographic Services Branch
395 Wellington Street
Ottawa, Ontario
K1A 0N4

Bibliothèque nationale du Canada
Direction des acquisitions et des services bibliographiques
395, rue Wellington
Ottawa (Ontario)
K1A 0N4

Your file Votre référence

Our file Notre référence

NOTICE

The quality of this microform is heavily dependent upon the quality of the original thesis submitted for microfilming. Every effort has been made to ensure the highest quality of reproduction possible.

If pages are missing, contact the university which granted the degree.

Some pages may have indistinct print especially if the original pages were typed with a poor typewriter ribbon or if the university sent us an inferior photocopy.

Reproduction in full or in part of this microform is governed by the Canadian Copyright Act, R.S.C. 1970, c. C-30, and subsequent amendments.

AVIS

La qualité de cette microforme dépend grandement de la qualité de la thèse soumise au microfilmage. Nous avons tout fait pour assurer une qualité supérieure de reproduction.

S'il manque des pages, veuillez communiquer avec l'université qui a conféré le grade.

La qualité d'impression de certaines pages peut laisser à désirer, surtout si les pages originales ont été dactylographiées à l'aide d'un ruban usé ou si l'université nous a fait parvenir une photocopie de qualité inférieure.

La reproduction, même partielle, de cette microforme est soumise à la Loi canadienne sur le droit d'auteur, SRC 1970, c. C-30, et ses amendements subséquents.

Canada

UNIVERSITY OF ALBERTA

IDENTIFICATION OF MAGNETIC MINERALS IN ARCHAEOMAGNETIC SAMPLES

BY

LI JIANG

A thesis submitted to the Faculty of Graduate Studies and Research in partial fulfillment of the requirements for the degree of Master of Science.

IN

GEOPHYSICS

DEPARTMENT OF PHYSICS

EDMONTON, ALBERTA

FALL 1995

National Library
of Canada

Acquisitions and
Bibliographic Services Branch

395 Wellington Street
Ottawa, Ontario
K1A 0N4

Bibliothèque nationale
du Canada

Direction des acquisitions et
des services bibliographiques

395, rue Wellington
Ottawa (Ontario)
K1A 0N4

Your file Votre référence

Our file Notre référence

THE AUTHOR HAS GRANTED AN IRREVOCABLE NON-EXCLUSIVE LICENCE ALLOWING THE NATIONAL LIBRARY OF CANADA TO REPRODUCE, LOAN, DISTRIBUTE OR SELL COPIES OF HIS/HER THESIS BY ANY MEANS AND IN ANY FORM OR FORMAT, MAKING THIS THESIS AVAILABLE TO INTERESTED PERSONS.

L'AUTEUR A ACCORDE UNE LICENCE IRREVOCABLE ET NON EXCLUSIVE PERMETTANT A LA BIBLIOTHEQUE NATIONALE DU CANADA DE REPRODUIRE, PRETER, DISTRIBUER OU VENDRE DES COPIES DE SA THESE DE QUELQUE MANIERE ET SOUS QUELQUE FORME QUE CE SOIT POUR METTRE DES EXEMPLAIRES DE CETTE THESE A LA DISPOSITION DES PERSONNE INTERESSEES.

THE AUTHOR RETAINS OWNERSHIP OF THE COPYRIGHT IN HIS/HER THESIS. NEITHER THE THESIS NOR SUBSTANTIAL EXTRACTS FROM IT MAY BE PRINTED OR OTHERWISE REPRODUCED WITHOUT HIS/HER PERMISSION.

L'AUTEUR CONSERVE LA PROPRIETE DU DROIT D'AUTEUR QUI PROTEGE SA THESE. NI LA THESE NI DES EXTRAITS SUBSTANTIELS DE CELLE-CI NE DOIVENT ETRE IMPRIMES OU AUTREMENT REPRODUITS SANS SON AUTORISATION.

ISBN 0-612-06486-7

Canada

UNIVERSITY OF ALBERTA
LIBRARY RELEASE FORM

NAME OF AUTHOR: **LI JIANG**

TITLE OF THESIS: **IDENTIFICATION OF MAGNETIC MINERALS IN ARCHAEOMAGNETIC SAMPLES**

DEGREE: **Master of Science**

YEAR THIS DEGREE GRANTED: **1995**

Permission is hereby granted to the University of Alberta Library to reproduce single copies of this thesis and to lend or sell such copies for private, scholarly of scientific research purpose only.

The author reserves all other publication and other rights in association with the copyright in the thesis, and except as hereinbefore provided neither the thesis nor any substantial portion thereof may be printed or otherwise reproduced in any material form whatever without the author's prior written permission.

Li Jiang

Li Jiang
11147-82 Ave, #607
Edmonton, Alberta
Canada T6G 0T5

July 1, 1995

UNIVERSITY OF ALBERTA

FACULTY OF GRADUATE STUDIES AND RESEARCH

The undersigned certify that they have read, and recommend to the Faculty of Graduate Studies and Research for acceptance, a thesis entitled **IDENTIFICATION OF MAGNETIC MINERALS IN ARCHAEOMAGNETIC SAMPLES** submitted by **LI JIANG** in partial fulfillment of the requirements for the degree of **Master of Science** in **GEOPHYSICS**.

M E Evans
Dr. M.E. Evans (supervisor)

Dr. F.W. Jones

J.A. Kernahan
Dr. J.A. Kernahan

M L Wayman
Dr. M.L. Wayman

Date July 1, 1995

ABSTRACT

Archaeological material has been a significant source of information concerning the long-term behaviour of the geomagnetic field. The actual magnetic minerals responsible for this signal have never been systematically investigated. In this project, I have studied 68 samples (kilns, 48 samples; sherds, 8 samples; bricks, 4 samples; bath houses, 8 samples) from Greece, Italy, China and North Africa. Using several kinds of laboratory techniques, results about the magnetic minerals contained in the samples have been obtained. Although different magnetic parameters are used to diagnose the minerals, the conclusions drawn from them are essentially the same; the dominant magnetic mineral contained in most samples is magnetite and/or titanomagnetite, only a few samples show evidence of small amounts (in the order of a few per cent) of hematite.

ACKNOWLEDGEMENTS

I wish to express my sincere appreciation to my supervisor, Dr. M.E. Evans for his invaluable guidance, encouragement and patience throughout my graduate study, and for his careful editing of the manuscript. Without his help, my M.Sc. study could not be accomplished.

I am deeply grateful to Dr. Yuchun Wang for providing valuable suggestions and prompt assistance in my research.

I would like to thank my wife, Lei Wei, for her whole support and great enthusiasm through my endeavour.

TABLE OF CONTENTS

CHAPTER	PAGE
1 Introduction	1
1.1 Geomagnetism and archaeomagnetism	1
1.2 Principles of rock magnetism	4
1.3 Magnetic minerals in archaeomagnetic samples	9
1.4 Aims of this thesis	10
2 Sample collection and laboratory techniques	12
2.1 The samples	12
2.2 Laboratory techniques	14
2.2.1 Remanence measurements	14
2.2.2 Demagnetisation	15
2.2.3 Laboratory remanence acquisition	17
2.2.4 Backfield method	18
3 Results	20
3.1 Introduction	20

3.2 Results 21

4 Discussion 49

4.1 Thermal treatment and magnetic mineralogy 49

4.1.1 Thermal demagnetisation of NRM 49

4.1.2 Thermal demagnetisation of SIRM 50

4.2 Coercivity spectra and magnetic mineralogy 54

4.2.1 IRM acquisition 54

4.2.2 Backfield 57

4.2.3 AF demagnetisation of IRM 60

4.2.4 AF demagnetisation of ARM 62

4.2.5 AF demagnetisation of NRM 64

5 Summary and Conclusions 66

Bibliography 70

Appendix A 73

Appendix B 101

LIST OF TABLES

TABLE	PAGE
2.1 Samples (N=23) from Greece	12
2.2 Samples (N=24) from Italy	13
2.3 Samples (N=12) from China	13
2.4 Samples (N=9) from North Africa	14
4.2.1 Δ values for 36 samples	57
4.2.2 Hcr (mT) values for 36 samples	58
4.2.3 MDF of IRM values for 10 samples	60
4.2.4 MDF of ARM (mT) values for 20 samples	62
4.2.5 MDF of NRM (mT) values for 40 samples	64
5.1 $H_{(1/2)I}$, H'_{cr} and Hcr values for 9 samples	68

LIST OF FIGURES

FIGURE		PAGE
1.1.	The main elements of geomagnetic field	2
1.2.	The spontaneous magnetisation vectors for three types of magnetism.	5
1.3.	Domain (Bloch) wall	6
1.4.	The magnetic hysteresis loop	7
1.5.	FeO-TiO_2-Fe_2O_3 ternary diagram	10
2.1.	AF demagnetisation curve	16
2.2.	Thermal demagnetisation curve	17
2.3.	IRM acquisition curve	18
2.4.	Back field method	19
3.2.1a	AF demagnetisation of NRM of Greek samples	23
3.2.1b	AF demagnetisation of NRM of Italian samples	25
3.2.1c	AF demagnetisation of NRM of Chinese samples	27
3.2.1d	AF demagnetisation of NRM of North African samples	28

3.2.2a	Thermal demagnetisation of NRM of Greek samples	29
3.2.2b	Thermal demagnetisation of NRM of Italian samples	31
3.2.2c	Thermal demagnetisation of NRM of Chinese samples	33
3.2.3a	AF demagnetisation of ARM of Greek samples	34
3.2.3b	AF demagnetisation of ARM of Italian samples	35
3.2.3c	AF demagnetisation of ARM of Chinese samples	37
3.2.4a	IRM acquisition and back field results of Greek samples	38
3.2.4b	IRM acquisition and back field results of Italian samples	40
3.2.4c	IRM acquisition and back field results of Chinese samples	42
3.2.4d	IRM acquisition and back field results of North African samples	43
3.2.5a	AF demagnetisation of IRM of Greek samples	45
3.2.5b	AF demagnetisation of IRM of Italian samples	46
3.2.6a	Thermal demagnetisation of IRM of Greek samples	47
3.2.6b	Thermal demagnetisation of IRM of Italian samples	48
4 1.1a	Thermal demagnetisation curves	51
4.1.1b	Thermal demagnetisation curves	51
4.1.1a	Thermal demagnetisation curves	52

4.1.2	Inclination vs. temperature for thermal demagnetisation SIRM.	53
4.2.1	Histogram of Δ for 36 samples	56
4.2.2	Histogram of Hcr for 36 samples	59
4.2.3	Histogram of MDF of IRM for 10 samples	61
4.2.4	Histogram of MDF of ARM for 20 samples	63
4.2.5	Histogram of MDF of NRM for 40 samples	65
5.1	$H_{(1/2)I}$ + H'cr vs 2*Hcr for 9 samples	68

Chapter 1 Introduction

1.1 Geomagnetism and archaeomagnetism

The Chinese discovered magnetism more than 2000 years ago (Needham, 1962). From about A.D. 83, Chinese observers noticed the directional characters of the Earth's magnetic field. This may be considered as the beginning of geomagnetism (Malin, 1987). In 1269, Petrus Peregrinus reported his famous experimental results with spherical pieces of lodestone (naturally occurring iron oxide). He defined the concept of polarity, discovered magnetic meridians and used several methods to determine the positions of poles of a lodestone sphere.

In 1600 William Gilbert published his notable scientific treatise *De Magnete* which strongly influenced the course of magnetic study. In this book he presented the results of many years of his study of magnetism. He stated that "the Earth itself is a great magnet". Gilbert's work indicated that the geomagnetic field is mainly dipolar.

The geomagnetic field at any location is a vector quantity, having both magnitude and direction. It is convenient to determine the geomagnetic field by three of the quantities illustrated in Figure 1.1. Inclination, I, is the angle between the horizontal plane and the magnetic vector. The inclination is reckoned positive

when the magnetic vector points downward and negative when it points upward. Declination, D, is the angle between geographical north and the horizontal component of the magnetic field vector. D is always measured clockwise from the present geographic north. F is the total intensity of the Earth's magnetic field. Sometimes it is convenient to resolve F to geographical directions; the north component X; the east component Y; the horizontal component H; and the vertical downward component Z.

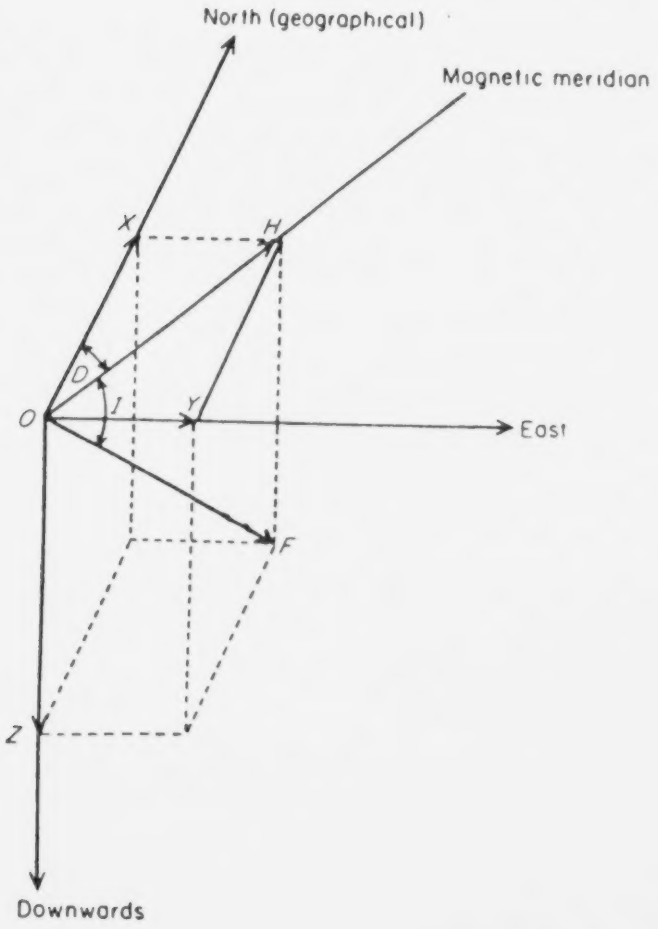

Figure 1.1. *The main elements of geomagnetic field*

It is now known that the magnetic field at any given location near the Earth's surface can be ascribed to three sources located (1) in the Earth's core, (2) in the Earth's crust, and (3) in the Earth's ionosphere and beyond. The magnetic field from the core is called the main field, and it is the largest in magnitude. The strength of the main field varies from approximately 30μT at the equator to 60μT at the poles. In 1837, C.F. Gauss was the first person to study the geomagnetic field by using spherical analysis. The present best fitting dipole is situated at the Earth's centre and its axis makes an angle of 11.5° with the rotation axis. When the dipole field is subtracted from the observed value, the residual is called the non-dipole field. The non-dipole field comprises only about 1/20 of the total field.

In 1634, Henry Gellibrand discovered that declination changes with time. It was later discovered that both inclination and intensity also vary with time. These changes in magnetic field are now called secular variation. Direct observation of the direction of the geomagnetic field began about 400 years ago, but it was more than 200 years later before the strength of the geomagnetic field was successfully measured. Since the geomagnetic field changes in a very complicated way, it is not enough for us to study the geomagnetic field by using only the data from direct instrumental observations. With the development of archaeomagnetism, it is now possible to learn more about the long-term history of the geomagnetic field.

One very important feature of magnetism is that it is the only geophysical property that can be measured and determined throughout time. Archaeomagnetic techniques make use of the phenomenon that certain minerals are capable of retaining a record of the past direction and intensity of the

geomagnetic field, and therefore the direction and strength of the geomagnetic field can be studied over archaeological time scales (Thellier, 1981; Walton, 1990).

1. 2 Principles of rock magnetism

Rock magnetism is the term applied to the study of the magnetic properties of rocks and minerals, and the origin and characteristics of the different types of remanent magnetisation which rocks and minerals can acquire.

The best way to introduce the different types of magnetism is to describe how materials respond to a magnetic field. In diamagnetic substances the electron shells are full and the precession of electron orbits creates a magnetic field in the opposite direction to the applied field. Because the induced magnetisation is in the opposite direction to the applied field, the susceptibility (the magnetisation acquired per unit field applied) is negative and typically of the order of 10^{-6} SI. In paramagnetic materials the electron shells are incomplete, and each atom has a magnetic moment due to the uncompensated electron orbits. When placed in a magnetic field, the electron orbits precess but the magnetic moment is aligned in the same direction as the applied field and produces susceptibilities of the order of 10^{-4} SI. Paramagnetism and diamagnetism exist only in the presence of the external magnetic field.

Some substances like iron, cobalt and nickel exhibit strong magnetic effects known as ferromagnetism and have much larger susceptibilities. In these magnetic materials, the atomic moments exhibit very strong interactions. These interactions are produced by electronic exchange forces and result in a parallel or

antiparallel alignment of atomic moments even in the absence of an applied magnetic field. Ferromagnetic substances thus exhibit spontaneous magnetisation, and may carry a permanent magnetisation in the absence of an applied magnetic field. These spontaneous magnetisation regions have dimensions of the order 10^{-6} m and are called magnetic domains. The ordering of atomic moments within a domain may follow one of three patterns (Figure 1.2). In ferromagnetic minerals, the atomic moments are parallel. In antiferromagnetic minerals they are arranged on two equal antiparallel sublattices, so there is no residual moment. In the third type of mineral, the moments are arranged in two unequal sublattices, therefore the net magnetisation is not zero; this is ferrimagnetism.

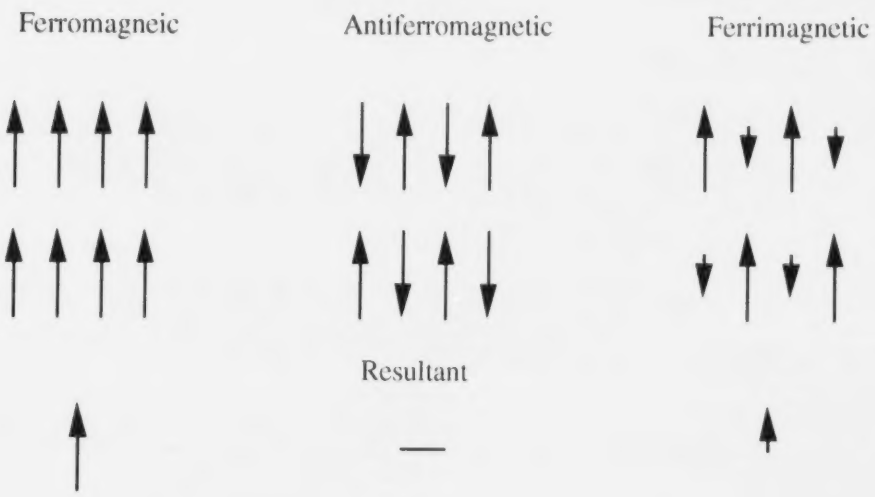

Figure 1.2. *The spontaneous magnetization vectors for three types of magnetism.*

As the temperature increases, thermal agitation may destroy the alignment. In ferromagnetic and ferrimagnetic minerals the spontaneous magnetisation falls

as the temperature increases, disappearing at a critical temperature called the Curie temperature or Curie point, T_C; above T_C the substance behaves like an ordinary paramagnetic. In antiferromagnetic minerals the ordering is lost at the Néel temperature, T_N, above which the minerals are paramagnetic.

The smallest magnetic mineral particles contain only one domain. The larger particles contain many domains. The boundary between two domains is called a Bloch wall, which is a narrow zone within which the directions of the magnetisation of the electron spins cant over from that of one domain to that of the next (Figure 1.3). Magnetic crystals have "easy" and "hard" directions. Therefore, there are directions, along which it is easier for a substance to become magnetised than along another; this is referred to as magnetocrystalline anisotropy.

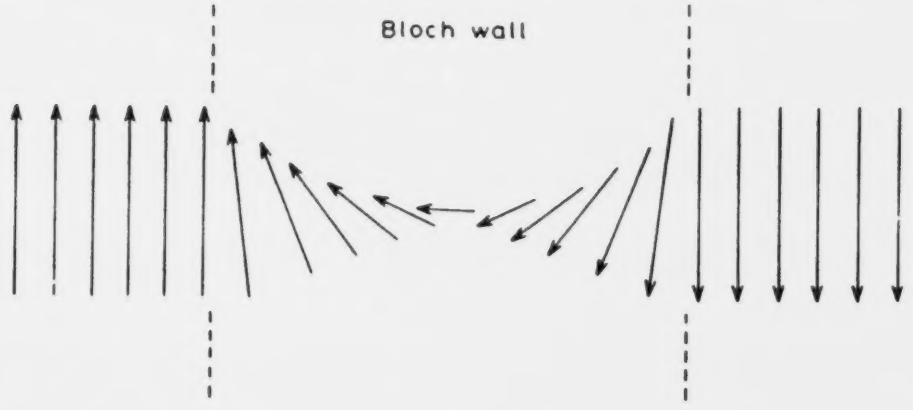

Figure 1.3. *Domain (Bloch) wall*

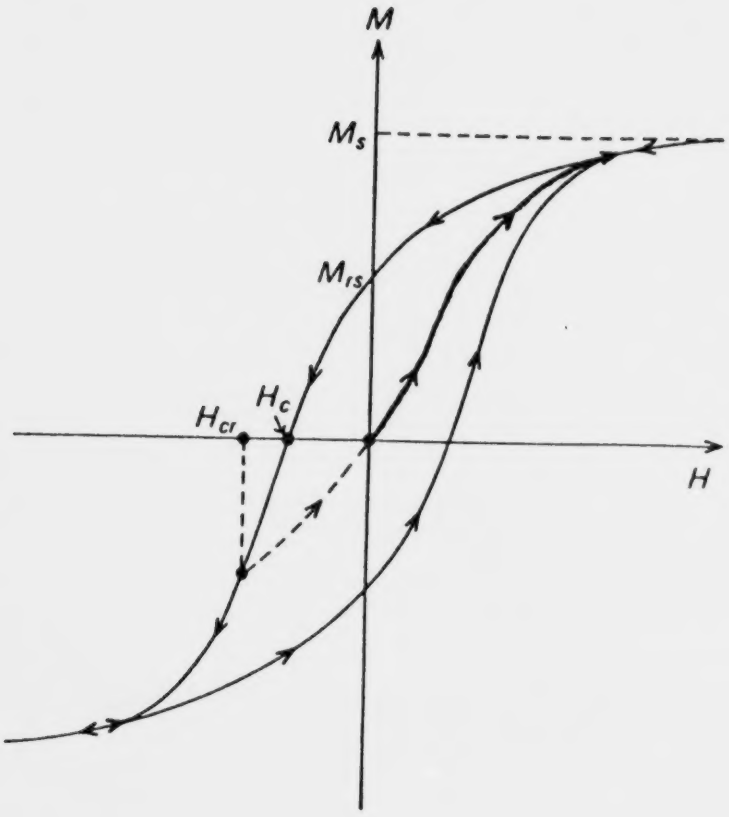

Figure 1.4. *The magnetic hysteresis loop*

A demagnetised material may acquire a remanence when a magnetic field is applied. The simplest situation is the effect of a magnetic field applied at room temperature for periods of the order of seconds or minutes. As the field increases the magnetisation eventually reaches a steady value, M_S, called the saturation magnetisation. The application of increasing magnetic fields, first in one direction and then in the opposite direction yields a hysteresis loop (Figure 1.4).

This loop defines some important magnetic parameters. The isothermal remanent magnetisation, M_{rs}, is the magnetisation remaining when the applied field has been removed. The coercive force, H_c, is the reverse field necessary to reduce the magnetisation to zero. The coercivity of remanence, H_{cr}, is the reverse field which, when reduced to zero, leaves the specimen in a demagnetised state.

Néel (1955) developed a theory of remanence in single domain particles based on thermal fluctuations. His model provides a simple way of looking at the effects of time, temperature and magnetic field on the magnetisation and demagnetisation process. Néel introduced the concept of relaxation time. Each particle has a specific relaxation time for it to acquire a magnetisation with a component in the direction of the applied field. The relaxation time τ is given by the formula

$$\tau = \frac{1}{C}\exp\left(\frac{vK}{kT}\right) \qquad (1)$$

where C is a frequency factor which is of the order of $10^{10}s^{-1}$, v is the volume of the grain, k is Boltzmann's constant, K is the anisotropy constant and T is the absolute temperature. τ is strongly dependent on the volume of the magnetic grains and the temperature :

$$\log \tau \propto \frac{v}{T}$$

When cooled from the Curie temperature, a single domain particle will show a logarithmic increase in its relaxation time. Similarly, as a crystal grows at constant temperature, it will show a logarithmic increase in its relaxation time. Consequently, there are two separate ways to acquire such remanence. One is to cool a specimen in a magnetic field over temperature ranges below the Curie point. The remanence acquired in this way is called thermoremanent

magnetisation (TRM). The other type of remanence is acquired when crystals grow in a magnetic field, which is termed chemical remanent magnetisation (CRM).

Most natural materials contain a large range of grain sizes. Just below the Curie point, the larger single domain particles will have relaxation times of the order of a few minutes, but the smaller particles will have shorter relaxation times. The magnetic grains of different sizes will show a wide range of relaxation times while cooling to room temperature. The larger magnetic grains will reach their blocking temperature, which is the temperature at which the remanence acquired becomes blocked within it for the duration of the experiment, at higher temperature than the smaller particles do. Therefore the total TRM is acquired over a range of blocking temperatures corresponding to the grain sizes present.

1.3 Magnetic minerals in archaeomagnetic samples

The magnetic minerals of the Earth are compounds of iron, commonly oxides. The most important iron oxides can be represented on the FeO - TiO_2 - Fe_2O_3 ternary diagram (Figure 1.5). Magnetite (Fe_3O_4) and Hematite (αFe_2O_3) are the two most important magnetic minerals found in natural samples.

Magnetite is a cubic mineral with inverse spinel structure and is ferrimagnetic. The saturation magnetisation at room temperature is in the range of 90 - 93 Am^2kg^{-1}. Its Curie point is 578 °C and the coercivity of remanence usually lies in the range 10 - 50 mT. Saturation remanence is achieved in fields of $\leq$ 300 mT.

Hematite is hexagonal and is a canted antiferromagnet. Its Curie point is 680°C. The saturation magnetisation is commonly in the range 0.2 - 0.4 Am^2kg^{-1}. The coercivity of remanence is very high (0.5 - 1.5 T), and saturation remanence requires fields > 3T.

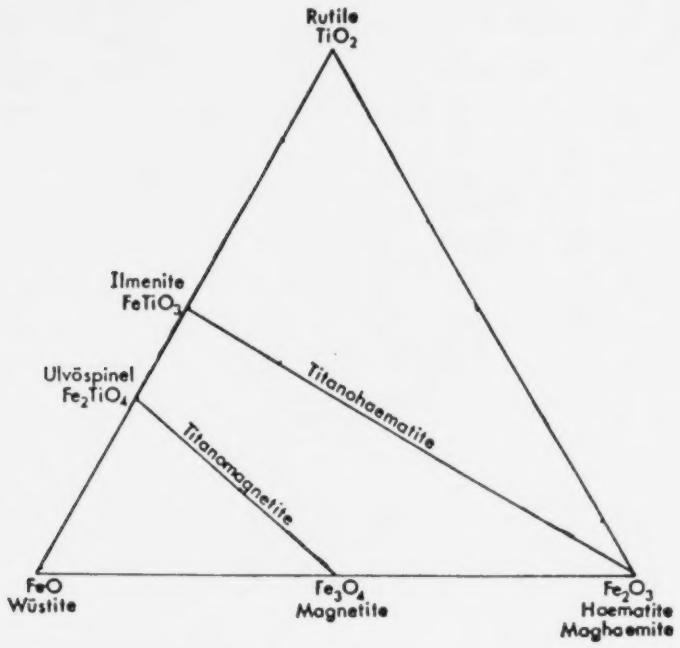

Figure 1.5. FeO-TiO_2-Fe_2O_3 *ternary diagram*

1.4 Aims of this thesis

Although it is well known that most archaeological materials contain magnetic minerals, there exists no systematic survey in terms of the magnetic minerals they contain. The aim of this project is to start such a survey using

representative samples from the large collection available in the University of Alberta Palaeomagnetism Laboratory. These represent ~100 sites in Italy, Greece and North Africa, and span the time interval from 2000B.C. to 600A.D. In addition, material representing an even wider age range is now available from Shandong Province in China.

Chapter 2 Sample collection and laboratory techniques

2.1 The samples

The samples for this study were collected from Greece (Evans & Mareschal, 1988) (Table 2.1), Italy (Evans & Mareschal, 1989) (Table 2.2), China (Table 2.3), and North Africa (Table 2.4). The time interval represented ranges from 3000 BC to 1300 AD. Altogether, 4 kinds of archaeological features are represented (kilns, 48 samples; sherds, 8 samples; bricks, 4 samples; bath houses, 8 samples). A total of 68 individual specimens is involved.

Table 2.1 Samples (N=23) from Greece

Site	Code	Latitude	Longitude	N	Type
Argos	AG	37.6 N	22.7 E	2	kiln
Avlis	AV	38.5 N	23.7 E	2	kiln
Corinth	CO	37.9 N	22.9 E	2	kiln
Corinth	CR	37.9 N	22.9 E	1	kiln
Delos	DE	37.4 N	25.3 E	2	kiln
Gortyn	GO	35.1 N	25.0 E	2	kiln
Kalochorio	KC	35.1 N	25.7 E	2	kiln
Knossos	KN	35.3 N	25.3 E	2	kiln
Palaikastro	PK	34.9 N	26.3 E	2	kiln
Pella	PE	40.7 N	22.3 E	1	kiln
Stylos	SY	35.4 N	24.1 E	1	kiln
Thessaloniki	MO	40.6 N	23.0 E	2	kiln
Thessaloniki	TH	40.6 N	23.0 E	2	kiln

Table 2.2 Samples (N=24) from Italy

Site	Code	Latitude	Longitude	N	Type
Apani	AP	40.7 N	17.9 E	2	kiln
Bisignano	BI	39.5 N	16.3 E	2	kiln
Capocolonna	CN	39.1 N	17.1 E	2	kiln
Sibari	CA	39.6 N	16.5 E	2	kiln
Metapontum	IN	40.4 N	16.8 E	2	kiln
Metapontum	KE	40.4 N	16.8 E	2	kiln
Metapontum	TM	40.4 N	16.8 E	2	kiln
Motya	MT	37.8 N	12.5 E	2	kiln
Pompeii	PP	40.8 N	14.5 E	1	kiln
Ruoti	RU	40.6 N	16.8 E	2	kiln
Sant'Angelo	GR	40.4 N	16.8 E	2	kiln
Sant'Angelo	UE	40.4 N	16.7 E	2	kiln
Segesta	SE	37.9 N	12.8 E	1	kiln

Table 2.3 Samples (N=12) from China

Site	Code	Latitude	Longitude	N	Type
Linzhi	ST09	36.8 N	118.4 E	2	brick
Linzhi	ST16	36.8 N	118.8 E	2	brick
Tianwan	ST15	36.8 N	118.2 E	2	sherd
Zhangqiu	ST05	36.7 N	117.4 E	2	sherd
Zhangqiu	ST11	36.7 N	117.4 E	2	sherd
Zoubin	ST24	36.8 N	117.7 E	2	sherd

Table 2.4 Samples (N=9) from North Africa

Site	Code	Latitude	Longitude	N	Type
Banassa	BA	34.6 N	6.1 W	2	bath house
Carthage	CT	36.9 N	10.3 W	1	kiln
Sala	SA	34.0 N	6.9 W	2	bath house
Thamusida	TS	34.4 N	6.5 W	2	bath house
Tippassa	TI	36.6 N	2.4 E	2	bath house

2.2 Laboratory techniques

2.2.1 Remanence measurements

The laboratory techniques involved in the measurement of remanent magnetisation are now routine and have been well documented (see e.g., Collinson, 1983). All measurements of remanent magnetisation were carried out using a Schonstedt SSM-2 spinner magnetometer. This magnetometer has 4 sample positions that change the distance between the sample and sensor (position 0 being the closest to the sensor). Since the remanent magnetisations of the samples vary over a large range, all four positions had to be used. Each measurement of a sample involves six spins, with two components (X, Y or Z component) measured each time. Therefore, each component is measured four times. A useful quality index is the discrepancy of the measurement described by the angle theta (θ):

$$\theta = \sin^{-1}\left(\frac{\sqrt{\text{disX}^2 + \text{disY}^2 + \text{disZ}^2}}{\text{RM}}\right)$$

where $\text{dis}X^2 = \sqrt{\sum_{i=1}^{4} (X_i - \overline{X})^2/4}$

and similarly for disY and disZ, and

$$RM = \sqrt{\overline{X}^2 + \overline{Y}^2 + \overline{Z}^2}$$

Thus, the angle θ conveniently describes the consistency of the six spins within each measurement. The smaller the angle, the more reliable are the results.

2.2.2 Demagnetisation

(a)Alternating field (AF) demagnetisation

In this project, the AF method has been applied to the initial magnetisation possessed by the samples upon collection (the so-called natural remanent magnetisation, NRM), and to the laboratory remanences anhysteretic remanent magnetisation (ARM) and saturation isothermal remanence (SIRM). In the AF method a sample is subjected to an alternating magnetic field that is smoothly reduced to zero from a pre-set peak value. The sample orientation is randomised by means of a pair of tumbling gears attached to the sample holder. The ambient field is annulled by two orthogonal pairs of coils carrying DC current. AF demagnetisation is useful for characterising the coercivity spectrum, the AF value needed to reduce the initial remanence by one half being referred to as the median destructive field (MDF, Figure 2.1).

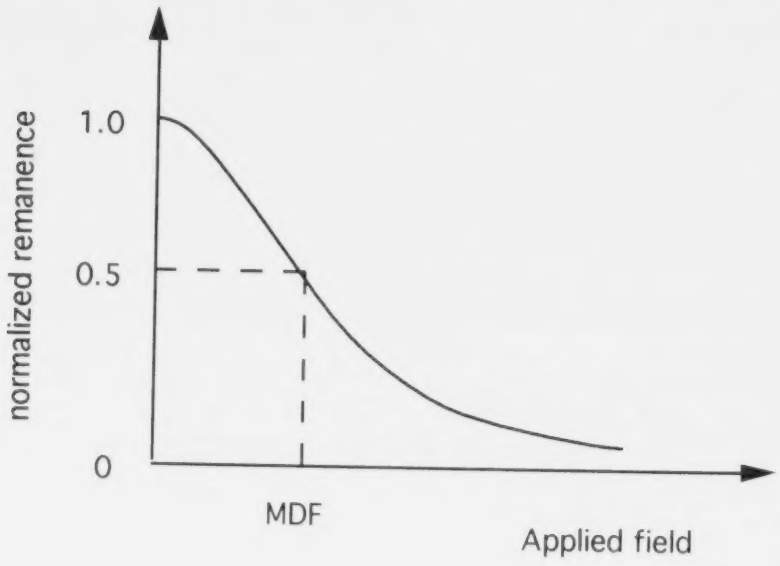

Figure 2.1. *AF demagnetisation curve*

(b) Thermal demagnetisation

From equation (1) (section 1.2), it is obvious that relaxation time is greatly dependent on temperature. When the temperature of a sample is increased, the relaxation time of the lower part of its blocking temperature spectrum is reduced to a time period of the same order as the laboratory experiment. If cooling takes place in a zero magnetic field, the remanence in this part will be removed and the unblocked fraction will not acquire a new TRM. In this project the samples were heated and cooled in a magnetically shielded room in which the ambient field is less than 60 nT (Maillol, 1992). After each temperature increment the remaining remanence was measured (Figure 2.2).

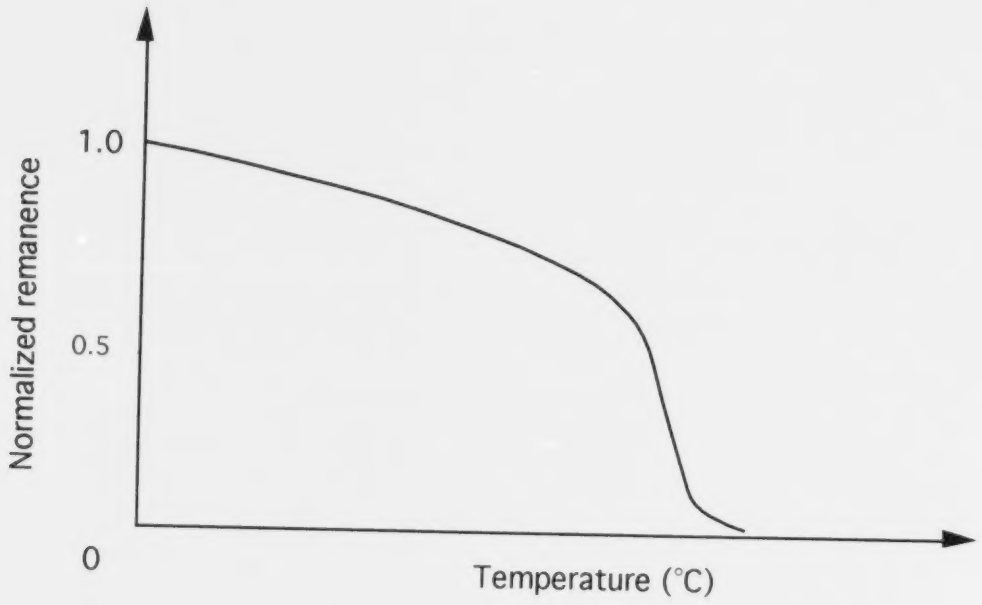

Figure 2.2. *Thermal demagnetisation curve*

2.2.3 Laboratory remanence acquisition

Two types of remanence acquisition experiment are involved in this project.

(a) ARM acquisition: The anhysteretic remanent magnetisation (ARM) is produced by the combined actions of a large AF and a smaller constant DC field. In this project, the AF peak value was 180mT and the DC field is 0.1mT.

(b) IRM acquisition: Isothermal remanent magnetisation (IRM) is the remanence left in the sample after a steady field has been applied for a short time (20 seconds) and then switched off. This steady field was increased from 0 to a maximum value (usually 1.2 T) step by step. After each step the remaining remanence is measured. The maximum remanence is the saturation isothermal remanence (SIRM) (Figure 2.3).

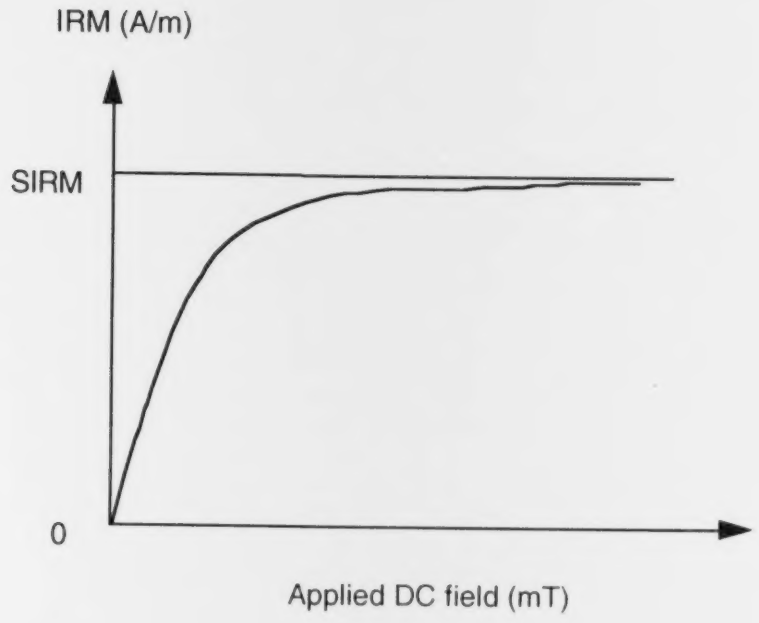

Figure 2.3. *IRM acquisition curve*

2.2.4 Backfield method

This procedure involves first giving a sample a saturation IRM (SIRM), and then successively increasing the DC field in the opposite sense to the SIRM. The back field required to reduce SIRM to zero is called the coercivity of remanence (H_{cr}) (Figure 2.4, see also Figure 1.4).

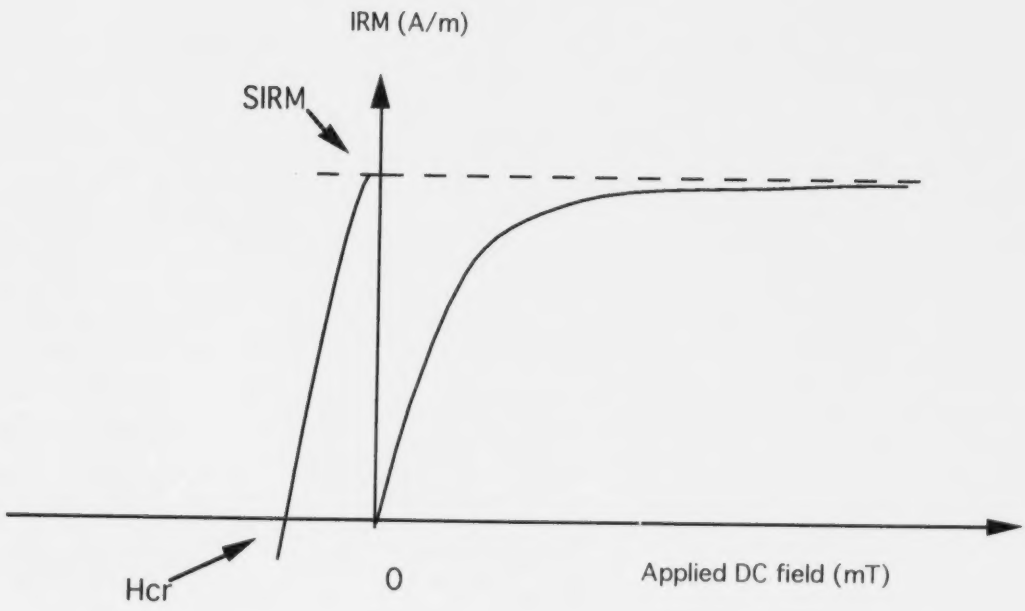

Figure 2.4. *Back field method*

Chapter 3 Results

3.1 Introduction

The magnetic properties of the samples described in Chapter 1 have been characterised by means of the techniques described in Chapter 2. All the measurement data can be found in Appendix A. The experiments performed on the individual samples are listed in Appendix B. In summary, the experiments involved are:

(a) AF demagnetisation of NRM (40 samples) (section 3.2 (a)).

(b) Thermal demagnetisation of NRM (22 samples) (section 3.2 (b)).

(c) ARM acquisition and its AF demagnetisation (20 samples) (section 3.2 (c)).

(d) IRM acquisition and backfield demagnetisation (33 samples) (section 3.2 (d)).

(e) AF demagnetisation of SIRM (10 samples) (section 3.2 (e)).

(f) Thermal demagnetisation of SIRM (5 samples) (section 3.2 (f)).

Since the primary aim of this project was to survey the relevant magnetic properties of representative archaeomagnetic samples, the results obtained are

given here in detail. In this chapter the observations are simply documented without comment. Chapter 4 summarises them and discusses their significance.

3.2 Results

(a) The AF demagnetisation technique has the advantage of leaving the samples intact, as opposed to thermal demagnetisation that presents the potential risk of chemical alteration of the minerals. This technique was applied to the NRM of 40 samples. The maximum field available for AF demagnetisation is 180 mT. Figures 3.2.1a - d show the results from Greece (N=14), Italy (N=11), China (N=6) and North Africa (N=9), respectively.

(b) Thermal demagnetisation was carried out on the NRM of 22 samples; 7 were collected from Greece, 9 from Italy and 6 from China. Figures 3.2.2a - c present the curves obtained.

(c) Using the ARM technique described in section 2.2.3(a), 20 samples were investigated. After the samples acquired ARM, AF demagnetisation was performed on them as for AF demagnetisation of NRM. The results are presented in Figures 3.2.3a - c.

(d) The IRM acquisition and backfield method have been applied to 36 samples from Greece (N=9), Italy (N=12), China (N=6) and North Africa (N=9). The results are given in Figures 3.2.4a - d.

(e) Figures 3.2.5a and b illustrate the AF demagnetisation curves of SIRM for 4 samples from Greece and 6 samples from Italy.

(f) Five samples (3 from Greece and 2 from Italy) were chosen for thermal demagnetisation of SIRM. First the samples were given a SIRM. Then by using the method described in section 2.2.2(b), we obtained the thermal demagnetisation results (Figure 3.2.6a-b).

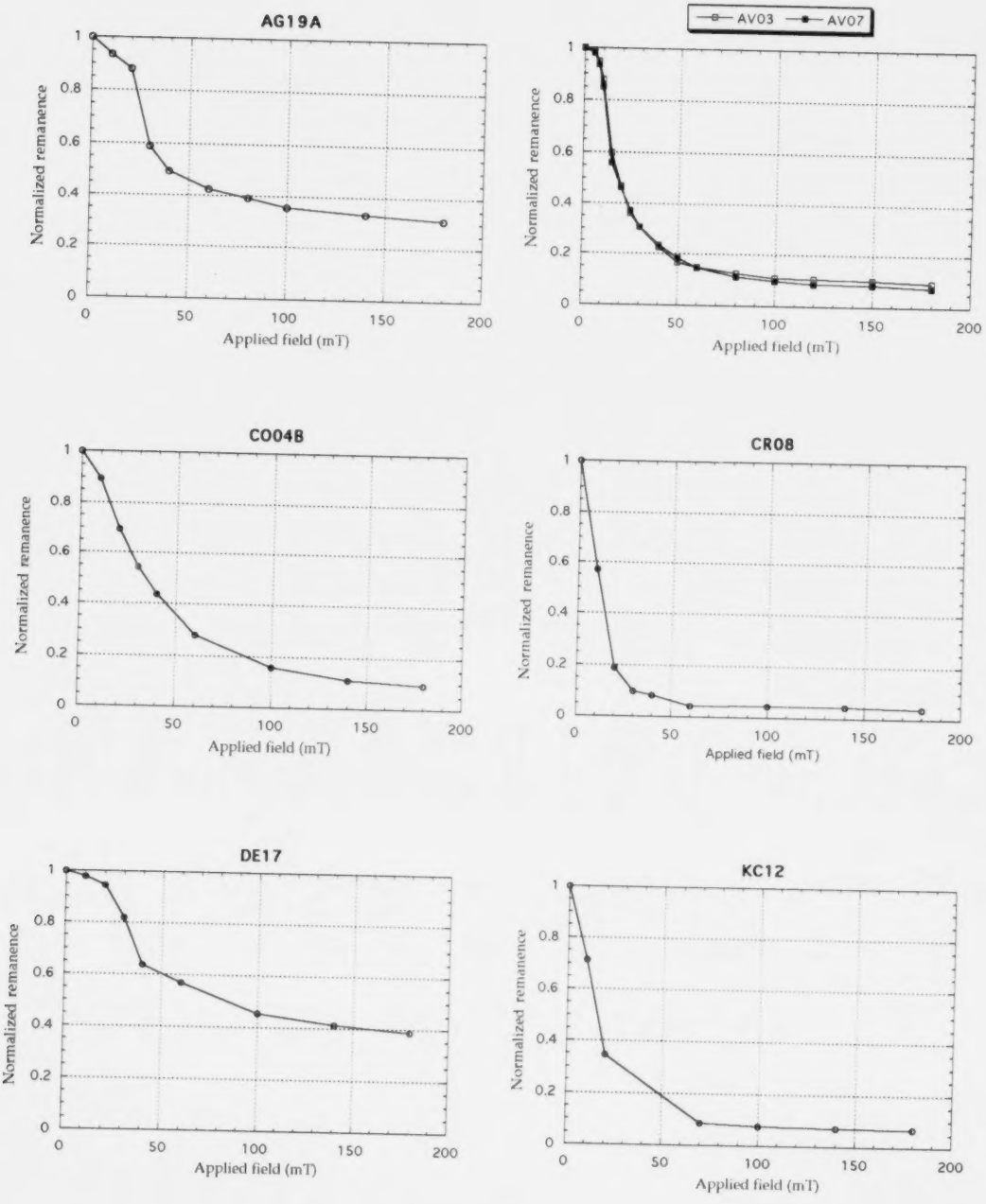

Figure 3.2.1a *AF demagnetisation of NRM of Greek samples*

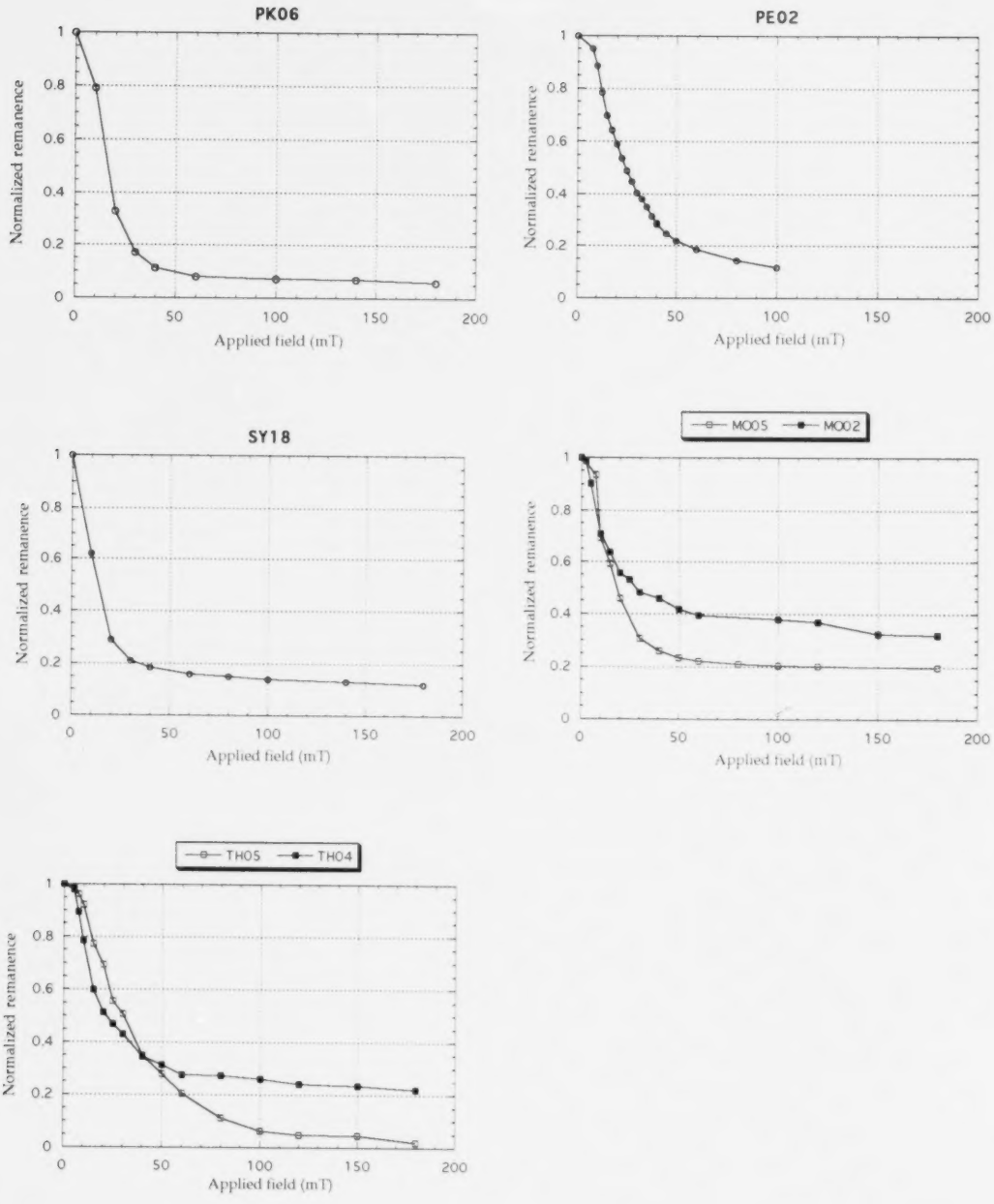

Figure 3.2.1a *Continued*

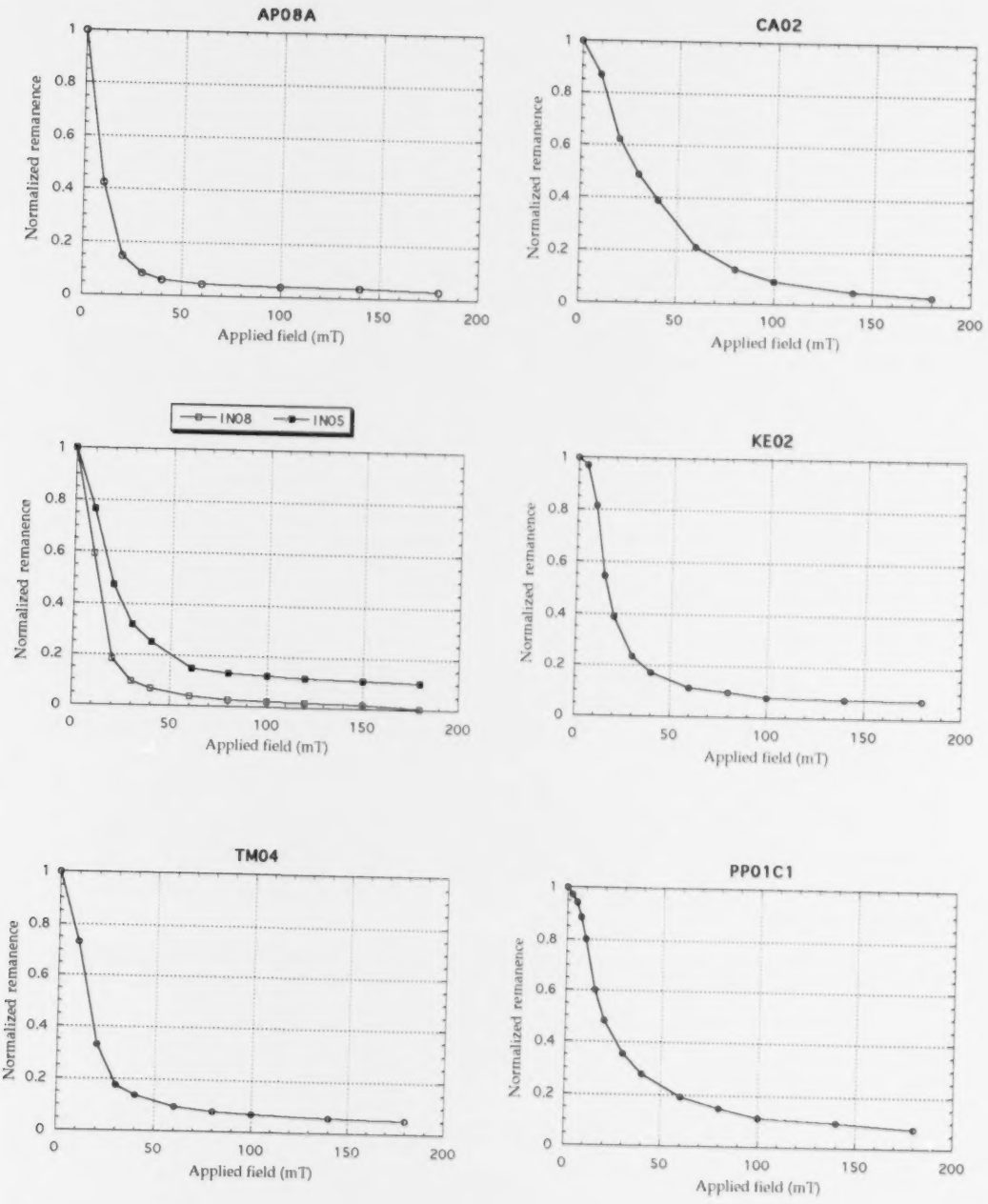

Figure 3.2.1b *AF demagnetisation of NRM of Italian samples*

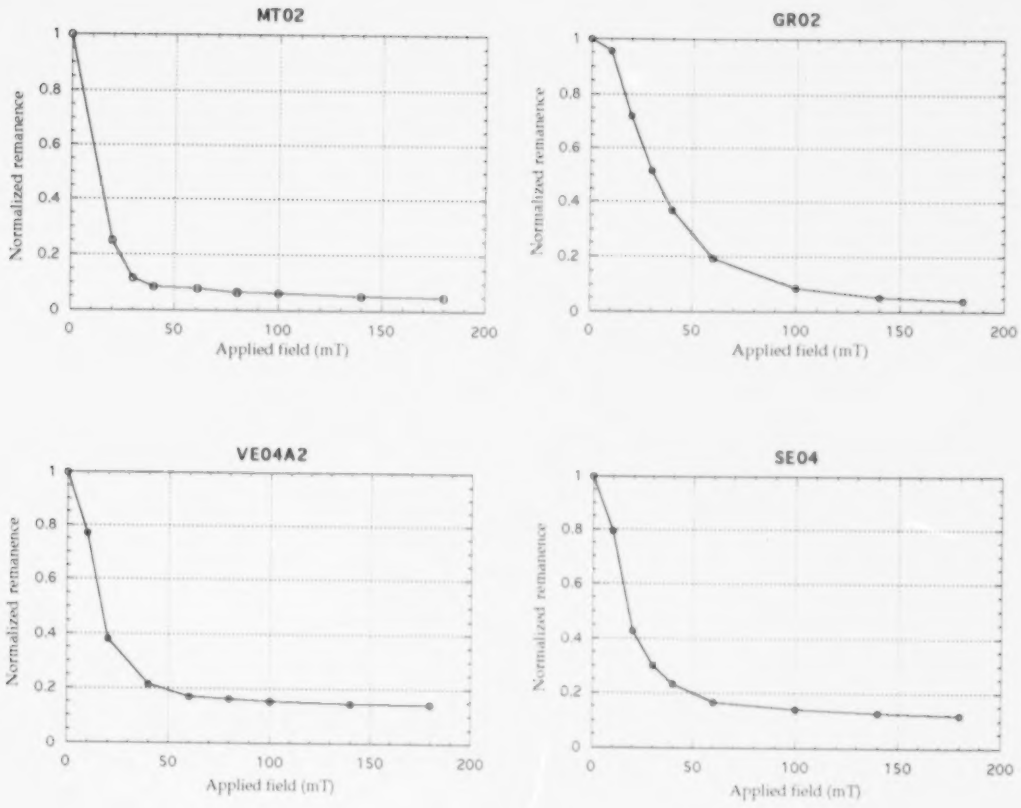

Figure 3.2.1b *Continued*

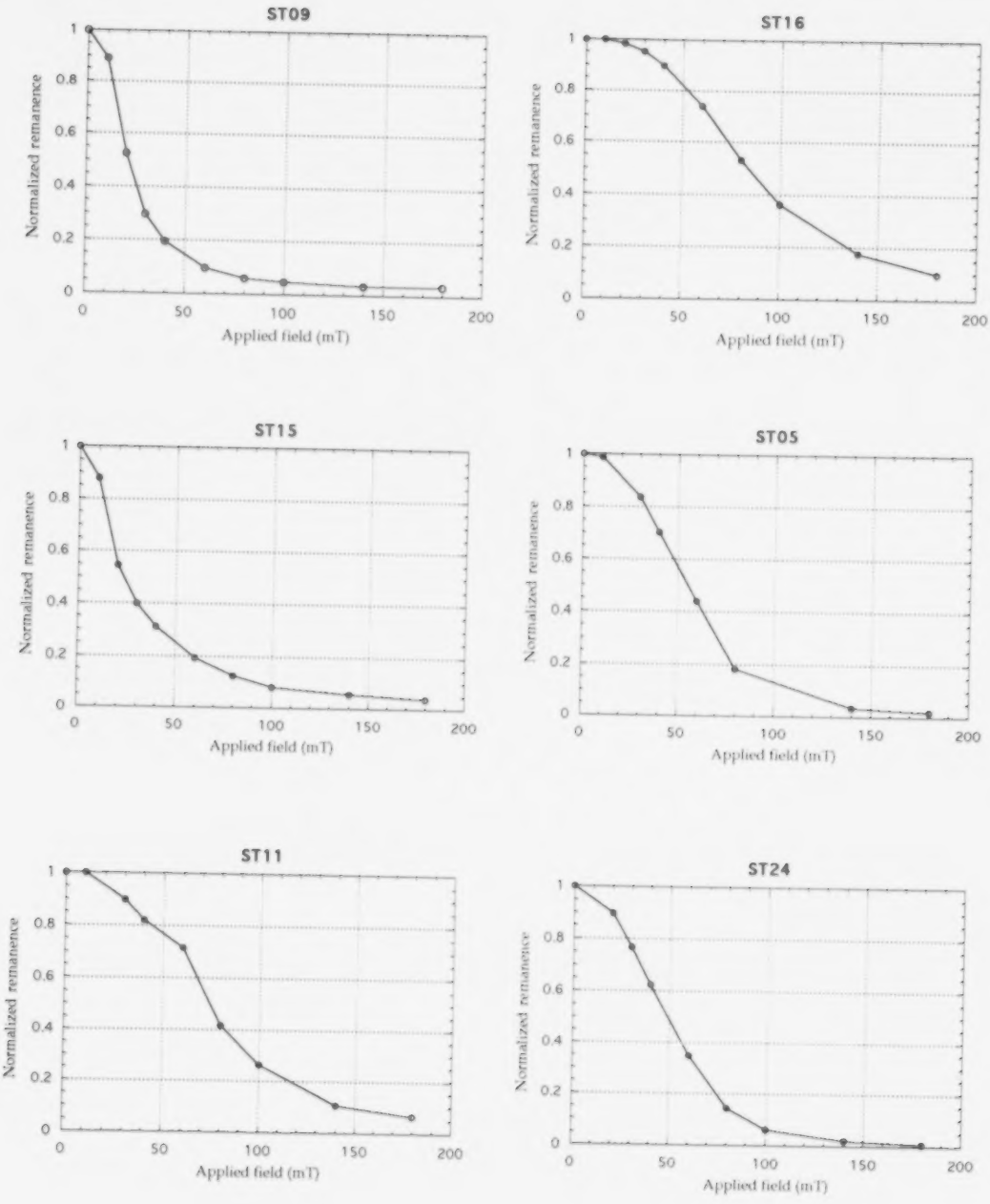

Figure 3.2.1c *AF demagnetisation of NRM of Chinese samples*

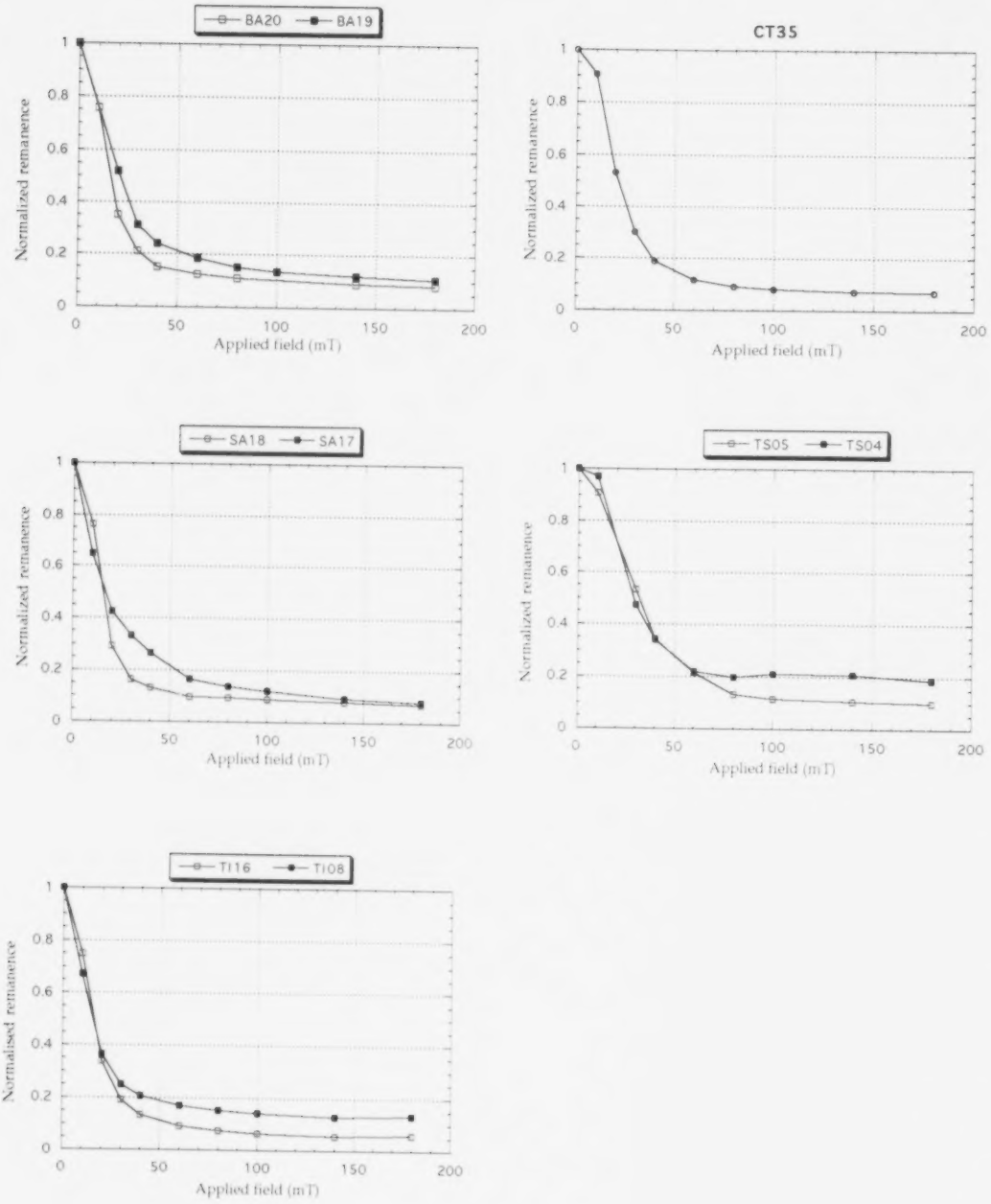

Figure 3.2.1d *AF demagnetisation of NRM of North African samples*

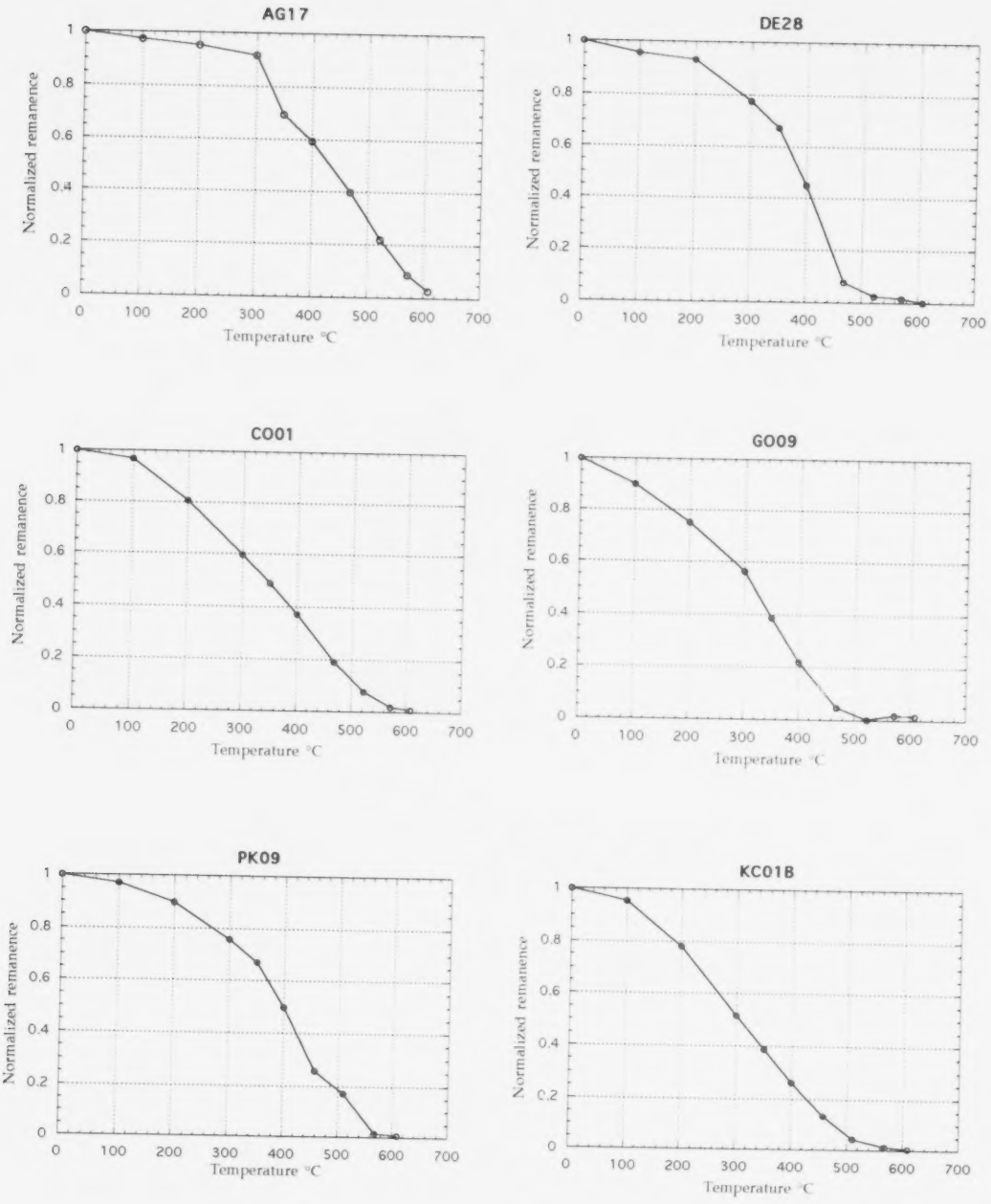

Figure 3.2.2a *Thermal demagnetisation of NRM of Greek samples*

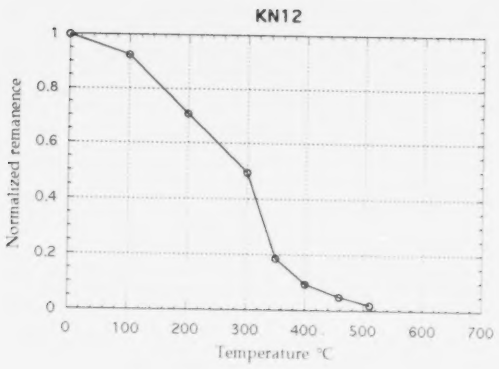

Figure 3.2.2a *Continued*

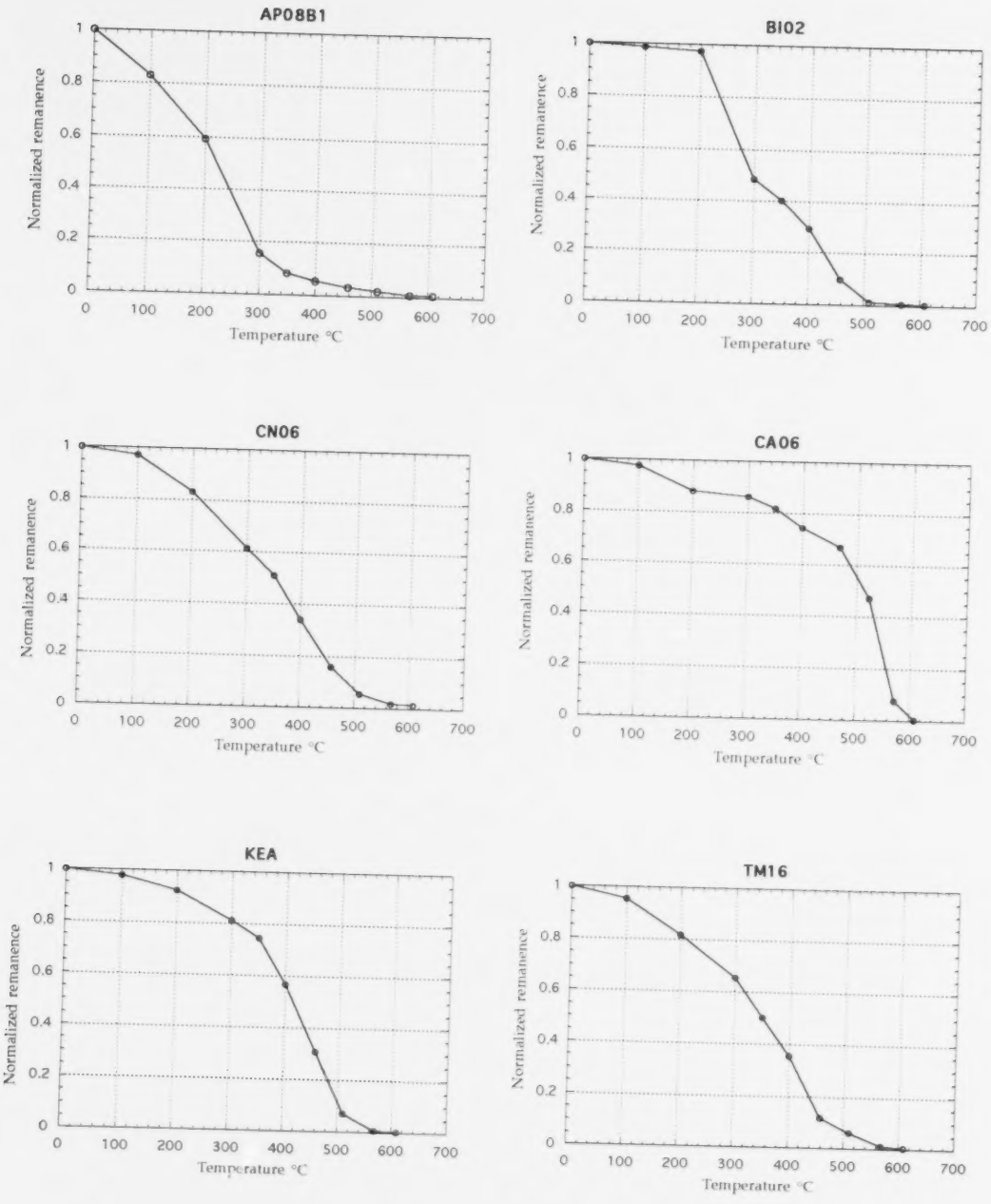

Figure 3.2.2b *Thermal demagnetisation of NRM of Italian samples*

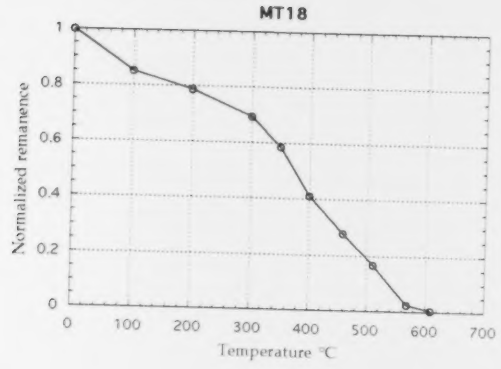

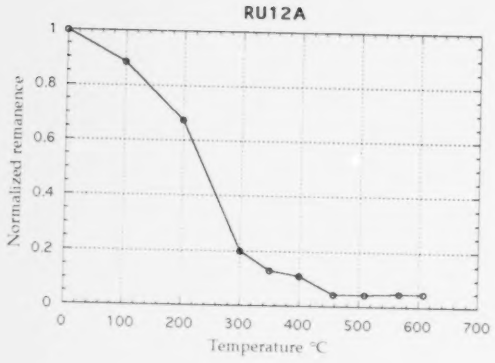

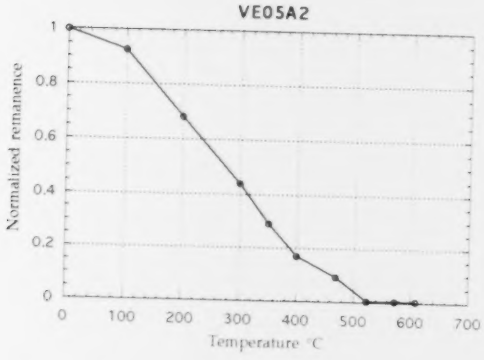

Figure 3.2.2b *Continued*

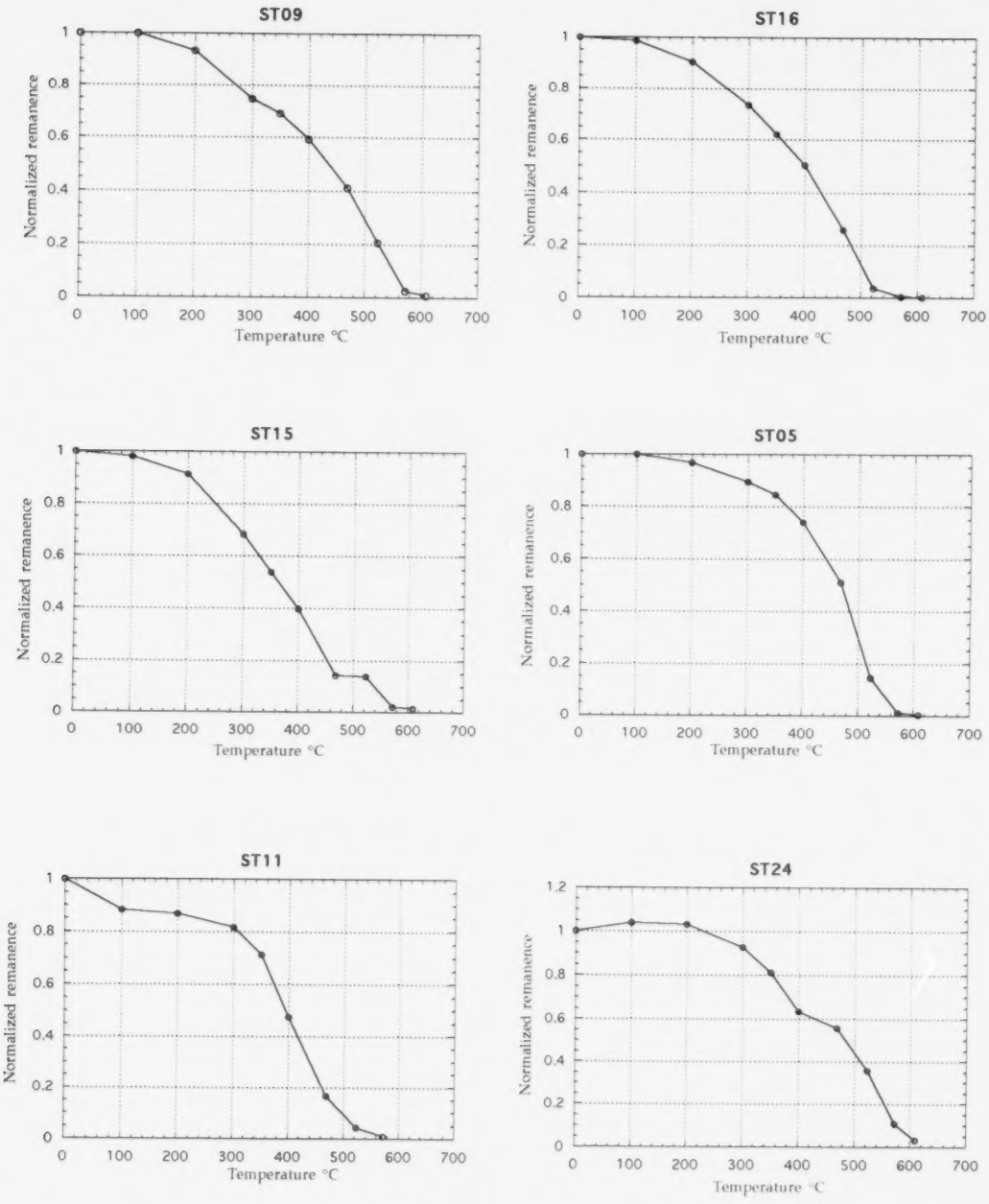

Figure 3.2.2c *Thermal demagnetisation of NRM of Chinese samples*

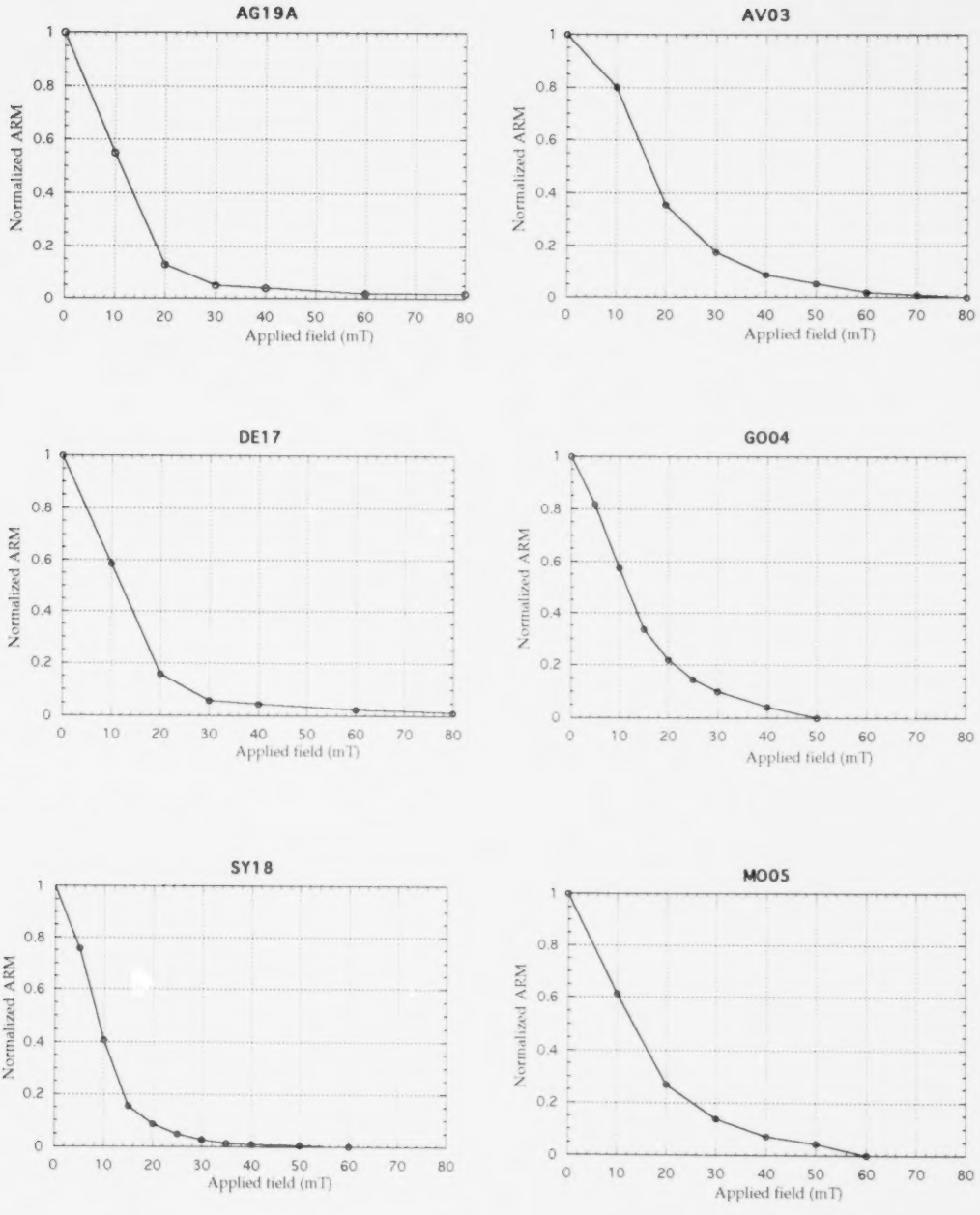

Figure3.2.3a *AF demagnetisation of ARM of Greek samples*

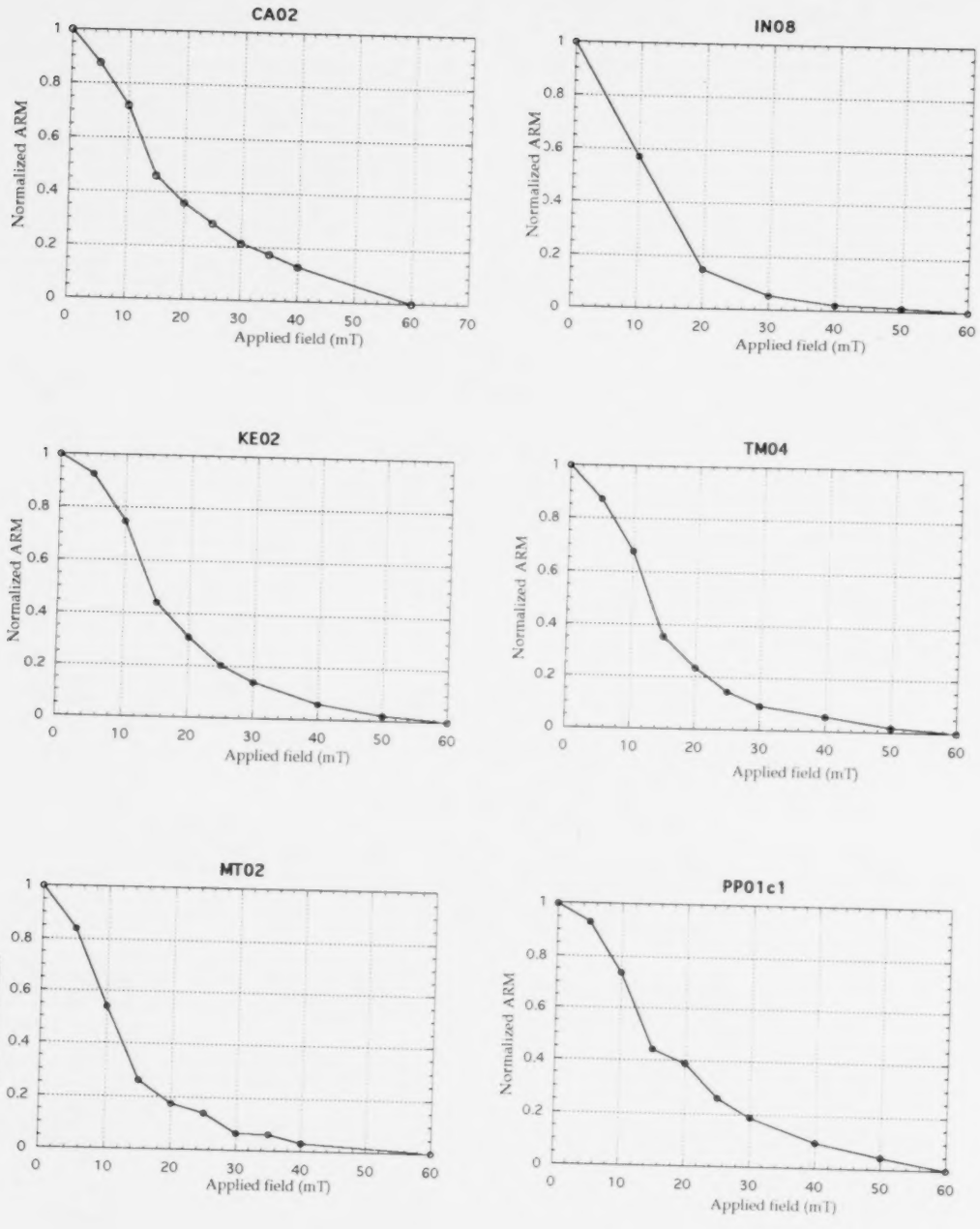

Figure3.2.3b *AF demagnetisation of ARM of Italian samples*

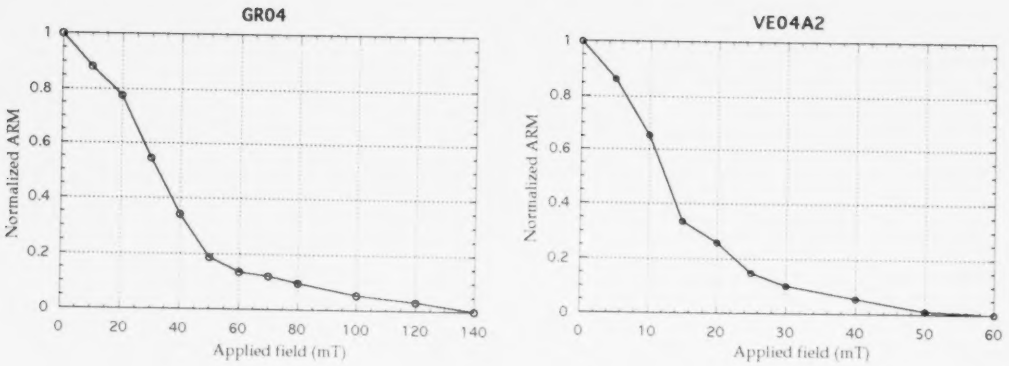

Figure3.2.3b *Continued*

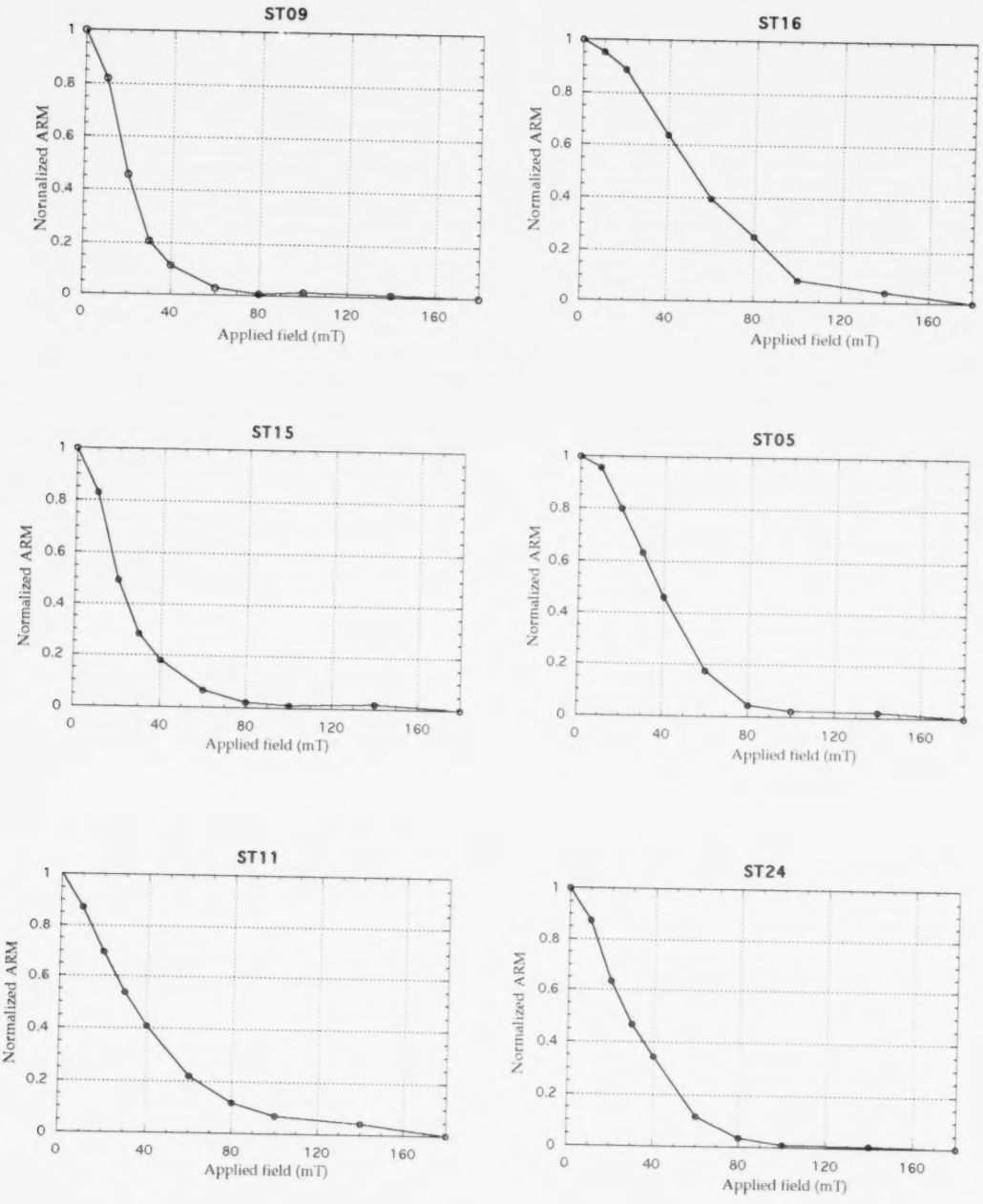

Figure3.2.3c *AF demagnetisation of ARM of Chinese samples*

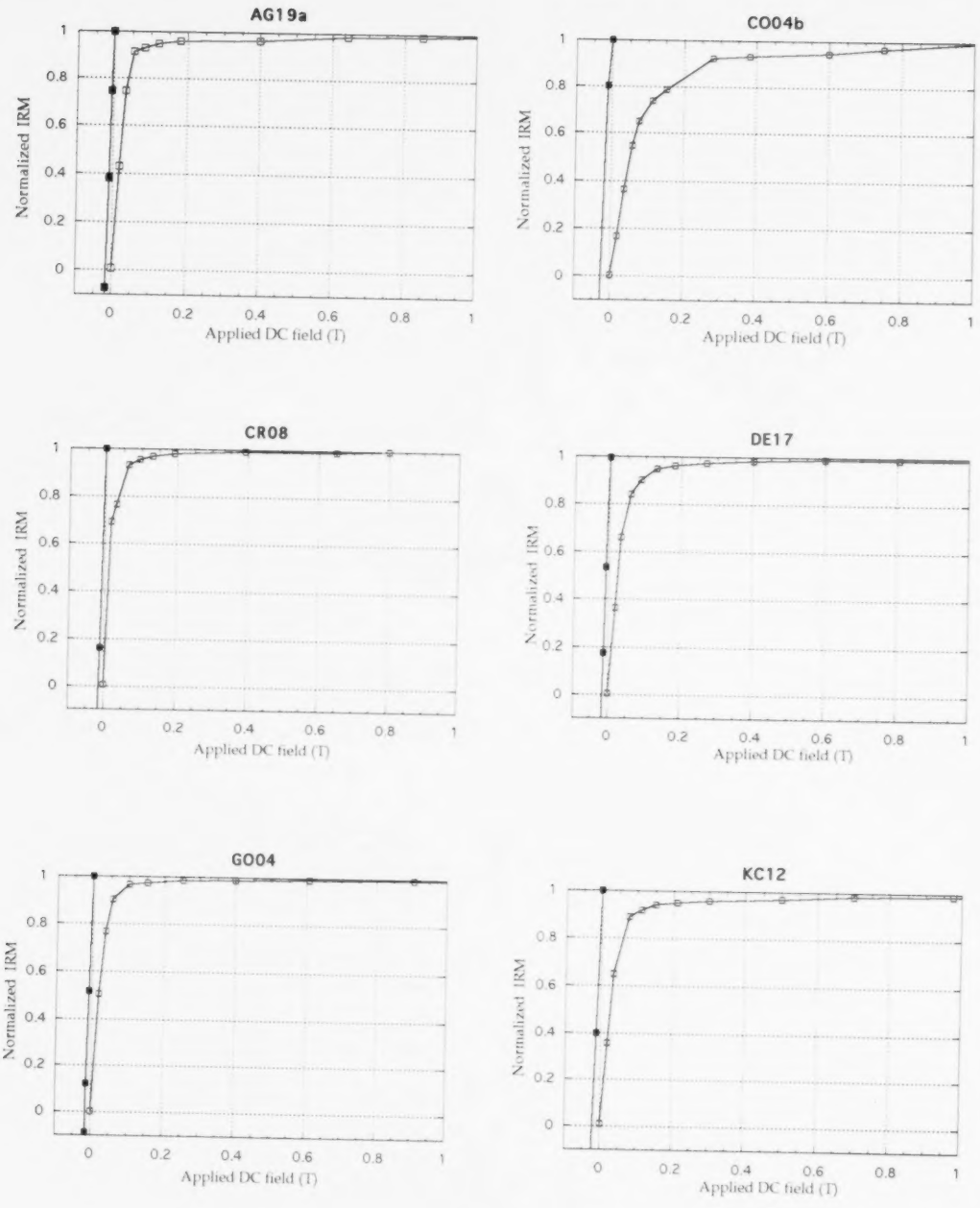

Figure 3.2.4a *IRM acquisition and back field results of Greek samples*

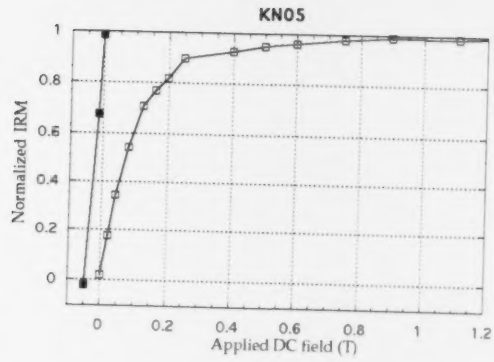

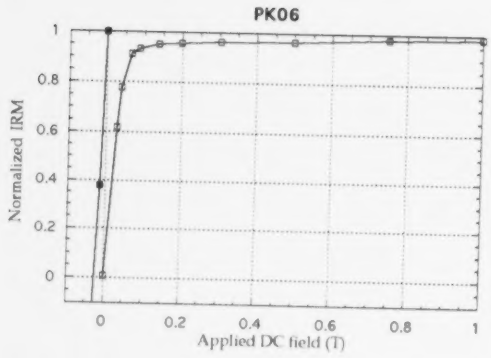

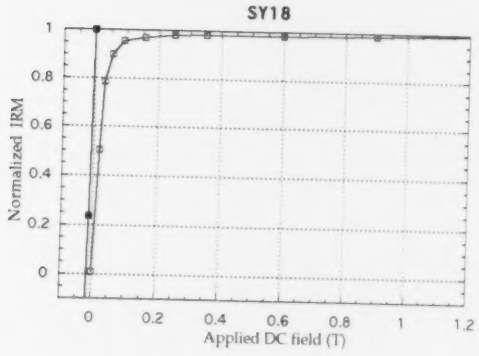

Figure 3.2.4a *Continued*

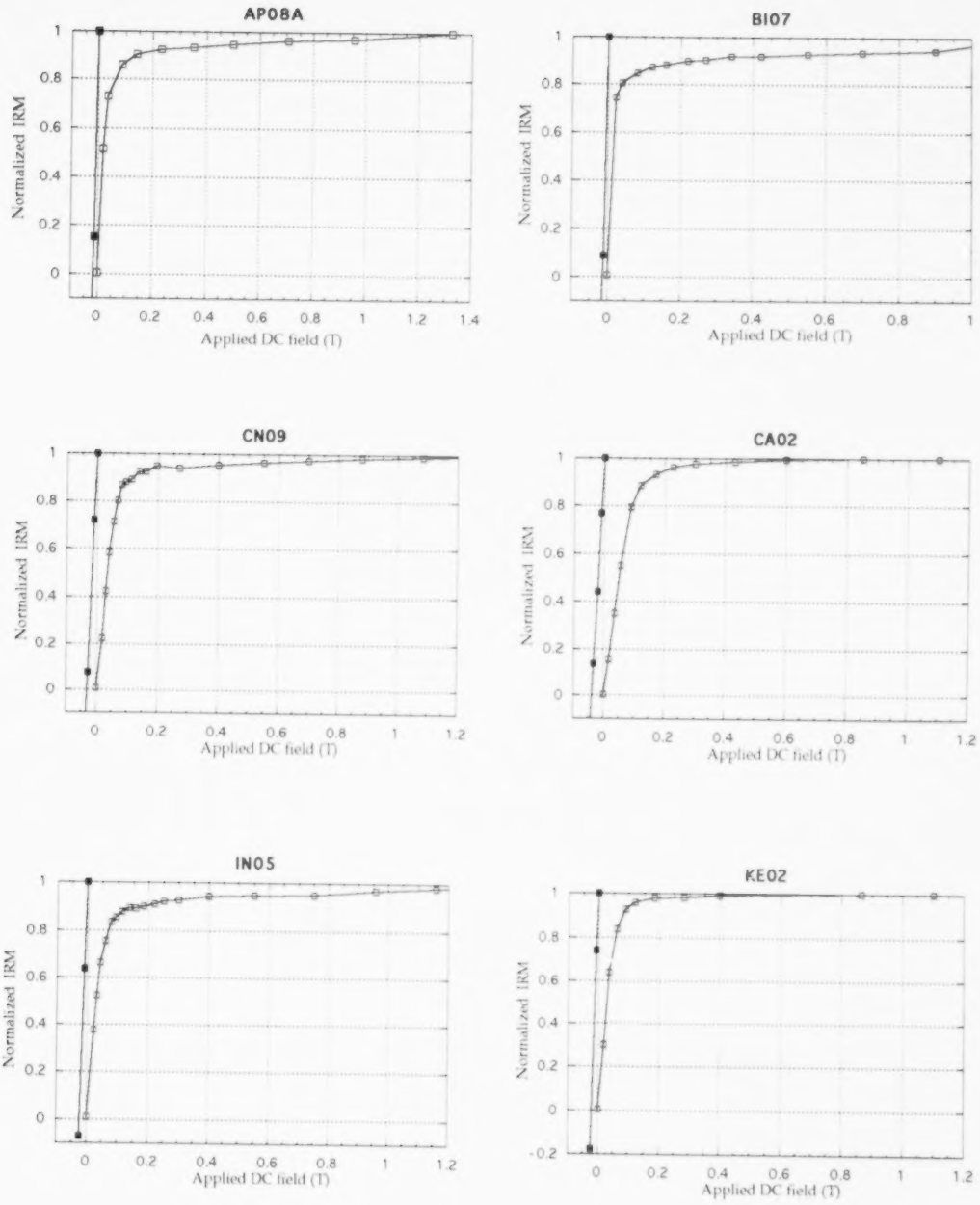

Figure 3.2.4b *IRM acquisition and back field results of Italian samples*

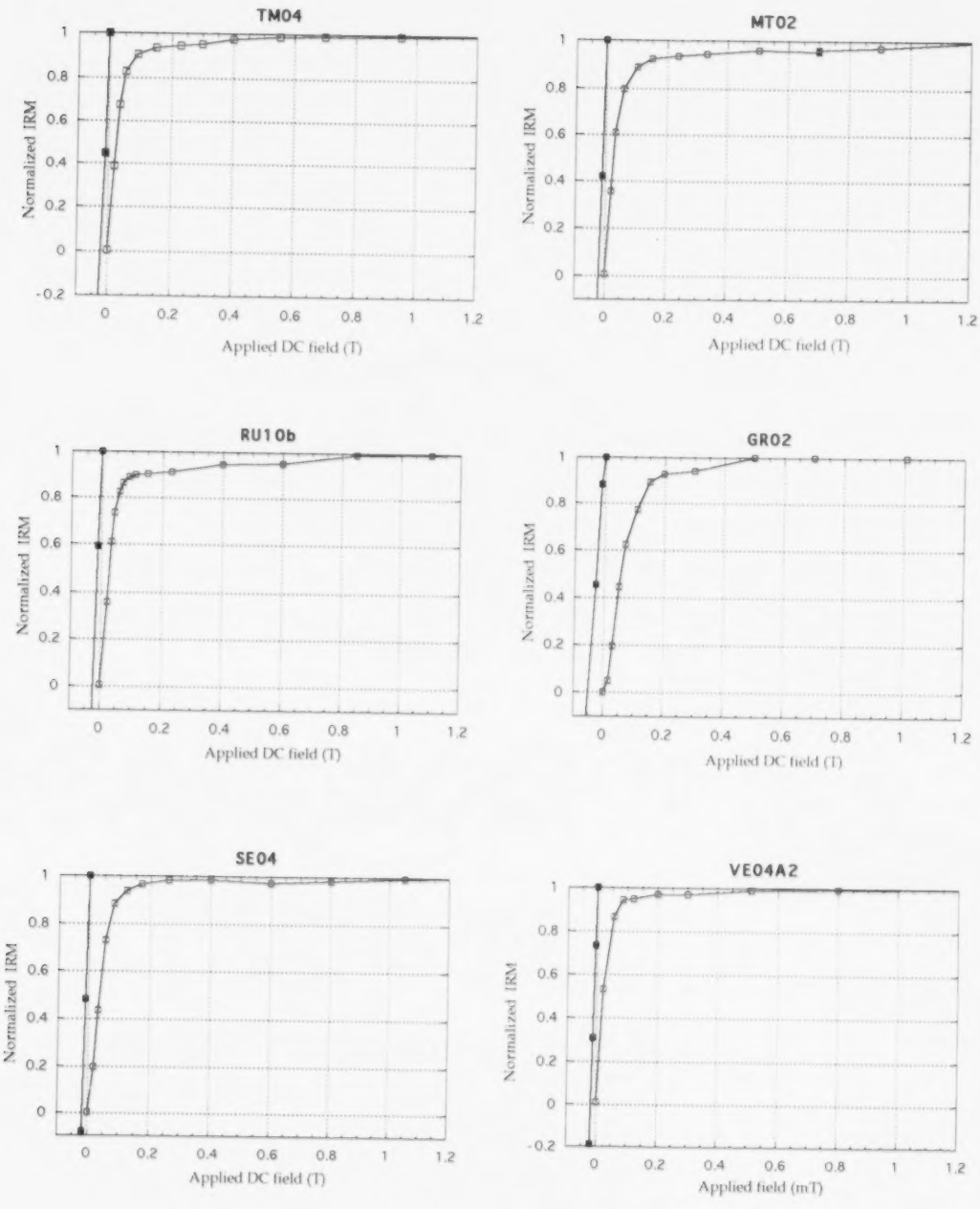

Figure 3.2.4b *Continued*

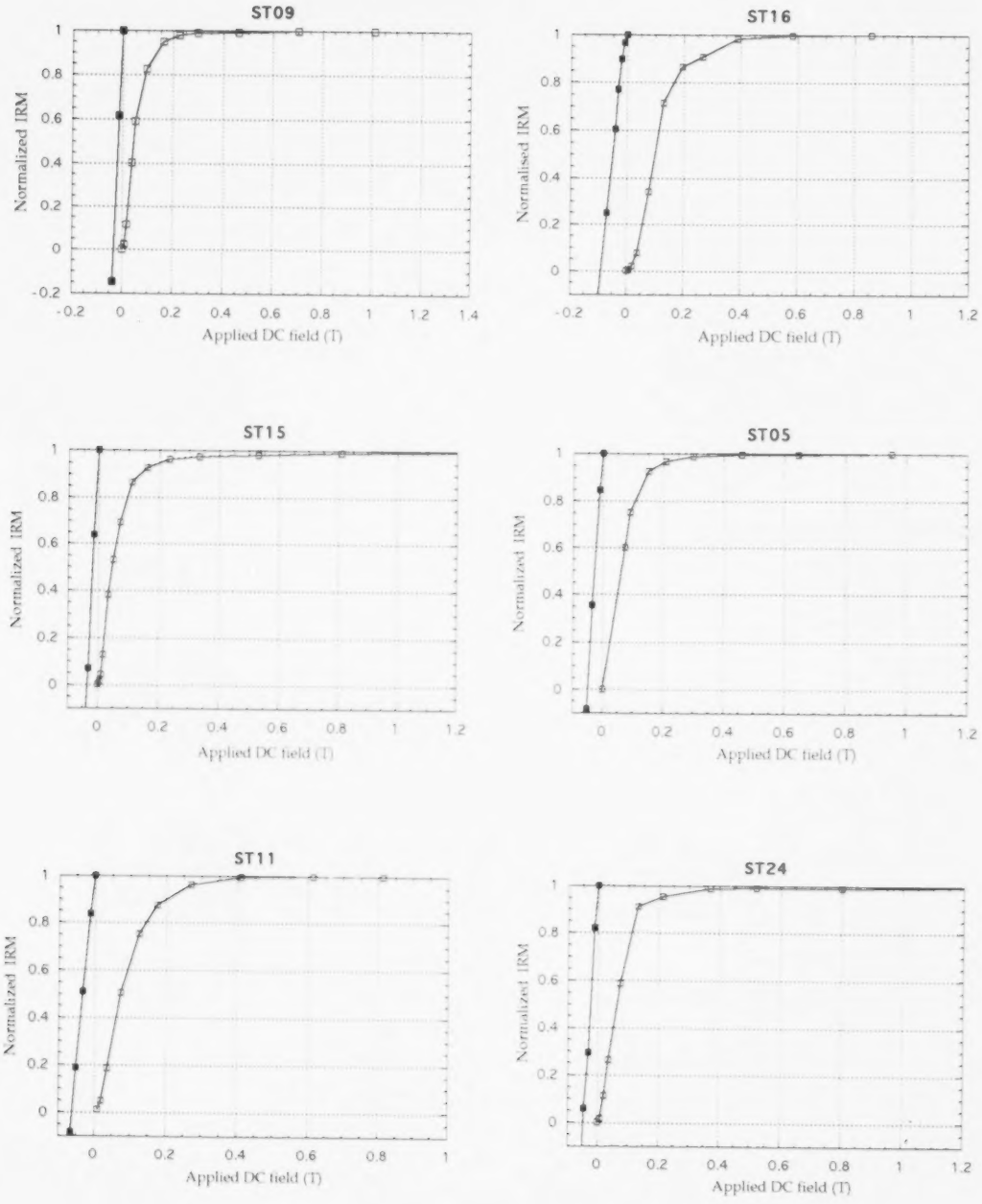

Figure 3.2.4c *IRM acquisition and back field results of Chinese samples*

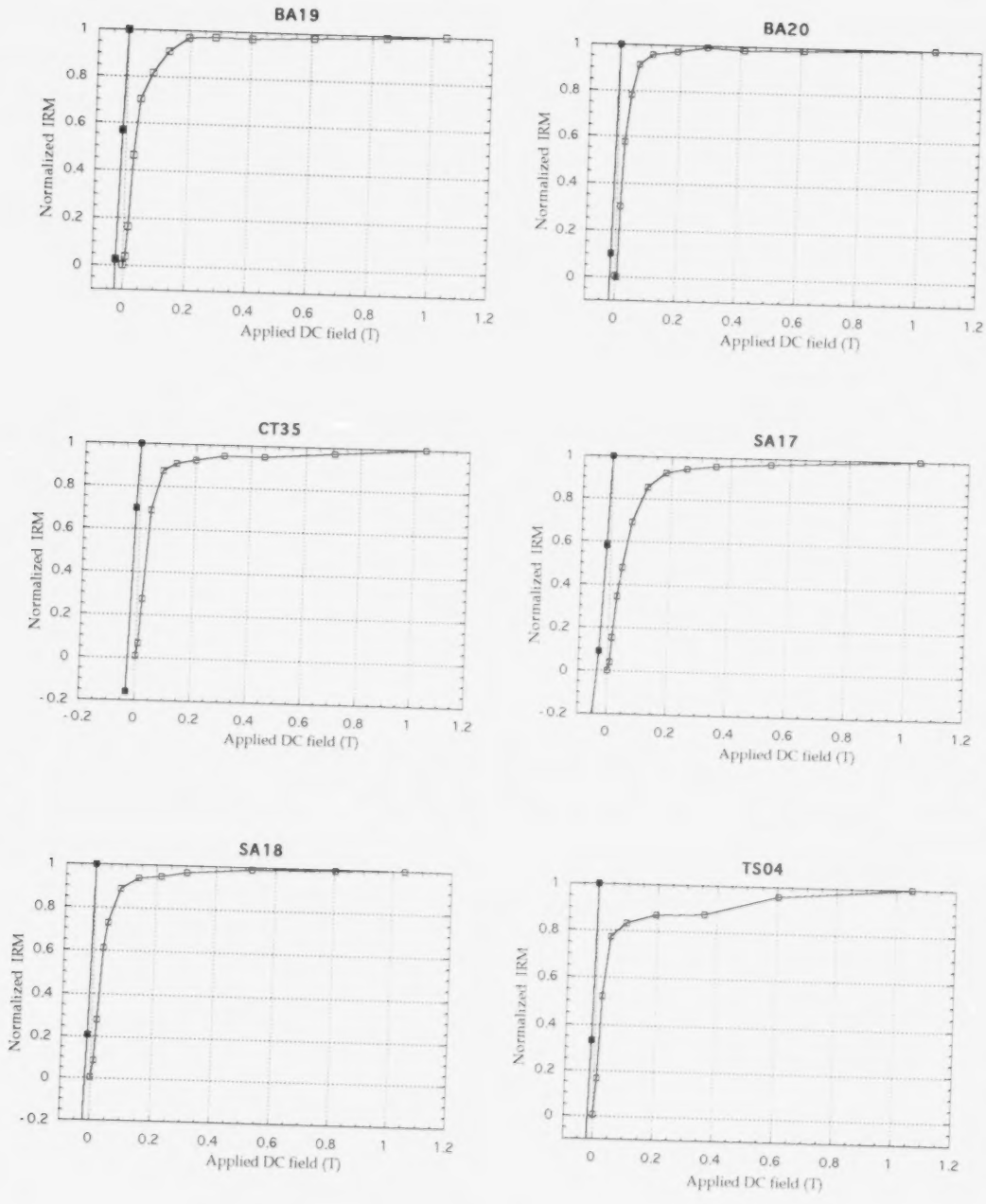

Figure 3.2.4d *IRM acquisition and back field results of North African samples*

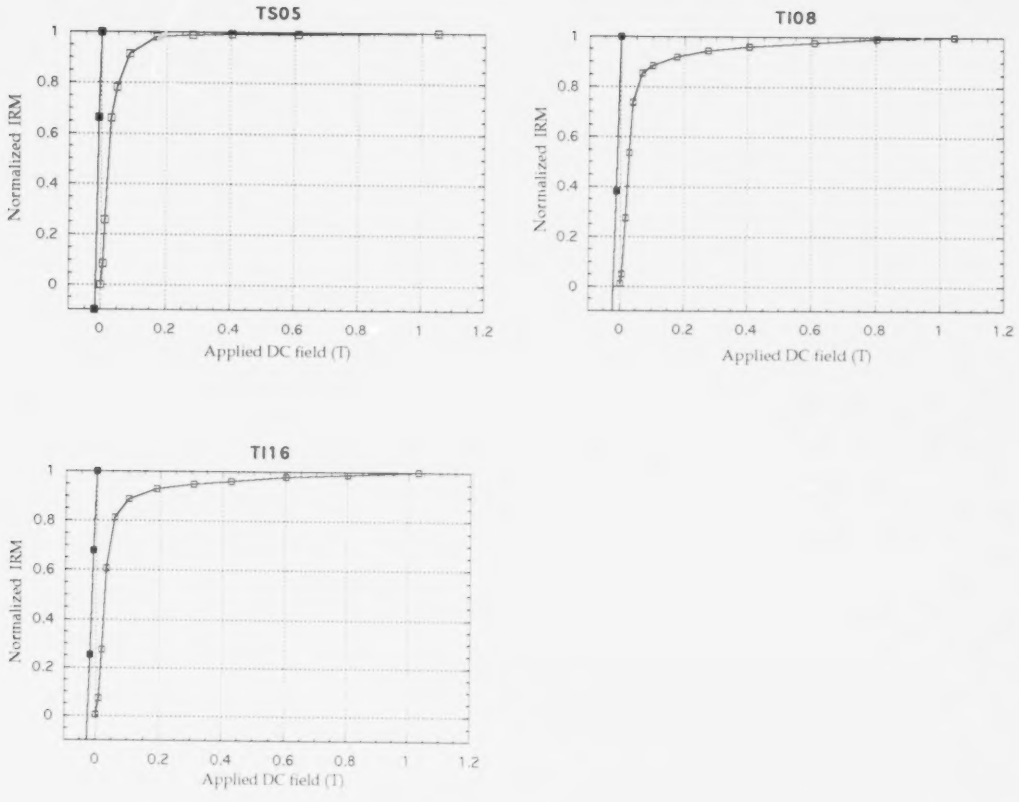

Figure 3.2.4d *Continued*

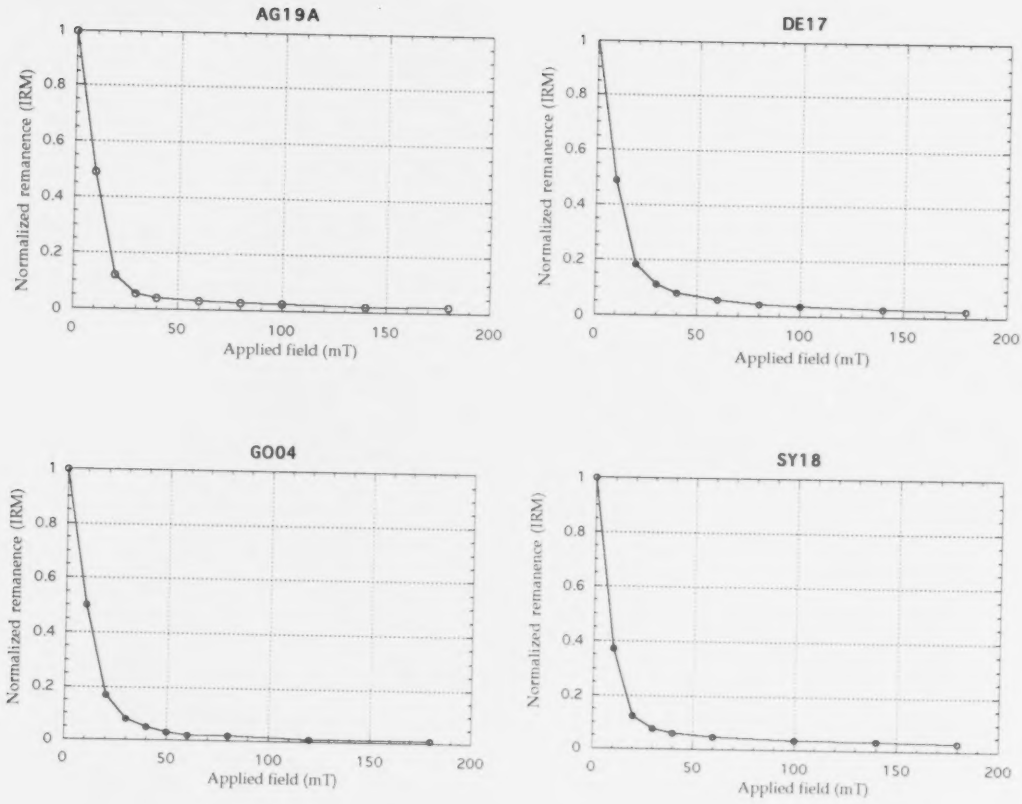

Figure 3.2.5a *AF demagnetisation of IRM of Greek samples*

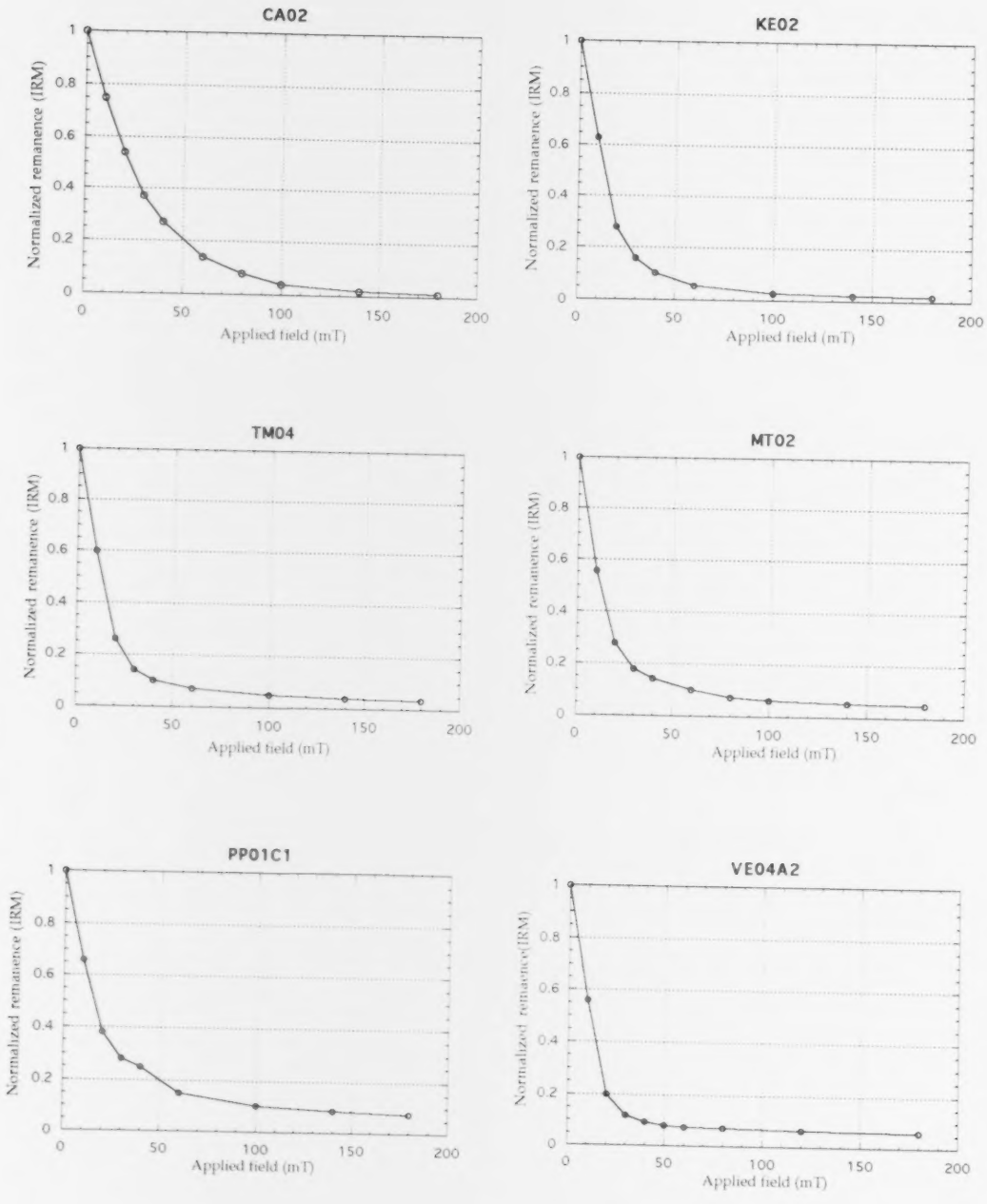

Figure 3.2.5b *AF demagnetisation of IRM of Italian samples*

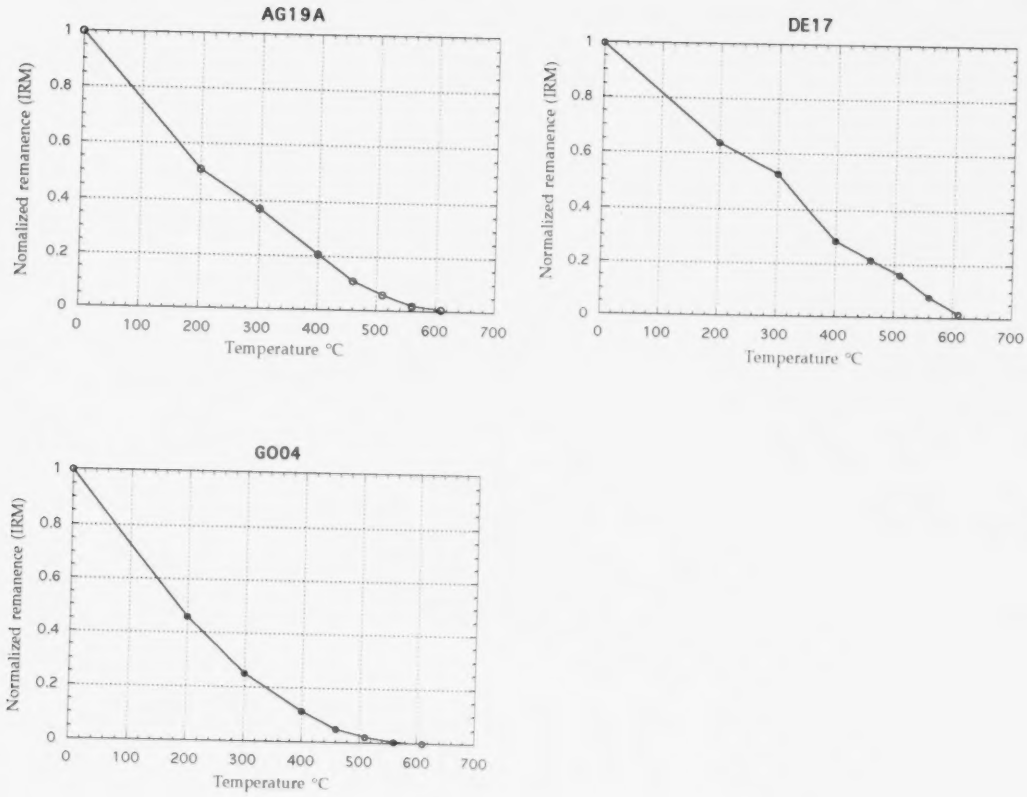

Figure 3.2.6a *Thermal demagnetisation of IRM of Greek samples*

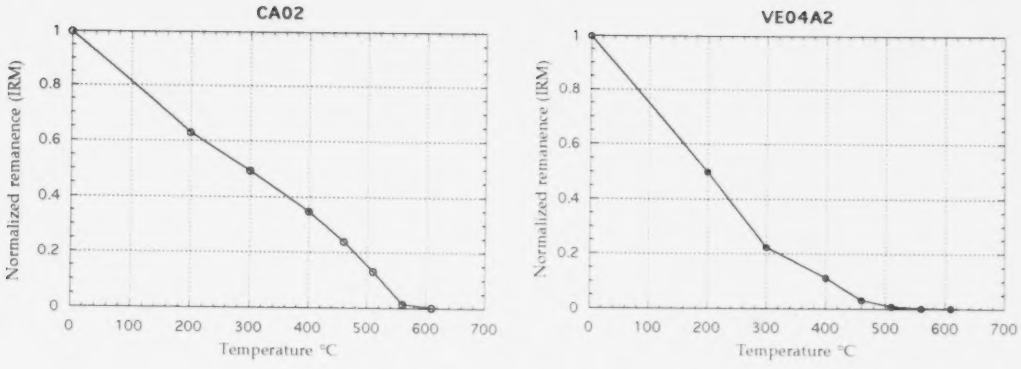

Figure 3.2.6b *Thermal demagnetisation of IRM of Italian samples*

Chapter 4 Discussion

4.1 Thermal treatment and magnetic mineralogy

4.1.1 Thermal demagnetisation of NRM

Since each specific composition of magnetic mineral has a particular Curie temperature, it is possible to identify minerals by means of thermal demagnetisation. Figures 3.2.2a - c present the thermal demagnetisation curves of all 22 samples. It is clear that the Curie temperatures of all these samples are below 600°C, except, perhaps, for sample RU12A. The behaviour of RU12A is somewhat different from that of the other samples. The intensity decreases rapidly up to ~300°C, and then decreases much more slowly until 610°C. Even at the highest temperature, there is still 5% of the NRM remaining in this sample. One possible interpretation is that there is some hematite (αFe_2O_3) contained in the sample. However, when the directions of remanence are considered, it is noted that beyond 400°C there is no stable magnetisation. This indicates that the NRM of this sample is <u>not</u> carried by hematite.

From the discussion above, at least, we know that there is basically no hematite playing a significant role in these archaeomagnetic materials. The demagnetisation curves have variable degrees of convexity. The curves of twelve

samples (AG17, KEA, DE28, MT18, PK09, CA06, ST05, ST09, ST11, ST15, ST16, ST24) (Figure 4.1.1a) have the typical shape for single-domain (SD) magnetite (Hunt, 1991). The intensity of NRM of these samples is reduced near to zero when the heating temperature reaches about 570°C. Therefore, the dominant magnetic mineral contained in these samples appears to be magnetite (Fe_3O_4).

In a second group of samples (GO09, TM16, BI02, CN06, VE05A2, KC01B, CO01), the relationship between the intensity of NRM and the temperature is much more linear (Figure 4.1.1b), indicating the presence of a distributed spectrum of blocking temperatures. However, the NRM still falls to near-zero values at relatively high temperatures (>500°C). This type of curve is typical of multi-domain (MD) magnetite (Hunt, 1991).

Finally, there are 3 remaining samples (KN12, AP08B1, RU12A)) which have highly convex curves (Figure 4.1.1c), but with Curie points in the 350 to 400°C range. This *could* be due to a titanomagnetite with a particular composition (x~0.4 in the formula $[(1-x)Fe_3O_4]$ $[xFe_2TiO_4]$) (Tarling, 1983), but it is much more likely to represent maghemite (γFe_2O_3). This is a common mineral, which is metastable and converts to hematite (αFe_2O_3) at ~350°C (O'Reilly, 1984).

4.1.2 Thermal demagnetisation of SIRM

Five saturation isothermal remanent magnetisations (SIRM's) were thermally demagnetised (Figure 3.2.6a and b). As can be seen, the curves obtained are generally more linear than the corresponding NRM curves (Figure 3.2.2a-c). This probably indicates that magnetically soft MD particles are more important in the

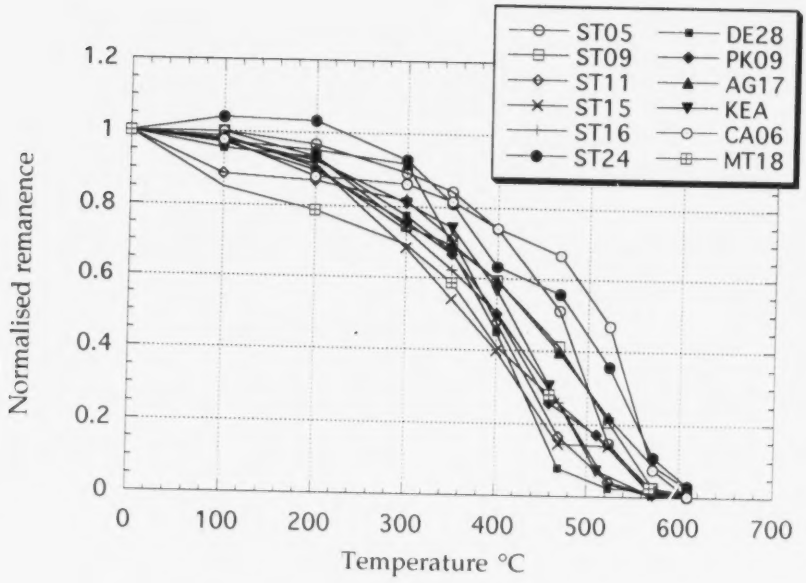

Figure 4.1.1a Thermal demagnetisation curves

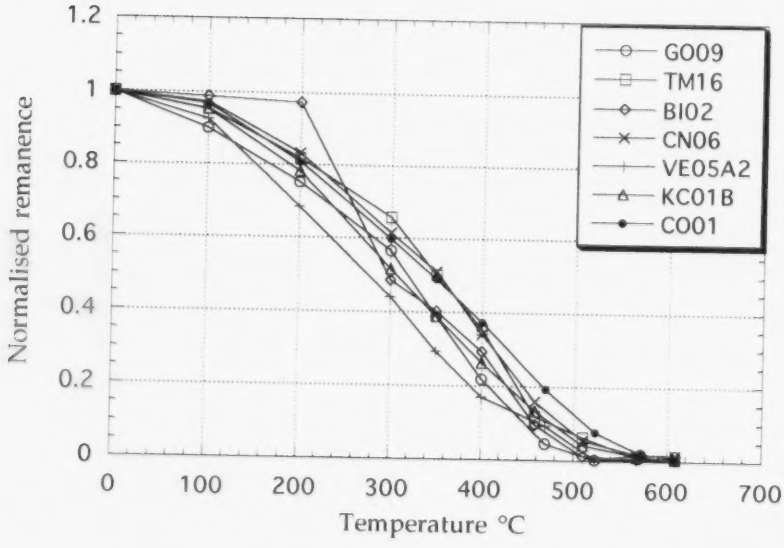

Figure 4.1.1b Thermal demagnetisation curves

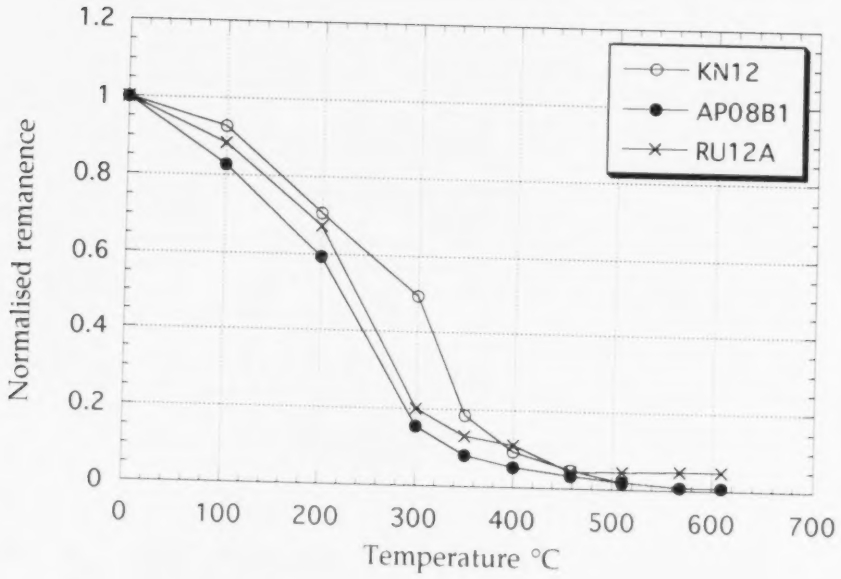

Figure 4.1.1c Thermal demagnetisation curves

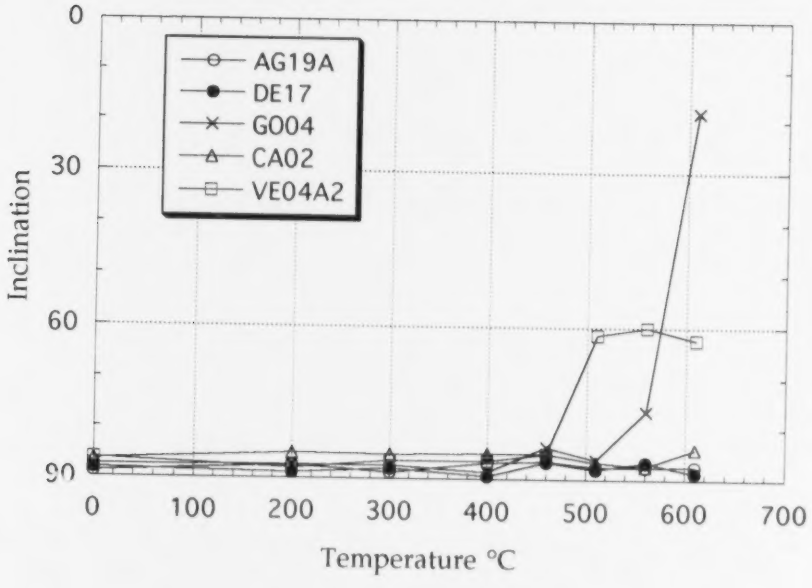

Figure 4.1.2 Inclination vs. temperature for thermal demagnetisation SIRM. Inclination is expected to be 90° due to the way in which the sample is placed in the laboratory electromagnet.

SIRM; in the NRM these particles would have preferentially decayed. Figure 4.1.2 shows the directional behaviour during demagnetisation. Three samples are stable throughout the entire temperature range (AG19A, DE17, CA02), but the other two (GO04, VE4A2) diverge beyond 500°C. These results agree with the data shown in Figure 4.1.1a and b (compare with samples AG17, CA06, GO09, VE5A2). (Note that no samples from site DE were included in the thermal demagnetisation of NRM).

These few SIRM results favour magnetite, or a very low-titanium titanomagnetite, as the dominant magnetic mineral present. The directional stability of 3 of the samples up 610°C suggests that hematite may play a small role. However, this fraction is always less than 2%.

4.2 Coercivity spectra and magnetic mineralogy

4.2.1 IRM acquisition

Magnetite and hematite are the two commonest magnetic minerals in nature. The difference in the magnetic coercivity of magnetite and hematite makes the IRM acquisition method an effective means of distinguishing between these two minerals. Magnetite is typically saturated in fields less than 0.3T, while hematite does not saturate until fields of over 3T (Hunt, 1991; Tarling, 1983). The main advantage of this method is that it does not involve any heating and possible chemical changes.

The IRM acquisition curves are given in Figures 3.2.4a-d. Most samples acquire little IRM in fields greater than 0.3T. This behaviour indicates that the remanence in these samples is carried by magnetite and/or titanomagnetite (Butler, 1982), hematite being either absent or negligible. However, a few samples such as BI07, KN05, TS04 show increasing IRM in fields greater than 0.3T. These samples may contain a small amount of high-coercivity hematite.

In order to investigate the possible relation of IRM acquisition to properties of NRM, it is appropriate to define a parameter which in some way quantifies the IRM acquisition behaviour (Butler, 1982; Verosub, 1995). Let

$$\Delta = [SIRM - IRM(0.3T)]/[IRM(0.3T)]$$

where IRM(0.3T) is the IRM acquired by exposure to a magnetising field of 0.3T. $\Delta = 0$ would indicate an IRM acquisition curve in which no additional IRM was acquired for applied fields > 0.3T. Such a curve would indicate that there is no hematite playing a significant role in the sample. From the results, using the formula above it is easy to obtain all Δ values (Table 4.2.1). In order to see more clearly, a histogram (Figure 4.2.1) was plotted. The Δ values for 33 of the 36 samples are less than 0.08, which indicates that the dominant magnetic mineral in these samples is magnetite and/or titanomagnetite. The Δ values for the remaining three samples (BI07, KN05, TS04) are in the range 0.1 to 0.15, which means that there is *some* hematite present, but it clearly does not dominate the overall magnetisation.

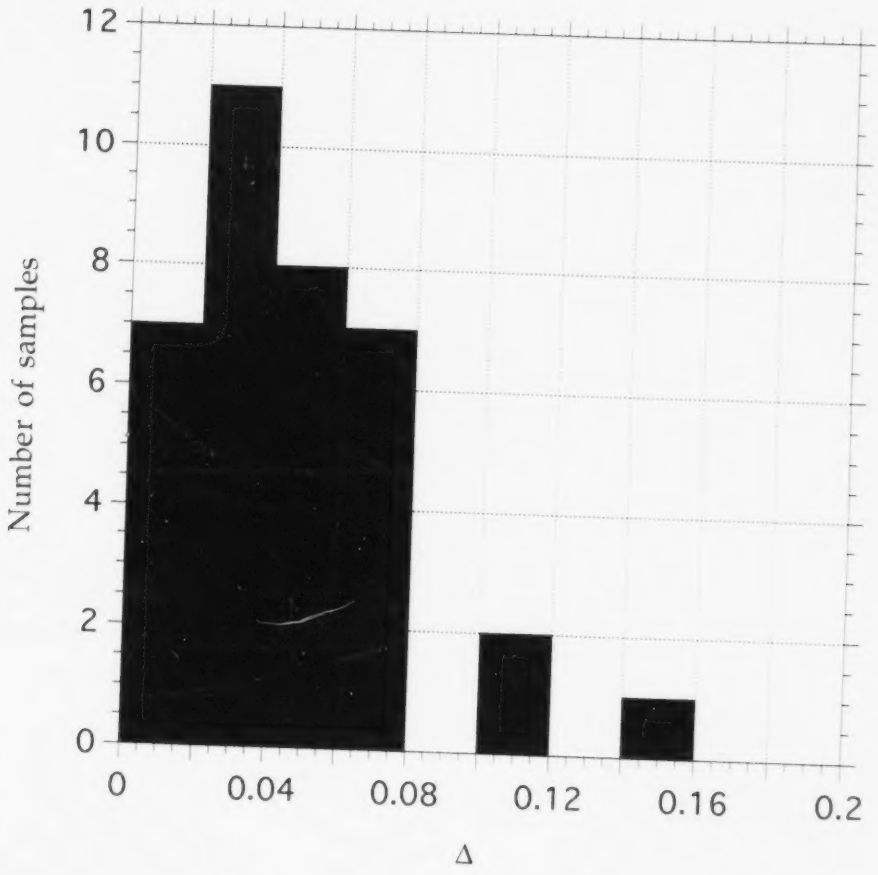

Figure 4.2.1 Histogram of Δ for 36 samples

Table 4.2.1 Δ values for 36 samples

Sample	Δ	Sample	Δ	Sample	Δ	Sample	Δ
KC12	0.043	CA02	0.024	CN09	0.058	SA18	0.031
CO04B	0.079	GR02	0.058	AP08A	0.074	SA17	0.047
AG19A	0.083	IN05	0.079	BI07	0.101	CT35	0.053
CR08	0.09	TM04	0.053	ST09	0.01	BA20	0.02
DE17	0.024	KE02	0.01	ST24	0.028	BA19	0.029
SY18	0.014	MT02	0.064	ST11	0.033	TS05	0.014
GO04	0.009	VE04A2	0.03	ST16	0.079	TI08	0.058
KN05	0.101	RU10B	0.079	ST15	0.028	TI16	0.053
PK06	0.038	SE04	0.02	ST05	0.014	TS04	0.14

4.2.2 Backfield

The coercivity of remanence, H_{cr}, is a useful magnetic parameter to identify minerals contained in samples. It is usually more convenient to measure H_{cr} than to measure H_c. The backfield method has been applied to 36 samples and the results are shown in Figure 3.2.4a-d. All H_{cr} values can be found in Table 4.2.2. The H_{cr} values for 34 samples are less than 50 mT. Only two samples (ST16 and ST11) have relatively high values (63 and 87mT) (Figure 4.2.2). Day et al (1976) studied synthetic titanomagnetites [(1-x) Fe_3O_4] [xFe_2TiO_4] ($0 \leq x \leq 0.6$) and found that H_{cr} values are in the range of 9 to 220 mT. The Hcr values for

hematite are much higher, at least in the order of several hundred mT (Irving, 1964; Dankers, 1981). Therefore, it is reasonable to consider that the main magnetic minerals contained in these samples are magnetite and/or titanomagnetite.

Table 4.2.2 Hcr (mT) values for 36 samples

Sample	Hcr	Sample	Hcr	Sample	Hcr	Sample	Hcr
KC12	20	CA02	35	CN09	27	SA18	13
CO04B	23	GR02	47	AP08A	12	SA17	31
AG19A	14	IN05	20	BI07	8	CT35	25
CR08	8	TM04	21	ST09	31	BA20	13
DE17	14	KE02	21	ST24	48	BA19	24
SY18	9	MT02	19	ST11	63	TS05	10
GO04	14	VE04A2	17	ST16	87	TI08	13
KN05	47	RU10B	17	ST15	32	TI16	20
PK06	20	SE04	17	ST05	49	TS04	13

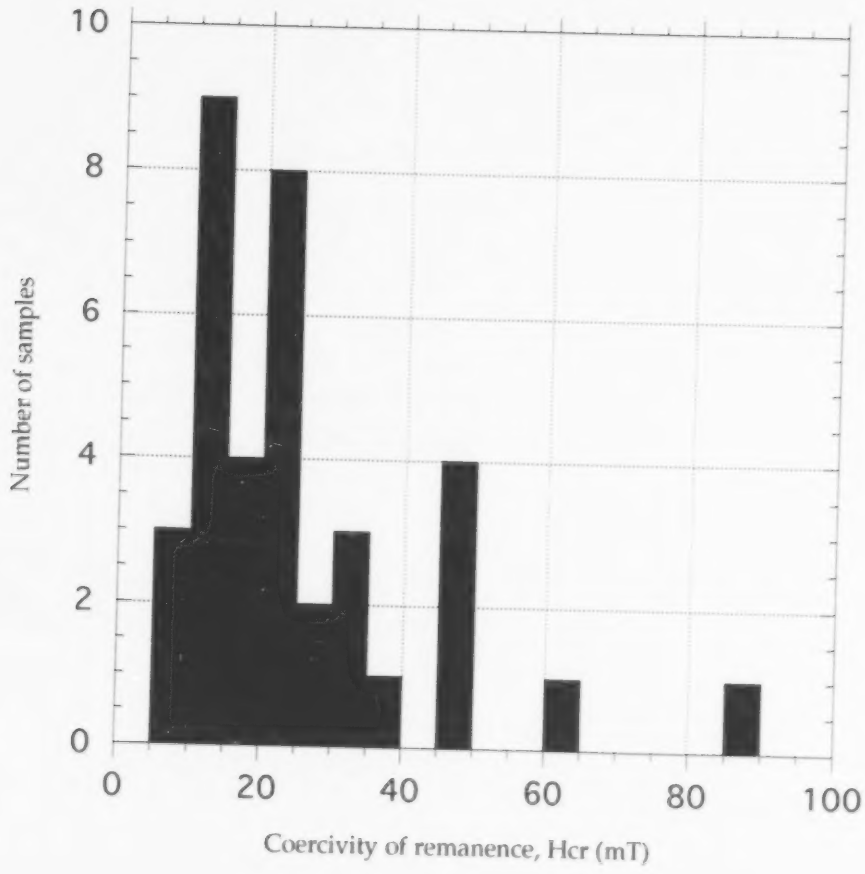

Figure 4.2.2 Histogram of Hcr for 36 samples

4.2.3 AF demagnetisation of IRM

Ten samples were investigated using AF demagnetisation of saturation IRM (Figure 3.2.5a and b). From these results, we obtain the values of median destructive field of IRM (MDF of IRM) (Table 4.2.3). The MDF of IRM values for 9 out of 10 are in the range of 7 - 16mT and the remaining one (CA02) is 22mT (Figure 4.2.3). Dankers (1981) studied the MDF of IRM for hematite, magnetite and titanomagnetite with different compositions. His results are: the MDF of IRM values for hematite are in the range 53 - 285mT; the MDF of IRM values for magnetite and titanomagnetite are in the range 5 - 19mT. Comparing our results with those of Dankers, it is clear that the main magnetic mineral contained in the 10 samples is magnetite and/or titanomagnetite, hematite being either absent or negligible.

Table 4.2.3 MDF of IRM values for 10 samples

Sample	MDF (mT)	Sample	MDF (mT)
VE04A2	12	SY18	7
PP01C1	15	GO04	10
AG19A	10	KE02	13
CA02	22	TM04	12
DE17	10	MT02	11

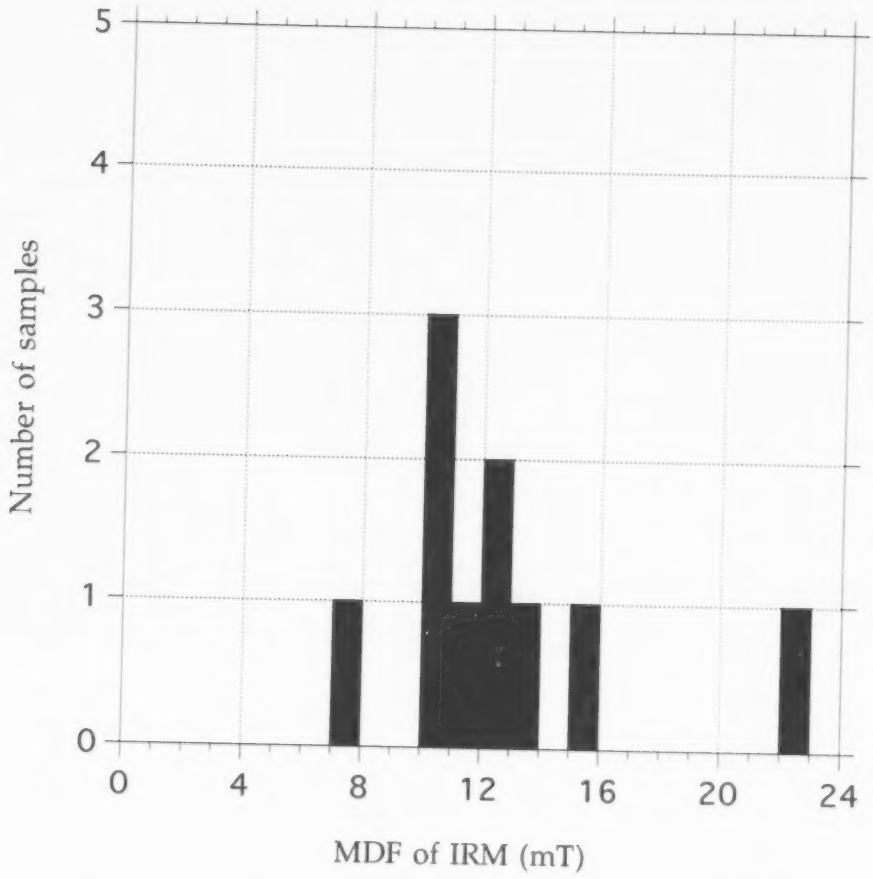

Figure 4.2.3 Histogram of MDF of IRM for 10 samples

4.2.4 AF demagnetisation of ARM

AF demagnetisation of ARM has been performed on 20 samples. The results are presented in Figure 3.2.3a-c. The values of median destructive field (MDF) of ARM are listed in Table 4.2.4. Most samples (18 out of 20 samples) have low values of MDF of ARM (between 11 - 33mT) (Figure 4.2.4). The other two ST05 and ST16) have the values of 38 and 48mT respectively. The MDF of ARM has been investigated by Maher (1988), by Levi et al (1976) and by Johnson et al (1974). The MDF of ARM values for magnetite with different grain size are in the range of 3 - 67mT. I could not find any corresponding values published for hematite.

Table 4.2.4 MDF of ARM (mT) values for 20 samples

Sample	MDF	Sample	MDF	Sample	MDF	Sample	MDF
CA02	14	MT02	11	AG19A	11	ST11	33
IN08	12	GR04	32	GO04	12	ST05	38
KE02	14	VE04A2	12	DE17	12	ST15	20
TM04	13	SY18	9	MO05	13	ST16	48
PP01C1	14	AV03	17	ST24	28	ST09	19

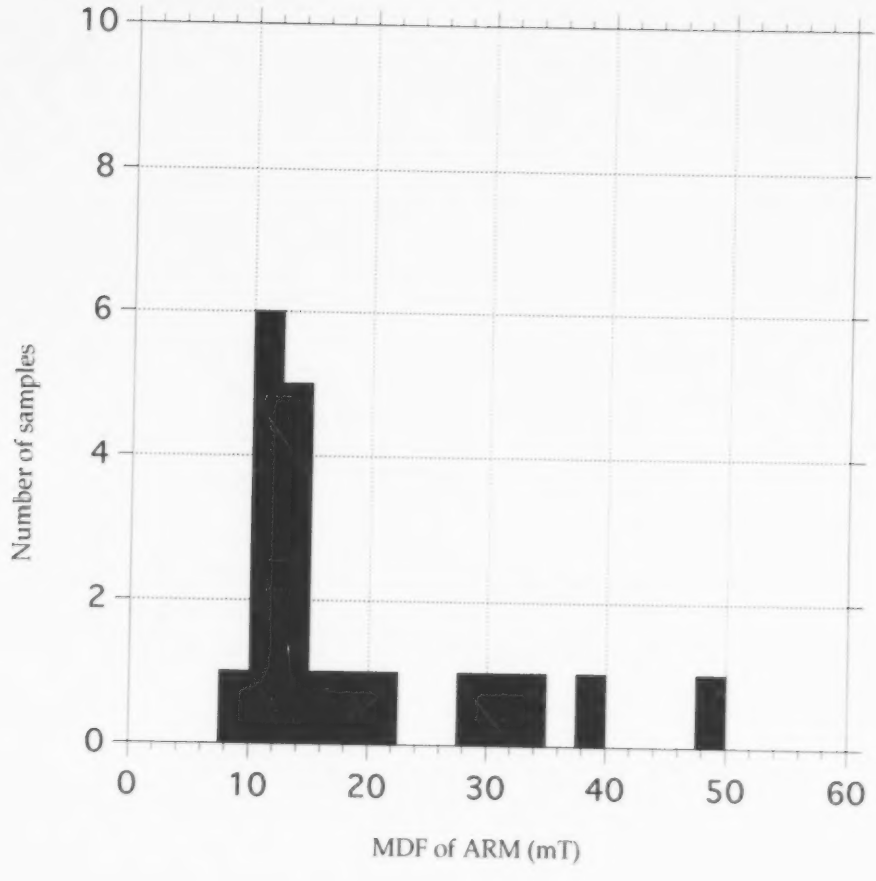

Figure 4.2.4 Histogram of MDF of ARM for 20 samples

4.2.5 AF demagnetisation of NRM

This technique has been applied to 40 samples. All the results are presented in Figure 3.2.1a - d. The median destructive field (MDF) of NRM is one of the useful magnetic parameters to identify those minerals responsible for the natural remanent magnetisation. The MDF values (Table 4.2.5) are plotted in Figure 4.2.5. It is found that the MDF of NRM of most samples (34) is low (< 35mT), and the other 6 samples are in the range of 40 - 85mT. These results indicate that a great deal of the NRM in these archaeomagnetic samples is carried by low coercivity magnetic minerals (magnetite and/or titanomagnetite). However, 4 Chinese, and 2 Greek samples are magnetically harder, and may therefore have significant hematite contributions to the NRM.

Table 4.2.5 MDF of NRM (mT) values for 40 samples

Sample	MDF	Sample	MDF	Sample	MDF	Sample	MDF
MO05	18	CA02	29	ST09	21	GR02	31
TH04	21	DE17	81	ST11	74	SE04	18
TH05	30	VE02A4	17	ST15	23	AP08A	9
MO02	27	KE02	17	ST16	82	CR08	12
IN08	12	PP01C1	19	ST24	49	TS04	29
PE02	25	MT02	13	IN05	19	TS05	31
AV07	19	SY18	14	KC12	16	BA19	21
AV03	19	TM04	15	CO04B	34	BA20	17
AG19A	40	ST05	54	PK06	16	TI08	16
SA16	16	SA17	17	CT35	22	TI16	17

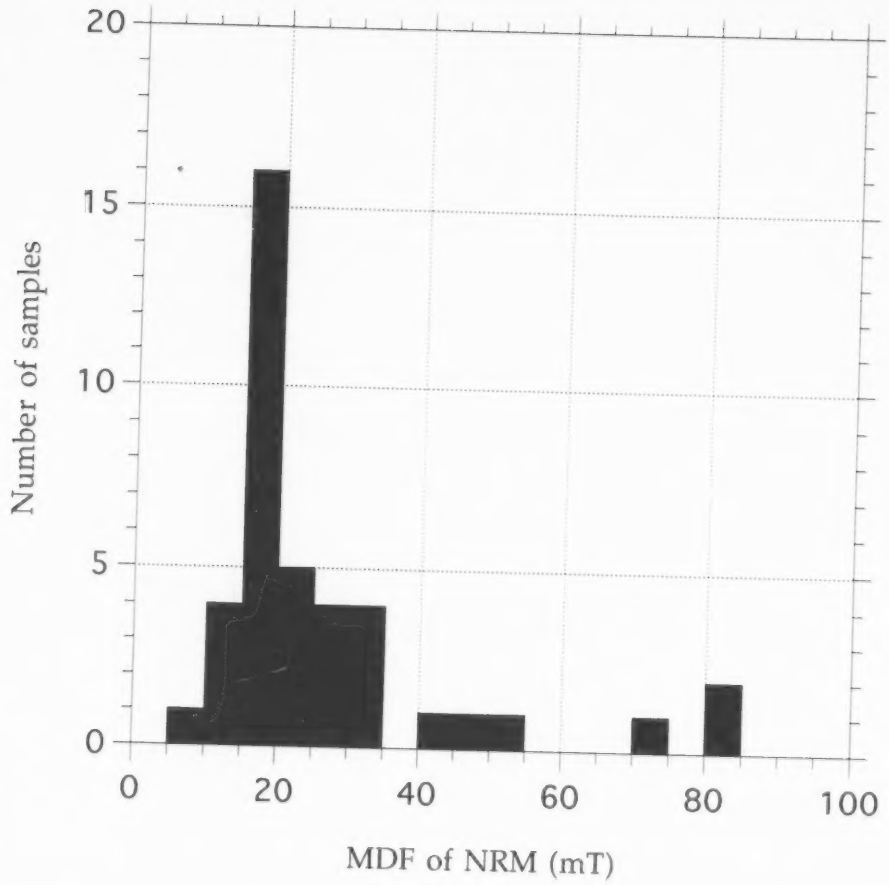

FIgure 4.2.5 Histogram of MDF of NRM for 40 samples

Chapter 5 Summary and Conclusions

Remanent magnetisation has proved useful in extending knowledge of geomagnetic secular variation back beyond historical observatory records (Aitken, 1974). One major source of such data is archaeological material. In contrast to geological materials, however, archaeological materials have never been systematically surveyed in terms of the magnetic minerals which they contain. In this project, I have investigated archaeomagnetic samples from Greece, Italy, China and North Africa in order to begin a systematic survey.

Thermal demagnetisation was applied to 27 samples (22 for NRM, 5 for IRM). The results of thermal demagnetisation of NRM clearly indicate that there is basically no hematite playing a significant role in these samples and the dominant magnetic mineral appears to be magnetite (Fe_3O_4). A similar conclusion follows from the results of thermal demagnetisation of saturation IRM. The results of three samples suggest that hematite may play a small role. However, this fraction is always less than 2 %.

The IRM acquisition method is an effective means of distinguishing those minerals with different magnetic coercivities. The IRM results from 33 of 36 samples suggest that the dominant magnetic mineral in these samples is magnetite and/or titanomagnetite. The results of the remaining three samples

indicate that there is *some* hematite present, but it clearly does not dominate the overall magnetisation. Backfield demagnetisation leads to the same conclusion.

The results of AF demagnetisation of IRM (10 samples), ARM (20 samples), and NRM (40 samples), all suggest that the main magnetic mineral contained in the samples is magnetite and/or titanomagnetite. Dankers (1981) found an interesting empirical relationship that appears to hold for dispersed magnetite, titanomagnetite, and hematite. The relationship is:

$$H'_{cr} + H_{(1/2)I} \approx 2\, H_{cr}$$

where H'_{cr} is the median remanent acquisition coercivity (see Figure 2.3), $H_{(1/2)I}$ is the median destructive field (MDF) obtained from AF demagnetisation of the saturation IRM (see Figure 2.1), and H_{cr} is the coercivity of remanence (see Figure 1.4).

In the present project there are 9 samples which can be used to check the results of Dankers. All the related values are listed in Table 5.1, and represented graphically in Figure 5.1. We see that the plot confirms Dankers' formula. At the same time, it indicates that the experimental results reported in this thesis are reliable.

Table 5.1 $H_{(1/2)I}$, H'_{cr} and Hcr values for 9 samples

Sample	$H_{(1/2)I}$	H'cr	Hcr	Sample	$H_{(1/2)I}$	H'cr	Hcr
AG19A	10	21	14	MT02	11	26	19
CA02	22	48	35	TM04	12	29	21
DE17	10	20	14	SY18	7	16	9
GO04	10	19	14	VE04A2	12	21	17
KE02	13	30	21				

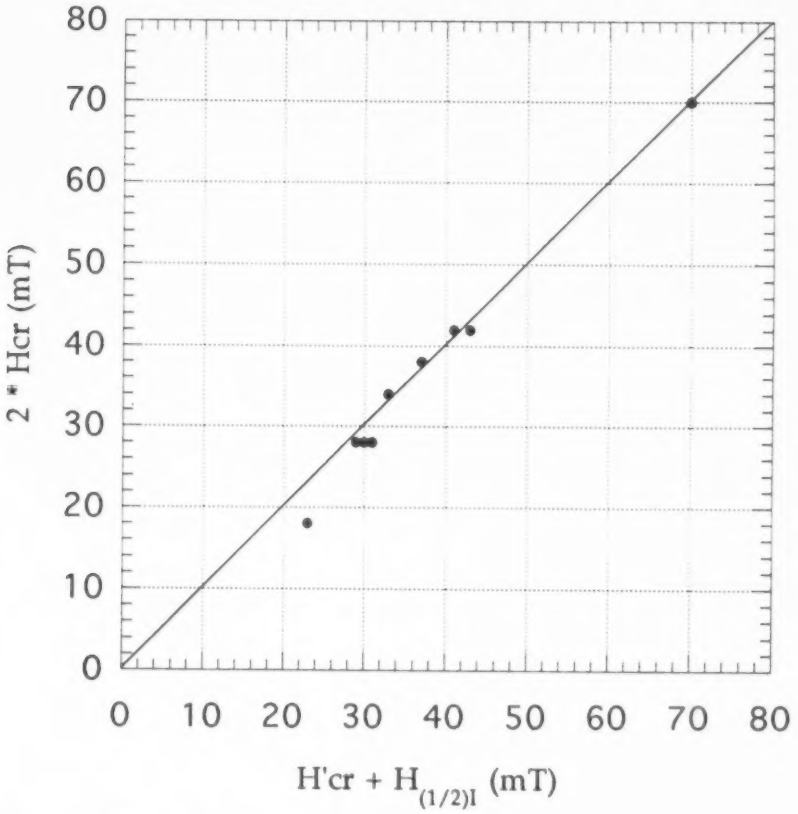

*Figure 5.1 $H_{(1/2)I}$ + H'cr vs 2*Hcr for 9 samples*

I have investigated the magnetic minerals contained in 68 archaeomagnetic samples using several different techniques. The conclusions drawn from the different methods is essentially the same; the dominant magnetic mineral contained in most samples is magnetite and/or titanomagnetite. Only a few samples show evidence of small amounts (in the order of a few per cent) of hematite.

BIBLIOGRAPHY

Aitken M. J., 1974. Physics and archaeology, second edition, pp. 291, Clarendon press.

Butler R. F., 1982. Magnetic mineralogy of continental deposits, San Juan Basin, New Mexico, and Clark's Fork Basin, Wyoming, Journal of Geophysical Research, **87**, 7843-7852.

Collinson D.W., 1983. Methods in rock magnetism and palaeomagnetism: techniques and instrumentation, pp.503, Chapman and Hall.

Dankers P., 1981. Relationship between median destructive field and remanent coercive forces for dispersed natural magnetite, titanomagnetite and hematite, Geophys. J. R. astr. Soc. **64**, 447-461.

Day R., Fuller M. D. and Schmidt V. A., 1976. Magnetic hysteresis properties of synthetic titanomagnetites, Journal of Geophysical Research, **81**, 873-880.

Dunlop D. J., 1972. Magnetic mineralogy of unheated and heated red sediments by coercivity spectrum analysis, Geophys. J. R. astr. Soc. **27**, 37-55.

Dunlop D. J., Xu S., Özdemir Ö., AlMawalwi D. and Moskovits M., 1993. Magnetic properties of arrays of oriented iron particles as a function of particle size, shape and spacing, Physics of the Earth and Planetary interiors, 76, 113-121.

Evans M. E. and Mareschal M., 1988. Secular variation and dating of fired structures in Greece, Proceedings of the 26th International Archaeometry Symposium, 75-79.

Evans M. E. and Mareschal M., 1989. Secular variation and dating of fired structures in southern Italy, Proceedings of the 25th International Archaeometry Symposium, 59-68.

Hunt C. P., 1991. Handbook, Environmental Magnetism Workshop, pp.240, University of Minnesota.

Irving E., 1964. Paleomagnetism and its application to geological and geophysical problems, pp. 399, John Wiley & Sons.

Johnson H. P., Lowrie W. and Kent D.V., 1975. Stability of anhysteretic remanent magnetization in fine and coarse magnetite and maghemite particles, Geophys. J. R. astr. Soc., **41**, 1-10.

Levi S. and Merrill R.T., 1976. A comparison of ARM and TRM in magnetite, Earth and Planetary Science Letters, **32**, 171-184

Lowrie W., 1990. Identification of ferromagnetic minerals in rock by coercivity and unblocking temperature properties, Geophysical Research Letters, **17**, 159-162.

Lowrie W. and Fuller M., 1971. On the alternating demagnetization characteristics of Multidomain thermoremanent magnetization in magnetite, Journal of Geophysical Research, **76**, 6339-6348.

Maher B. A., 1988. Magnetic properties of some synthetic sub-micron magnetite, Geophysical Journal, **94**, 83-96.

Maillol J. -M., 1992. A paleo-geomagnetic investigation of the Permo-Carboniferous Superchron, Ph. D. thesis, pp. 202, University of Alberta.

Malin S., 1987. Historical Introduction to Geomagnetism, 1-49, in Geomagnetism Vol.1, Ed: J.A.Jacobs, Academic Press.

McElhinny M. W., 1973. Palaeomagnetism and Plate Tectonics, pp. 358, Cambridge University Press.

Needham J., 1962. Science and Civilization in China, **4**, Cambridge University Press.

Néel L. 1955. Some theoretical aspects of rock magnetism, Adv. Phys., **4**, 191-243.

O'Reilly W., 1984. Rock and mineral magnetism, pp. 220, Blackie & Son.

Tarling D.H., 1983. Palaeomagnetism: principles and applications in geology, geophysics, archaeology. pp. 379, Chapman and Hall.

Thellier E., 1981. Sur la direction du champ magnétique terrestre, en France, durant les deux derniers millenaires, Physics of the Earth and Planetary Interiors, **24**, 89-132.

Verosub K. L., and Roberts A. P., 1995. Environmental magnetism: Past, present, and future, Journal of Geophysical Research, **100,** 2175-2192.

Walton D., 1990. Changes in the intensity of the geomagnetic field, Geophysical Research Letters, 17 2085-2088.

APPENDIX A

This Appendix lists all the data obtained from the experiments carried out on each individual sample.

Experiment 1 = Alternating field demagnetisation of natural remanent magnetisation;

Experiment 2 = Alternating field demagnetisation of anhysteretic remanent magnetisation;

Experiment 3 = Isothermal remanent magnetisation acquisition;

Experiment 4 = Back field;

Experiment 5 = Alternating field demagnetisation of isothermal remanent magnetisation;

Experiment 6 = Thermal demagnetisation of isothermal remanent magnetisation;

Experiment 7 = Thermal demagnetisation of natural remanent magnetisation.

The columns contain the following data:-

Column 1 -= Temperature (°C) or applied field (mT)

Column 2 -= magnetic moment (mAm^2)

Column 3 -= declination (degrees)

Column 4 -= inclination (degrees)

Column 5 -= theta (degrees) (see chapter 2)

Note: The columns continue downwards from page to page (e.g. DE17 at bottom of page 75 continues onto top of page 76. The same true in the right-hand column e.g. KC12).

Experiment 1 (p75 - 80)

AG19A

1	2	3	4	5
0	0.0219	202	55	5.5
10	0.0205	196	57	9.9
20	0.0193	194	64	9.1
30	0.0129	198	63	9.2
40	0.0108	197	63	6.2
60	0.0093	203	56	11.5
80	0.0086	198	62	5.6
100	0.0078	200	61	6.3
140	0.0072	198	63	6.1
180	0.0068	194	62	5.7

CO04B

1	2	3	4	5
0	0.0123	34	55	8
10	0.011	35	57	6
20	0.0086	34	56	7.9
30	0.0067	34	57	8.3
40	0.0054	33	55	12.6
60	0.0035	30	54	11.1
100	0.0019	36	58	12.8
140	0.0014	32	58	13
180	0.0012	33	58	14

CR08

1	2	3	4	5
0	0.028	66	51	8.1
10	0.0159	67	50	9.1
20	0.0053	67	53	11.1
30	0.0027	58	47	10.3
40	0.0023	56	44	8.9
60	0.0012	57	41	6.6
100	0.0012	59	46	6.8
140	0.0012	69	45	13.7
180	0.0011	57	35	28.1

DE17

1	2	3	4	5
0	0.0016	327	64	2.2
10	0.0016	323	62	3.8
20	0.0015	321	64	6.9
30	0.0014	305	68	9.4
40	0.0011	296	67	3
60	0.0009	293	73	12.5

AV03

1	2	3	4	5
0	0.0796	4	58	3.7
5	0.0786	5	58	3.7
8	0.0753	4	58	3.6
10	0.0699	5	58	3.4
15	0.0476	4	58	4.1
20	0.0372	4	58	4.2
25	0.0287	6	58	2.7
30	0.0244	-2	58	7.6
40	0.018	2	56	9.3
50	0.0133	6	56	6.4
60	0.0117	7	59	2.9
80	0.0099	8	62	6.5
100	0.0085	6	65	10.6
120	0.0083	3	63	7.8
150	0.008	6	62	7.9
180	0.0074	8	65	9.2

AV04

1	2	3	4	5
0	0.0105	27	61	15.8
5	0.0103	29	61	12.7
8	0.0098	30	56	17.5
10	0.0089	30	55	16.9
15	0.0059	29	58	12.9
20	0.0049	30	60	14.4
25	0.0039	30	59	13.5
30	0.0032	31	59	14.5
40	0.0025	28	58	14.9
50	0.0019	29	59	14.1
60	0.0015	26	61	17.9
80	0.0012	35	59	16.6
100	0.001	31	55	15.6
120	0.0009	31	57	14.7
150	0.0009	36	58	12.5
180	0.0008	25	55	17.6

KC12

1	2	3	4	5
0	0.0641	144	71	4.2
10	0.0457	147	72	3.7
20	0.0221	144	69	3.8
70	0.0056	142	69	3.7
100	0.0049	139	67	3.8

100	0.0008	289	66	5.4
140	0.0007	280	61	7.1
180	0.0006	281	65	3.6

PK06

1	2	3	4	5
0	0.3446	66	-11	11
10	0.2727	62	-9	12
20	0.1137	63	-8	11
30	0.0586	65	-8	10
40	0.0385	62	-10	11.1
60	0.0273	62	-8	15.8
100	0.0244	64	-7	19.7
140	0.0236	65	-7	15.8
180	0.0204	68	-13	20.9

SY18

1	2	3	4	5
0	0.019	77	77	2.1
10	0.0118	78	75	2.2
20	0.0055	91	76	2.2
30	0.004	84	77	2.2
40	0.0035	67	77	2.9
60	0.003	92	76	4.1
80	0.0029	91	75	2.9
100	0.0026	92	75	3.6
140	0.0025	92	76	3.4
180	0.0023	89	75	4

MO02

1	2	3	4	5
0	0.0016	9	60	4.1
3	0.0016	11	59	5.8
5	0.0015	6	60	3.5
10	0.0012	7	58	4.2
15	0.001	5	59	7
20	0.0009	14	54	8.8
25	0.0009	9	57	6.4
30	0.0008	7	60	6.6
40	0.0008	7	58	4.5
50	0.0007	8	59	4.2
60	0.0007	8	59	3.6
100	0.0006	7	62	12.1
120	0.0006	6	63	11.7
150	0.0005	7	60	4
180	0.0005	6	58	3.8
140	0.0045	141	70	3.7
180	0.0044	140	74	3.8

PE02

1	2	3	4	5
0	0.0043	351	68	4.9
8	0.0041	357	66	4.7
10	0.0038	356	66	4.3
13	0.0034	358	66	3.8
15	0.003	355	66	3.4
18	0.0027	355	66	3.1
20	0.0025	356	66	2.9
22	0.0023	355	65	2.6
25	0.0021	358	63	2.4
27	0.0019	356	66	2.2
30	0.0017	357	64	2
32	0.0016	351	69	1.9
35	0.0015	352	65	1.7
37	0.0013	357	67	1.5
40	0.0012	352	67	1.4
40	0.0012	355	65	1.4
45	0.0011	352	65	1.2
50	0.0009	356	66	1.1
60	0.0008	360	61	0.9
80	0.0006	354	65	0.7
100	0.0005	358	64	0.6

MO05

1	2	3	4	5
0	0.0181	97	65	13.1
8	0.0169	97	67	16.4
10	0.0125	95	62	20.1
15	0.0107	99	68	11.6
20	0.0083	99	67	15.3
30	0.0056	98	65	8
40	0.0047	99	65	7.1
50	0.0042	96	65	9.3
60	0.004	97	65	8.7
80	0.0038	98	65	8.5
100	0.0037	99	65	8.3
120	0.0037	100	63	7
180	0.0036	95	64	8.5

TH05

1	2	3	4	5
0	0.0041	30	45	7.5
5	0.0041	28	45	6.5

TH04

1	2	3	4	5
0	0.0044	8	64	3.6
5	0.0043	8	64	4.2
8	0.0039	10	65	3.4
10	0.0034	10	64	3.1
15	0.0026	9	65	3.3
20	0.0023	10	65	3
25	0.0021	9	65	4.8
30	0.0019	8	66	5.1
40	0.0015	11	66	4.9
50	0.0014	11	66	5.2
60	0.0012	20	64	9.8
80	0.0012	13	67	7.4
100	0.0011	9	67	7.5
120	0.0011	16	67	12.1
150	0.001	10	67	6.6
180	0.001	12	67	8.9

CA02

1	2	3	4	5
0	0.0484	64	31	2.2
10	0.0421	62	30	3.6
20	0.0302	62	30	4.8
30	0.0236	63	30	4
40	0.0188	62	30	2.1
60	0.0103	65	31	5.7
80	0.0064	64	30	6.6
100	0.0042	64	30	7.8
140	0.0023	63	31	8.8
180	0.0016	62	35	8.6

IN08

1	2	3	4	5
0	0.0631	41	51	3.3
10	0.0374	39	54	3.6
20	0.0115	38	52	4.8
30	0.006	44	51	5.7
40	0.0042	40	51	4.5
60	0.0025	73.3	53.8	4
80	0.0017	38.5	45.4	5.3
100	0.0014	37.2	45.3	6.1
120	0.0013	30	49.3	5.3
150	0.001	39	41	6.2
180	0.0001	27.3	53.5	5.7
8	0.004	30	45	6.5
10	0.0038	29	45	6.6
15	0.0032	30	45	7
20	0.0029	30	46	7.6
25	0.0023	32	47	9.2
30	0.0021	33	44	8.8
40	0.0014	29	42	10
50	0.0012	34	48	10.3
60	0.0008	30	47	13.3
80	0.0005	22	45	14
100	0.0003	34	42	10.6
120	0.0002	14	37	13.5
150	0.0002	23	55	32.2
180	0.0001	18	39	7

AP08A

1	2	3	4	5
0	0.0075	198	61	4.5
10	0.0032	185	60	2.8
20	0.0011	188	62	3.6
30	0.0006	190	59	3.8
40	0.0005	194	54	4.4
60	0.0004	200	60	3.8
100	0.0003	194	61	4.5
140	0.0003	193	62	11.9
180	0.0002	183	52	20.1

IN05

1	2	3	4	5
0	0.0619	77	50	5.1
10	0.0474	75	51	6.2
20	0.0292	74	49	6.3
30	0.0198	76	51	4.5
40	0.0155	77	53	4.2
61	0.0092	76	50	5.6
80	0.0081	74	53	7.4
100	0.0076	74	51	7.5
120	0.0072	74	49	7.6
150	0.0067	80	51	6.6
180	0.0064	77	51	7.7

KE02

1	2	3	4	5
0	0.0883			
5	0.0856			
10	0.0719			
15	0.048			

TM04

1	2	3	4	5
0	0.0904			
10	0.0661			
20	0.0298			
30	0.016			
40	0.0125			
60	0.0086	42	67	3.9
80	0.0071	29	62	2.7
100	0.0062	32	64	3
140	0.0053	32	62	3
180	0.0047	30	63	3.1

MT02

1	2	3	4	5
0	0.027			
20	0.0068			
30	0.0031			
40	0.0023			
61	0.0021	101	11	
80	0.0018	106	13	
80	0.0018	108	13	
100	0.0017	106	10	
140	0.0014	106	11	
180	0.0013	109	9	

GR02

1	2	3	4	5
0	0.0206			
10	0.0196			
20	0.0148			
30	0.0106			
40	0.0076			
60	0.004	81.9	53.1	3.8
100	0.0018	80	56.6	4.3
140	0.0011	78.8	50.6	2.2
180	0.0008	91	48.1	6.1

SE04

1	2	3	4	5
0	0.0807			
10	0.0641			
20	0.0345			
30	0.0242			
40	0.0186	106	36	6.1
60	0.0134	98	33	6.6
100	0.0112	100	32	10
20	0.0343			
30	0.0207			
40	0.0151			
60	0.01			
80	0.0083			
100	0.0067			
140	0.0063			
180	0.0061			

PP01C1

1	2	3	4	5
3	0.0106			
5	0.0103			
8	0.0096			
10	0.0087			
15	0.0066			
20	0.0052			
30	0.0038			
40	0.003			
60	0.0021			
80	0.0016			
100	0.0012			
140	0.0011			
180	0.0008			

VE04A2

1	2	3	4	5
0	0.0523	45	56	6.2
10	0.0402	57	17	3.3
20	0.0199	59	7	4.1
40	0.0112	58	17	2.5
60	0.0089	61	13	4.4
80	0.0084	61	17	7.6
100	0.008	60	15	7.1
140	0.0075	59	16	6.1
180	0.0074	61	16	8.9

ST09

1	2	3	4	5
0	0.0184	7	-24	5.3
10	0.0164	5	-27	5.6
20	0.0097	5	-24	2.9
30	0.0054	5	-23	2.8
40	0.0036	8	-23	5.6
60	0.0018	5	-25	3.6
80	0.0011	5	-24	8.4

140	0.0103	99	32	9.8
180	0.0096	97	31	9.9

ST16

1	2	3	4	5
0	0.0667	335	-17	3.8
10	0.0667	335	-17	3.9
20	0.0656	335	-17	3.7
30	0.0636	335	-17	3.8
40	0.0599	336	-17	3.5
60	0.0492	336	-17	3.8
80	0.0355	336	-18	2.9
100	0.0242	336	-17	4.7
140	0.0117	334	-18	5.6
180	0.0065	335	-15	6.1

ST05

1	2	3	4	5
0	0.0306	340	-3	2.9
10	0.0302	340	-3	2.5
30	0.0256	340	-4	3.1
40	0.0215	340	-4	3
60	0.0134	342	-4	6.9
80	0.0056	341	-3	4
140	0.0011	334	-4	9.1
180	0.0006	329	-7	4.7

ST24

1	2	3	4	5
0	0.0045	80	-75	4.6
20	0.004	83	-74	4.1
30	0.0034	82	-75	3.6
40	0.0028	77	-75	4.9
60	0.0016	87	-76	5.2
80	0.0006	90	-75	5
100	0.0003	90	-71	4
140	8E-05	45	-62	10.8
180	3E-05	37	-23	13.6

BA20

1	2	3	4	5
0	0.063	154	48	1.2
10	0.0477	151	48	1.3
20	0.022	147	49	3.5
30	0.0133	145	46	5.7
40	0.0094	155	47	2.3
60	0.0078	154	45	2
100	0.0009	4	-28	6.3
140	0.0006	7	-30	6.6
180	0.0006	13	-25	7.3

ST15

1	2	3	4	5
0	0.0064	66	-66	2.5
10	0.0056	65	-66	2.8
20	0.0035	60	-67	3.1
30	0.0026	63	-67	4.5
40	0.002	67	-68	3.4
60	0.0012	60	-67	3.8
80	0.0008	61	-74	9.2
100	0.0005	57	-73	3.8
140	0.0004	62	-80	4.3
180	0.0003	68	-87	5

ST11

1	2	3	4	5
0	0.0014	164	23	6.6
10	0.0013	168	22	13.6
30	0.0012	164	22	7.9
40	0.0011	164	22	8.1
60	0.001	166	19	9.2
80	0.0006	164	22	8
100	0.0004	166	21	8.3
140	0.0002	167	23	12.4
180	9E-05	188	35	18.5

BA19

1	2	3	4	5
0	0.0341	50	58	6.1
20	0.0177	51	59	5.1
30	0.0106	46	60	7.4
40	0.0082	53	58	4
60	0.0063	48	55	3.7
80	0.0052	47	58	4.7
100	0.0046	46	57	4.6
140	0.0041	50	56	4.9
180	0.0037	53	57	5.5

CT35

1	2	3	4	5
0	0.007	302	19	6.1
10	0.0064	301	19	6
20	0.0037	301	19	5.2
30	0.0021	302	21	6.9

80	0.0069	156	47	3
140	0.0057	156	47	3
180	0.0053	159	45	2.6

SA17

1	2	3	4	5
0	0.0482	280	48	2.1
10	0.0312	278	48	2.4
20	0.0204	278	50	5.4
30	0.016	276	51	3.3
40	0.0128	270	49	3.6
60	0.008	270	49	8.9
80	0.0066	279	50	4.2
100	0.0058	269	46	5.5
140	0.0045	273	41	6.3
180	0.0038	293	52	8.8

TS04

1	2	3	4	5
0	0.0075	39	62	3
10	0.0073	39	50	4.6
30	0.0035	25	45	3.1
40	0.0025	18	36	4.8
60	0.0016	8	35	4.3
80	0.0015	10	29	5.9
100	0.0016	9	26	4.4
140	0.0016	8	25	9.5
180	0.0014	3	25	9.3

TI08

1	2	3	4	5
0	0.0216	243	64	7.1
10	0.0145	244	63	3.7
20	0.0079	244	64	3.2
30	0.0054	248	66	4.2
40	0.0044	250	67	3.9
60	0.0037	244	68	4.8
80	0.0033	250	70	6
100	0.0031	243	71	4.6
140	0.0028	258	69	8.7
180	0.0029	247	71	7.9
40	0.0013	301	19	5.2
60	0.0008	304	24	9.1
80	0.0006	300	20	6.2
100	0.0006	299	20	4.9
140	0.0005	298	19	4.7
180	0.0005	300	17	4.7

SA18

1	2	3	4	5
0	0.008	4	42	6.4
10	0.0061	3	42	5.9
20	0.0023	1	40	6.3
30	0.0013	358	40	5.6
40	0.0011	360	37	6.9
60	0.0008	356	37	7
80	0.0007	0	39	8.3
100	0.0007	2	38	4.6
140	0.0006	358	33	5.8
180	0.0006	358	36	6.3

TS05

1	2	3	4	5
0	0.0079	345	43	2.6
10	0.0072	354	46	2.3
30	0.0042	356	43	1.5
40	0.0027	347	46	2.4
60	0.0017	358	43	10
80	0.001	24	45	3.4
100	0.0009	32	47	4.2
140	0.0008	337	48	3.5
180	0.001	45	55	10

TI16

1	2	3	4	5
0	0.0207	339	50	4.4
10	0.0155	327	50	4.4
20	0.007	315	45	6.7
30	0.004	317	45	6.1
40	0.0028	318	49	6.5
60	0.0019	325	45	7.7
100	0.0013	321	44	9.1

Experiment 2 (p81 - 83)

AG19A

1	2	3	4	5
0	0.0327	149	7	6.8
10	0.0194	154	13	5.3
20	0.0087	172	43	5.9
30	0.0072	186	56	6.5
40	0.0076	190	62	6.2
60	0.0069	197	62	6.2
80	0.0069	202	63	6.5
100	0.0064	193	62	6.1
140	0.0063	195	62	6.3
180	0.0063	199	63	6.6

GO04

1	2	3	4	5
0	0.0677	145	1.3	2.6
5	0.056	144.4	0.8	3.8
10	0.0404	143.6	2.2	5.3
15	0.0252	139.9	3.8	7.4
20	0.0177	137.2	4.2	8.1
25	0.0129	135.2	6.4	10.3
30	0.0104	132.1	17	8.4
40	0.0065	125.1	17.3	8.7
50	0.0039	123	10.9	9.6

MO05

1	2	3	4	5
0	0.0116	340	17	13
10	0.0079	336	25	7.3
20	0.0051	344	41	7.4
30	0.0042	353	52	6.4
40	0.0039	0	59	6
50	0.0039	7	64	6.6
60	0.0035	14	66	8.4

CA02

1	2	3	4	5
0	0.0181	142	4	5.1
5	0.0161	141	0	5.8
10	0.0136	142	3	4.7
15	0.0095	136	5	4.9
20	0.0079	135	2	4.8
25	0.0067	132	3	4.5
30	0.0056	130	4	5.4

AV03

1	2	3	4	5
0	0.0294	319	6	1.5
10	0.0244	318	7	3.3
20	0.0143	302	17	7.1
30	0.0105	295	30	5.8
40	0.0084	287	30	3
50	0.0082	280	33	8.8
60	0.0075	276	37	2.8
70	0.0073	272	39	3
80	0.0073	271	37	2.2

DE17

1	2	3	4	5
0	0.0035	151	6	6.5
10	0.002	153	10	8.6
20	0.0007	169	54	5.2
30	0.0006	230	75	4.5
40	0.0007	275	76	4.4
60	0.0006	288	72	7
80	0.0006	283	67	7.2
100	0.0006	277	62	3.3

SY18

1	2	3	4	5
0	0.0108	144.6	8.4	6.3
5	0.0083	143.6	11.3	5.6
10	0.0049	140.7	23	4.6
15	0.0029	132.5	47.8	3.8
20	0.0025	125.9	60	4.6
25	0.0024	118.8	69.1	4.2
30	0.0024	105.7	71.8	4.2
35	0.0024	98.4	73.9	5.9
40	0.0024	93.9	75.1	4.5
50	0.0023	89.6	76.1	4.7
60	0.0024	85.9	75.6	5

IN08

1	2	3	4	5
0	0.0231	327	11	6.2
10	0.0138	327	16	8.1
20	0.0057	325	48	8.5
30	0.0047	329	68	10.4
40	0.0044	319	78	8.5

35	0.005	127	4	5.1
40	0.0043	125	12	5.4
60	0.0023	113	3	6

KE02

1	2	3	4	5
0	0.0073	144	-9	5.9
5	0.0067	144	-10	5.3
10	0.0053	143	-11	4.4
15	0.0032	139	-25	5.4
20	0.0023	137	-37	5.3
25	0.0016	129	-53	8.6
30	0.0016	118	-70	9.6
40	0.0014	23	-79	9.6
50	0.0016	353	-70	8.7
60	0.0016	343	-65	8.7

MT02

1	2	3	4	5
0	0.0094	143	0	3.7
5	0.0081	142	1	3.6
10	0.0057	139	1	3.6
15	0.0034	136	1	4.2
20	0.0028	127	3	3.5
25	0.0025	125	5	4.6
30	0.002	121	7	3.1
35	0.0018	124	14	3.2
40	0.0017	117	7	6.6
60	0.0015	113	12	9.1

GR04

1	2	3	4	5
0	0.0034	318	13	5
10	0.003	317	12	6.2
20	0.0028	316	15	6.8
30	0.0022	308	19	6.1
40	0.0017	304	25	7.4
50	0.0013	300	33	7.6
60	0.0011	295	40	6.3
70	0.001	300	47	6.1
80	0.001	292	45	6.1
100	0.0009	287	35	4.8
120	0.0009	292	33	6.3
140	0.0008	289	33	6.8
180	0.0004	283	36	12.1

50	0.0044	312	83	8.4
60	0.0044	343	83	9.5

TM04

1	2	3	4	5
0	0.0228	145	7	4.2
5	0.0198	142	7	2.6
10	0.0153	142	11	6.6
15	0.0087	134	29	2.6
20	0.0066	125	40	3.6
25	0.0055	109	55	3.8
30	0.0054	86	67	4.1
40	0.0054	44	69	3.6
50	0.0046	30	67	3.5
60	0.0042	29	66	4.3

PP01C1

1	2	3	4	5
0	0.0206	149	-2	5.1
5	0.0194	150	-2	5
10	0.0161	152	-4	6.7
15	0.011	153	-2	9.7
20	0.0102	158	-2	7.2
25	0.0079	158	-2	5.4
30	0.0067	160	-2	6.1
40	0.0052	164	-4	5.7
50	0.0044	168	-4	5.2
60	0.0037	172	-2	4.6

VE04A2

1	2	3	4	5
0	0.0214	131	1	7.1
5	0.0186	131	2	4.8
10	0.0156	119	6	7.5
15	0.0099	105	9	5.6
20	0.0096	95	11	6.1
25	0.0082	84	13	5.4
30	0.0087	74	13	14.5
40	0.0084	66	14	14.1
50	0.0076	63	16	5.1
60	0.0075	62	17	4.2

ST09

1	2	3	4	5
0	0.0133	328	-3	2.3
10	0.011	329	-3	2.5

ST11

1	2	3	4	5
0	0.0005	323	1	7.9
10	0.0004	321	3	5.9
20	0.0003	320	4	6
30	0.0002	318	8	6.6
40	0.0002	314	10	5
60	7E-05	295	30	5.9
80	6E-05	225	49	10.8
100	6E-05	187	38	6.4
140	6E-05	172	29	5.8
180	6E-05	151	31	7.2

ST15

1	2	3	4	5
0	0.0073	327	0	4
10	0.0061	326	-1	4.1
20	0.0037	326	-2	4.3
30	0.0021	325	-3	5.7
40	0.0014	325	-6	6.6
60	0.0006	331	-18	5.1
80	0.0003	341	-42	4.3
100	0.0002	348	-56	4.4
140	0.0002	117	-68	6.4
180	0.0002	24	-60	4.2

ST24

1	2	3	4	5
0	0.0052	324	0	4.9
10	0.0045	324	0	5.8
20	0.0033	323	0	6
30	0.0024	321	1	6.8
40	0.0018	322	-1	7.8
60	0.0006	312	-3	10.2
80	0.0002	325	-13	9.1
100	6E-05	20	-30	11.2
140	7E-05	111	-51	10.8
180	6E-05	72	-35	8.7
20	0.0063	330	-3	2.2
30	0.0031	332	-6	2.9
40	0.0019	333	-8	4.6
60	0.0009	349	-19	7.9
80	0.0005	360	-20	9.5
100	0.0004	8	-40	13.7
140	0.0005	16	-34	8.6
180	0.0004	9	-25	7.9

ST16

1	2	3	4	5
0	0.0172	314	-4	6.1
10	0.0167	314	-4	5.6
20	0.0159	314	-5	6.9
40	0.0126	312	-6	6.5
60	0.0101	319	-8	5.4
80	0.0086	323	-10	7.3
100	0.0069	331	-13	4.6
140	0.0063	334	-13	4.3
180	0.0064	338	-15	3.4

ST05

1	2	3	4	5
0	0.0137	327	-2	2.3
10	0.0132	325	-1	5.7
20	0.0111	327	-1	3.2
30	0.0089	326	-1	2.8
40	0.0067	326	-1	3.6
60	0.0029	325	-1	7
80	0.0012	333	-5	9.1
100	0.0009	332	-7	11.7
140	0.0005	346	2	5.3
180	0.0006	321	-2	15.1

Experiment 3 (p84 - 90)

AG19a

1	2	3	4	5
0	0.003	192	62	10.4
18	0.159	286	86	6.4
32	0.277	299	89	8
54	0.34	228	89	5.8
83	0.346	223	88	6.1
121	0.352	242	89	6.2
180	0.357	252	88	6.3
400	0.358	186	90	5.8
643	0.366	284	89	5.8
850	0.367	244	88	5.7
1101	0.37	152	90	6.8
1314	0.371	260	88	5.7

CO04B

1	2	3	4	5
0	0.0004	28	73	17.3
19	0.0218	220	87	4.3
37	0.0478	258	87	3.6
58	0.0714	201	88	3
78	0.085	184	89	3.1
114	0.0965	150	89	2.9
153	0.103	172	89	2.7
280	0.121	130	90	12.8
382	0.122	108	90	7.5
599	0.124	145	87	8.5
750	0.131	91	89	13.8
1020	0.134	97	89	6.6

CR08

1	2	3	4	5
0	0.0011	39	72	13.9
18	0.113	86	88	21
31	0.125	141	86	12.3
64	0.152	208	89	7.9
95	0.156	112	89	11.3
131	0.158	111	87	8.6
191	0.16	148	89	8.8
391	0.162	125	84	10.2
650	0.162	129	89	10.8
800	0.163	104	87	8.8
1011	0.163	72	88	9

DE17

1	2	3	4	5
0	0	275	68	3.9
18	0.02	239	86	1.3
32	0.037	224	85	2.3
59	0.047	218	90	1.3
87	0.05	242	89	1.2
131	0.053	220	87	1.3
181	0.053	196	86	1.3
270	0.054	252	88	1.1
401	0.055	231	87	1.2
600	0.055	216	85	0.9
807	0.055	227	88	1.1
1061	0.055	182	88	1.2
1300	0.056	184	88	1.3

GO04

1	2	3	4	5
0	0.002	107	19	9.7
18	0.277	222	85	4.2
35	0.42	210	85	3.2
55	0.494	183	88	3.5
99	0.528	220	86	3.4
152	0.532	165	88	3.5
251	0.539	200	90	3.8
400	0.54	160	86	4.6
608	0.542	184	88	3.8
906	0.544	159	88	3.6
1400	0.546	170	89	3.8

KC12

1	2	3	4	5
0	0.0038	137	80	5.8
19	0.161	15	88	4.6
34	0.293	37	88	4.8
77	0.402	59	88	4.6
111	0.414	56	88	4.3
150	0.425	29	89	4.3
210	0.429	48	88	4.3
300	0.433	60	88	4.2
500	0.438	57	88	4.1
700	0.444	63	88	4.2
977	0.446	57	88	4.2

KN05

1	2	3	4	5
0	1E-05	328	68	44.1
21	8E-05	149	88	7.4
42	0.0002	167	88	8.5
80	0.0002	130	88	9.6
123	0.0003	92	89	11
161	0.0004	102	88	11.3
200	0.0004	131	89	12.6
250	0.0004	134	89	11.6
400	0.0004	116	88	13.4
500	0.0004	117	88	13.8
600	0.0004	158	88	13.6
750	0.0004	105	88	14
900	0.0005	110	89	14.2
1111	0.0005	119	88	14.2
1433	0.0005	111	88	14.2

SY18

1	2	3	4	5
0	0.003	140	69	4.2
18	0.141	92	89	3.9
31	0.221	107	87	3
55	0.253	133	88	3.7
91	0.269	120	89	4.4
156	0.273	358	89	4.3
251	0.276	109	89	4.1
351	0.277	114	88	4.3
600	0.277	106	88	4.5
900	0.278	108	87	4.2
1397	0.281	25	88	3.5

BI07

1	2	3	4	5
0	0.0001	282	-63	10.8
22	0.0145	189	88	5.9
40	0.0157	216	87	2.6
80	0.0165	152	88	1.9
122	0.017	159	88	1.3
161	0.0172	206	87	1.6
220	0.0175	183	88	1.4
270	0.0176	257	89	1
340	0.0179	181	86	1.6
423	0.0179	147	88	1.3
550	0.0181	247	90	1.4
700	0.0182	238	87	1.4
900	0.0184	178	88	1.4
1293	0.451	22	89	4.1

PK06

1	2	3	4	5
0	0.0049	73	-27	8.3
29	0.487	249	83	2.9
41	0.61	262	85	1.8
66	0.717	252	83	1.5
88	0.733	247	86	1.4
139	0.747	304	89	1.7
199	0.751	245	87	1.8
303	0.756	229	83	2.1
500	0.759	194	88	1.8
750	0.769	319	88	1.6
1000	0.775	298	87	1.5
1314	0.786	201	87	2.1

AP08A

1	2	3	4	5
0	0.0002	198	53	3.9
18	0.0235	317	-89	6.4
35	0.0334	96	-88	2.1
87	0.0393	315	-88	1.6
140	0.0413	290	-88	1.6
232	0.0423	53	-88	1.5
352	0.0427	331	-89	1.3
500	0.0433	297	-87	1.4
707	0.044	7	-88	1.4
957	0.0444	292	-86	1.6
1325	0.0457	350	-89	2.2

CA02

1	2	3	4	5
0	0.001	126	2	2.1
18	0.054	307	88	1.5
36	0.124	126	88	1.6
57	0.195	184	90	1.3
90	0.281	152	87	3.1
121	0.313	139	87	3
171	0.33	139	87	1.3
229	0.341	70	89	1.5
300	0.346	121	88	1.2
431	0.349	152	89	1.2
601	0.352	108	88	1.7
851	0.354	127	88	1.5
1102	0.354	115	88	1.3

1123	0.0195	145	88	3.9

CN09

1	2	3	4	5
0	0.003	118	14	3.9
19	0.0957	146	87	2
29	0.181	190	84	3.5
40	0.251	231	86	0.7
55	0.306	265	86	2.5
69	0.345	267	87	0.7
80	0.373	260	88	4.2
93	0.378	245	89	2.2
112	0.383	242	89	1
138	0.397	162	89	1.8
161	0.397	238	88	0.8
196	0.407	202	89	2.2
270	0.403	124	88	0.8
400	0.409	206	89	0.9
550	0.414	153	89	0.7
700	0.418	229	89	0.9
880	0.422	135	90	0.6
1084	0.425	157	89	0.9
1309	0.429	229	89	0.7

KE02

1	2	3	4	5
0	0.002	20	69	9.1
19	0.097	294	84	5.1
34	0.206	181	87	4.7
60	0.27	165	86	3
89	0.299	167	87	4.8
120	0.309	181	89	2.3
184	0.316	295	89	3
281	0.317	99	90	3.6
400	0.32	174	86	2.1
865	0.322	125	88	2
1101	0.322	206	88	1.9
1384	0.322	76	89	3.5

MT02

1	2	3	4	5
0	0.001	122	7	4.7
18	0.029	126	88	1.4
31	0.049	177	85	2.3
58	0.065	239	88	1
102	0.072	223	87	1.1
1275	0.354	122	88	1.3

IN05

1	2	3	4	5
0	0.0043	83	55	3.2
21	0.166	9	82	2.5
31	0.232	316	88	5.5
43	0.294	205	87	6.1
58	0.335	320	87	2.8
78	0.37	360	89	3.3
93	0.379	271	85	6.5
112	0.389	284	87	6
136	0.397	249	88	8.4
159	0.395	289	86	9.1
184	0.4	285	86	6.2
220	0.404	262	85	6.8
250	0.409	274	84	6.6
300	0.411	258	85	5.9
400	0.418	257	85	4.7
550	0.421	275	85	4.2
751	0.422	313	84	3.2
956	0.43	251	85	1.3
1159	0.435	300	84	5.2
1341	0.443	271	86	9.6

TM04

1	2	3	4	5
0	0.002	40	70	5.4
19	0.157	254	87	4.2
35	0.273	194	86	3.4
53	0.334	199	86	4.1
91	0.366	211	87	3.7
151	0.378	86	88	4
230	0.382	163	89	4
300	0.385	185	87	3.6
401	0.394	150	88	4.7
553	0.399	176	88	5.3
700	0.4	172	87	4.4
950	0.401	78	89	5.6
1400	0.404	173	88	4

RU10B

1	2	3	4	5
0	0.0038	340	-46	4.9
20	0.322	237	79	1.2
32	0.551	214	85	4

151	0.075	195	86	1.1
237	0.076	194	87	1.1
331	0.076	216	87	1.1
503	0.078	170	86	1.6
700	0.078	150	87	1.2
700	0.078	170	88	1.2
901	0.079	151	88	1.1
1278	0.081	164	88	1.6

GR02

1	2	3	4	5
0	0.0002	90	54	14.4
17	0.0057	198	86	13.7
31	0.0237	209	89	11.4
52	0.0544	77	85	12
72	0.0761	81	87	10.2
110	0.0944	160	84	12.2
151	0.109	340	85	10.7
199	0.113	306	89	8.6
300	0.115	356	90	7.8
500	0.122	50	86	10.9
701	0.122	86	87	12.5
1006	0.122	110	88	10.5
1307	0.122	83	88	10.1

VE04A2

1	2	3	4	5
0	0.002	64	21	5.2
20	0.105	260	85	8.9
55	0.171	356	89	5.2
85	0.186	263	86	5
120	0.187	60	89	2.9
200	0.191	295	89	3.1
300	0.191	255	87	4.7
512	0.195	273	88	5.2
800	0.196	306	89	4.7
1390	0.197	280	86	3.7

ST11

1	2	3	4	5
10	0.0005	105	82	4.3
19	0.0024	59	89	3.4
35	0.0091	37	84	3.1
73	0.0248	165	89	3.2
124	0.037	63	81	4.1
175	0.043	45	83	2.8
42	0.662	225	84	1.4
58	0.745	230	85	1.4
70	0.778	183	88	1.5
90	0.802	207	86	1.6
110	0.81	209	86	1.4
150	0.814	216	88	1.6
230	0.823	206	87	1.5
400	0.855	202	86	2.2
600	0.859	201	87	1.8
849	0.895	159	87	1.7
1103	0.898	164	88	1.8
1250	0.901	198	85	1.6

SE04

1	2	3	4	5
0	0.001	108	39	5.7
19	0.0844	265	84	1.8
32	0.185	247	79	2.2
53	0.312	209	85	3.1
81	0.378	201	85	2.4
121	0.401	116	89	1.7
171	0.413	150	87	2.6
260	0.42	180	88	2.3
400	0.421	162	86	2.4
600	0.416	144	87	2.3
801	0.42	181	89	1.6
1051	0.425	164	87	1.5
1304	0.427	250	88	1.5

ST09

1	2	3	4	5
0	0.0002	9	21	7.5
8	0.0071	302	87	5.7
18	0.0374	354	86	5.4
38	0.132	62	88	3.8
52	0.193	109	85	6.9
95	0.27	55	87	3.5
162	0.311	354	87	3.5
225	0.327	314	87	3.7
299	0.331	306	88	3.1
463	0.325	292	88	3.7
704	0.327	269	86	3.4
1010	0.327	277	87	3.6
1408	0.327	278	88	3.7

ST16

270	0.0474	13	86	2.5
410	0.049	17	83	2.5
614	0.0492	30	87	2.6
815	0.0492	356	86	2.8
1419	0.0492	24	84	2.6

ST15

1	2	3	4	5
0	0.0002	9	-16	7.5
4	0.0043	295	87	2.9
10	0.0149	308	87	2
17	0.0441	41	87	2.4
32	0.131	1	87	7.1
48	0.183	196	89	2
72	0.239	294	89	1.8
110	0.299	247	88	2.4
161	0.32	329	88	1.9
233	0.332	320	89	1.9
334	0.336	273	88	1.9
531	0.339	270	87	2.2
811	0.342	283	87	2.4
1419	0.345	291	88	2.2

ST24

1	2	3	4	5
0	0.0001	45	10	6.4
7	0.004	38	83	6.4
20	0.0298	4	82	5.7
35	0.0692	13	83	4.8
73	0.155	27	85	6
131	0.241	35	81	5.3
214	0.252	31	81	4.5
369	0.261	23	80	4.3
519	0.262	40	81	5.5
800	0.262	28	81	4.2
1417	0.264	41	82	4.1

BA20

1	2	3	4	5
0	0.0024	143	45	5.7
8	0.0006	63	87	3.7
14	0.153	321	87	4.6
22	0.291	77	85	3.1
40	0.396	62	89	7
65	0.462	358	87	4.1
107	0.485	334	88	3.2

1	2	3	4	5
0	0.0022	341	-21	6
9	0.0029	342	-46	3.4
20	0.0129	343	-86	4.1
37	0.0503	57	-88	3.3
79	0.221	220	-85	3.3
130	0.463	212	-81	4.3
197	0.56	168	-86	3.2
267	0.587	228	-87	3.7
391	0.637	143	-86	3.4
583	0.646	164	-87	3.4
859	0.648	134	-86	3.5
1400	0.648	149	-87	3.2

ST05

1	2	3	4	5
0	0.0005	332	-16	6.4
74	0.498	223	88	1.6
93	0.626	160	87	1.6
152	0.772	113	86	1.7
209	0.804	110	88	1.8
300	0.822	86	86	1.8
462	0.828	199	89	2.1
646	0.829	21	88	1.7
951	0.832	235	88	2.2
1410	0.831	265	89	2.2

BA19

1	2	3	4	5
0	0.0016	57	57	7.9
6	0.0169	113	83	9
13	0.0719	143	83	2
26	0.201	131	87	0.7
43	0.306	144	83	2.7
82	0.356	155	83	5.6
133	0.397	160	84	0.8
197	0.423	148	86	3.9
284	0.425	164	84	1.5
404	0.424	158	84	1
608	0.428	151	84	0.9
850	0.432	149	84	0.9
1047	0.436	156	87	1

CT35

1	2	3	4	5
0	0.0005	295	18	4.9

190	0.492	315	88	3.2
290	0.502	304	88	2.9
413	0.498	313	88	3.3
613	0.5	296	86	3.4
1045	0.506	304	88	3.3

SA17

1	2	3	4	5
0	0.0025	287	50	8.7
8	0.042	282	85	6.8
14	0.158	309	88	7.7
27	0.358	338	88	3.6
42	0.497	324	87	3.3
71	0.718	339	87	2.7
120	0.889	335	88	2.8
181	0.96	325	87	2.6
252	0.981	328	88	2.4
350	0.997	320	87	2.5
536	1.01	309	87	2.3
1036	1.04	299	87	2.9

TS04

1	2	3	4	5
0	0.0006	339	23	2.6
8	0.0276	71	86	2.3
20	0.0872	71	86	2.4
44	0.13	99	87	2.2
95	0.14	91	88	4.6
196	0.146	75	88	1.8
358	0.147	80	88	2
604	0.161	75	89	4.1
1053	0.168	65	88	4.6

TI08

1	2	3	4	5
0	0.0014	244	67	6.4
6	0.0063	222	89	2.5
17	0.0338	172	89	2.8
27	0.066	3	86	3
40	0.0906	129	87	3.4
67	0.105	311	89	3
101	0.109	338	88	6.9
177	0.113	329	88	3
276	0.116	293	84	6.6
404	0.118	300	87	3.1
609	0.12	288	86	3.3
8	0.0039	316	86	4.6
19	0.016	71	86	4.9
42	0.0402	80	86	3.8
82	0.051	82	85	3.7
130	0.053	89	88	3.8
199	0.0541	94	87	3.7
303	0.0554	89	88	4.2
450	0.0554	84	88	3.6
706	0.0568	316	89	3.5
1040	0.0584	125	89	3.7

SA18

1	2	3	4	5
0	0.0008	25	29	6.4
8	0.019	22	87	9.5
15	0.0633	91	86	6.2
31	0.138	76	85	5.2
44	0.165	56	89	5.6
83	0.201	57	88	5.4
142	0.212	201	89	6.3
218	0.23	37	89	5.8
303	0.229	22	89	5.4
522	0.224	40	90	5.4
803	0.225	315	89	5
1040	0.226	69	90	5.3

TS05

1	2	3	4	5
0	0.0008	13	61	2.2
7	0.0584	216	-89	2.5
13	0.176	254	-87	2.1
30	0.45	252	-84	2.7
47	0.532	212	-88	2.8
86	0.621	238	-87	3.7
170	0.667	190	-89	3.3
282	0.672	175	-89	3.4
404	0.675	245	-88	4.6
612	0.676	115	-89	3.4
1052	0.68	168	-89	3.5

804	0.122	300	86	2.5
1045	0.123	335	87	3.1

TI16

1	2	3	4	5
0	0.0015	313	48	4.5
8	0.0351	32	87	2.9
18	0.134	69	88	2.4
32	0.294	74	83	2.4
57	0.395	102	84	2.8
102	0.432	83	86	3
189	0.452	77	88	2.9
307	0.461	78	88	3.1
427	0.467	91	88	2.8
602	0.476	92	86	2.9
801	0.481	13	89	2.8
1030	0.486	109	88	3

Experiment 4 (p91 - 93)

AG19A

1	2	3	4	5
0	0.369	87	87.3	5.9
5	0.275	112.7	87.1	5.8
10	0.141	104.6	88.8	5.5
17	-0.027	92.2	-74.5	11.5
22	-0.132	84.9	-84.9	7.3

CR08

1	2	3	4	5
0	0.16	230	87	11.2
11	0.0257	261	76	3.9
29	-0.105	26	-84	12

GO04

1	2	3	4	5
0	0.546	134.3	88.2	3.6
8	0.283	111.3	86.9	5.8
13	0.065	53.4	53.5	14.8
16	-0.048	61.1	-49	16.5
20	-0.166	81.2	-85.2	10.3

PK06

1	2	3	4	5
0	0.775	55	86.8	2.6
13.8	0.293	139.5	87.1	3.2
51	-0.624	262.6	-84.1	2.9

AP08A

1	2	3	4	5
0	0.045	303	-88	1.9
12	0.0069	129	-85	7.6
35	-0.028	360	88	1.8

CN09

1	2	3	4	5
0	0.42	218	-88	1
10	0.303	234	-88	1.5
28	0.0313	78	-2	2.4
46	-0.183	46	77	4.3

IN05

1	2	3	4	5
0	0.448	358	89	3.1

CO04B

1	2	3	4	5
0	0.108	77.4	-86.9	4
10	0.0866	87.1	-83.5	4.5
30	-0.025	73.5	83.2	9.5

DE17

1	2	3	4	5
0	0.056	235	88	2.1
8	0.03	133	88	2.8
14	0.01	72	80	5.9
24	-0.018	78	-75	3.5

KC12

1	2	3	4	5
0	0.46	230	88	5.2
13	0.183	265	71	7.7
30	-0.141	294	-86	7

KN05

1	2	3	4	5
0	0.0004	357	86	9.7
13	0.0003	15	88	12.4
50	-1E-05	311	-21	90

SY18

1	2	3	4	5
0	0.289	245.4	86.7	4.6
10.6	0.0686	224.5	84.6	3.6
23.3	-0.125	255.9	-86.4	5.1

BI07

1	2	3	4	5
0	0.0158	184	-89	3
11	0.0014	115	67	22.6
27	-0.009	100	88	6.2

CA02

1	2	3	4	5
0	0.354	85.4	87.2	1.5
9	0.272	85.1	85.8	1.9
20	0.156	86.7	84.3	3.3
33	0.048	97.4	64.8	4.4
44	-0.038	90.5	-58.9	3.1

10	0.286	3	89	3.3
24	-0.032	91	-76	3.6

KE02

1	2	3	4	5
0	0.31	331	-89.3	1.5
8.6	0.23	303.6	-89.2	1.2
25	-0.055	89.2	65.5	12.8

MT02

1	2	3	4	5
0	0.0843	223	-89	7.5
11	0.0355	12	-89	1.9
26	-0.023	61	78	4.6

GR02

1	2	3	4	5
0	0.108	19	-89	7.8
10	0.0951	12	-85	9.5
27	0.0491	110	-85	4
82	-0.068	40	80	21.6

VE04A2

1	2	3	4	5
0	0.195	252.4	86.1	0.9
7	0.143	257.1	86.9	1.1
13	0.06	41.6	83.1	1.8
21	-0.037	84.8	-81.2	1.8

ST15

1	2	3	4	5
0	0.334	262	85	2.1
15	0.213	260	83	2.1
32	0.0231	263	57	3.4
43	-0.054	278	-78	3.8

ST05

1	2	3	4	5
0	0.829	195.3	-89.2	2.3
10.1	0.703	194.3	-88.3	2.4
34.7	0.293	122.1	-77	7.1
51.6	-0.071	129.4	22.4	12.9

ST24

1	2	3	4	5
0	0.255	30.5	80.8	7.7
13.3	0.209	30.7	79.9	5.5

TM04

1	2	3	4	5
0	0.401	9.5	88.3	3.4
12	0.18	110.6	88.7	5.8
26	-0.094	159.8	-82.8	7.6

RU10B

1	2	3	4	5
0	0.897	133	-88	2.8
11	0.53	102	-87	3.7
27	-0.131	79	62	1.6

SE04

1	2	3	4	5
0	0.432	342	88	2.4
14	0.208	257	85	4.6
27	-0.035	274	-67	5.6

ST09

1	2	3	4	5
0	0.325	88	-86	3.6
13	0.2	90	-84	11.6
39	-0.048	276	69	7.3

ST16

1	2	3	4	5
0	0.654	166	-88	3.2
10	0.632	115	-88	3.2
20	0.587	111	-87	3
30	0.504	104	-86	3.4
40	0.396	94	-83	3.6
70	0.163	78	-74	6.7
120	-0.225	350	76	3.3

ST11

1	2	3	4	5
0	0.0486	193.8	-82.4	2.5
12.4	0.0406	185.5	-85	2.6
32.7	0.0248	188.5	-85	2.6
51.9	0.0091	94.6	-44.9	5.3
65.3	-0.004	85.2	21.2	9.5

BA19

1	2	3	4	5

32.5	0.0745	18.1	83.4	4.5
46.1	0.0148	277.8	21.4	10
55	-0.037	263.2	-78.8	6.2

BA20

1	2	3	4	5
0	0.502	144	-87.4	3.5
13.5	0.05	269.9	-58.5	2.3
28.3	-0.262	40.1	89	3.2

SA17

1	2	3	4	5
0	0.1932	303	87	2.4
12	0.1121	287	85	3.4
28	0.0175	279	64	14.2
50	-0.049	205	-84	6.1

TS04

1	2	3	4	5
0	0.167	4.1	88.2	3.8
11	0.0551	307.7	87.4	2.3
25.5	-0.055	179.2	-88.3	2.5

TI08

1	2	3	4	5
0	0.121	147.1	-88.1	3.3
12.3	0.046	101.3	-81.4	5.8
28.2	-0.04	82.7	74.2	4.3

0	0.441	156	84	4
11	0.25	151	83	8.2
23	0.0117	132	45	6.5
42	-0.284	40	-87	1.4

CT35

1	2	3	4	5
0	0.0577	123.1	88.6	3.6
11.9	0.0403	287.4	89.7	3.5
31.9	-0.009	273.1	-68.3	5.7

SA18

1	2	3	4	5
0	0.232	253.9	-88.8	5.9
13	0.0486	113.7	-74.4	7.2
27.8	-0.081	92.5	89.2	10.8

TS05

1	2	3	4	5
0	0.679	194.8	-88	3.9
7.6	0.45	194.5	-87.6	4.6
18.3	-0.065	120.6	63.5	13.7

TI16

1	2	3	4	5
0	0.484	39.9	89.7	2.6
9.2	0.329	283.3	89	3.2
18.1	0.123	269.7	82.6	4.9
39.5	-0.248	254.3	-78.3	1.9

Experiment 5 (p94 - 95)

AG19A

1	2	3	4	5
0	0.361	47	89	6.1
10	0.177	269	89	5.9
20	0.0436	235	88	5.7
30	0.0199	226	87	5.7
40	0.0145	233	85	5.4
60	0.0111	193	87	4.5
80	0.0097	249	87	5.7
100	0.0091	163	89	6.3
140	0.0074	201	86	3.5
180	0.008	218	87	8.9

GO04

1	2	3	4	5
0	0.525	149	89	3.6
10	0.263	171	89	6.3
20	0.0883	168	85	9.5
30	0.0425	136	89	6.4
40	0.0261	137	88	6.2
50	0.0177	138	88	5.9
60	0.013	157	87	5.7
80	0.009	248	89	13.1
120	0.0066	129	82	7.7
180	0.0046	137	86	8.3

CA02

1	2	3	4	5
0	0.363	114	88	2.6
10	0.271	21	88	3.7
20	0.196	113	88	4.4
30	0.135	122	87	1.3
40	0.0983	128	88	1.7
60	0.0496	133	88	2.6
80	0.0275	144	88	2.8
100	0.0163	166	89	4.3
140	0.0077	177	88	4.4
180	0.0049	140	88	6.3

TM04

1	2	3	4	5
0	0.397	137	88	3.7
10	0.238	172	88	5.3
20	0.104	221	89	10.6

DE17

1	2	3	4	5
0	0.0551	173	87	2.6
10	0.0269	206	89	1.8
20	0.0101	190	87	4.5
30	0.0061	226	87	5.9
40	0.0045	218	83	9.5
60	0.0031	241	84	8.7
80	0.0024	228	82	6.2
100	0.002	245	84	8.9
140	0.0016	264	85	2.9
180	0.0013	260	85	2.6

SY18

1	2	3	4	5
0	0.28	22	84	6.3
10	0.104	7	88	4.5
20	0.0345	3	88	4.6
30	0.0212	313	89	4.9
40	0.0169	337	89	5.5
60	0.0133	80	89	6.2
100	0.0099	20	87	6.6
140	0.0092	38	89	6
180	0.0083	56	87	9.1

KE02

1	2	3	4	5
0	0.316	305	88	2.3
10	0.199	29	88	1.6
20	0.088	34	88	1.8
30	0.0499	33	88	2.9
40	0.0328	19	87	3.4
60	0.0176	357	87	4.1
100	0.0088	351	85	5.3
140	0.0071	13	84	4.3
180	0.0057	16	85	7.7

MT02

1	2	3	4	5
0	0.0791	201	88	1.8
10	0.0439	225	87	1.8
20	0.0221	184	88	3.9
30	0.0141	342	89	3
40	0.0112	9	87	5.5

30	0.056	225	89	6.4
40	0.04	249	89	6.8
60	0.0279	243	89	9.4
100	0.0193	294	87	6.5
140	0.016	354	79	16
180	0.0135	288	88	7.9

PP01C1

1	2	3	4	5
0	0.578	52	89	5.2
10	0.381	357	90	4.5
20	0.221	246	90	5.3
30	0.162	193	90	5.8
40	0.144	181	89	4.5
60	0.0868	194	89	2.4
100	0.0593	193	88	2.8
140	0.0489	188	87	3.5
180	0.0438	199	87	3

60	0.0079	58	90	8.5
80	0.0057	292	89	5.5
100	0.0049	102	88	6.9
140	0.0042	25	89	5
180	0.0039	86	89	4.4

VE04A2

1	2	3	4	5
0	0.204	351	90	5.1
10	0.114	275	88	5.1
20	0.0406	284	89	4.1
30	0.024	315	89	3.8
40	0.0187	257	89	3.2
50	0.0164	337	89	3.5
60	0.0151	340	89	3.5
80	0.0145	23	89	5.6
120	0.0132	36	89	4.4
180	0.0123	17	89	4

Experiment 6 (p96)

AG19A

1	2	3	4	5
0	0.364	176	89	5.9
200	0.185	178	87	6.9
300	0.135	327	89	6.1
400	0.075	151	87	9
460	0.04	133	87	4
510	0.021	180	88	2.8
560	0.007	163	88	1.5
610	0.002	170	87	5.3

DE17

1	2	3	4	5
0	0.056	195	88	2.3
200	0.036	235	89	2.8
300	0.03	204	88	1.8
400	0.016	281	89	2
460	0.012	204	87	2.1
510	0.009	173	88	2.2
560	0.004	171	87	1.8
610	0.001	186	89	1.6

GO04

1	2	3	4	5
0	0.545	133	88	3.6
200	0.249	120	87	6.5
300	0.135	115	87	10.3
400	0.062	157	89	8.7
460	0.027	163	84	7.7
510	0.012	191	86	12.5
560	0.002	169	77	8.7
610	0	128	18	23.6

CA02

1	2	3	4	5
0	0.353	92	87	1.7
200	0.222	89	85	4.8
300	0.174	90	85	3.1
400	0.123	132	85	5
460	0.085	93	85	1.5
510	0.046	85	87	1.3
560	0.005	117	87	1.9
610	0.001	149	84	9.9

VE04A2

1	2	3	4	5
0	0.195	239	86	1.2
200	0.0973	237	88	6.5
300	0.0434	242	87	2.1
400	0.0218	211	87	3.5
460	0.0064	145	85	1.9
510	0.0016	169	62	4.3
560	0.0006	144	60	6.9
610	0.0003	146	62	2.9

Experiment 7 (p97 - 100)

AG17

1	2	3	4	5
0	0.145	8	57	7.3
100	0.141	9	57	6.9
200	0.138	8	58	9.6
300	0.133	11	58	8.5
350	0.101	13	58	8.8
400	0.086	7	57	8.1
469	0.0577	6	57	7.6
523	0.0318	9	56	9.4
572	0.0126	358	54	18.2
609	0.00385	11	53	8.5

DE28

1	2	3	4	5
0	0.00013	260	-20	3.9
100	0.00013	257	-20	3.5
200	0.00013	260	-22	3.6
300	0.0001	260	-23	9.9
350	9.1E-05	259	-25	5.5
400	6E-05	257	-29	4.9
469	1E-05	248	-32	14.8
523	3.4E-06	260	-11	39.7
572	2.4E-06	267	-2	41.2
609	2E-07	275	-18	57.5

CO01

1	2	3	4	5
0	0.028	249	35	15.3
100	0.0271	254	35	14.5
200	0.0226	252	35	17.2
300	0.0167	255	34	16.8
350	0.0137	255	38	16.3
400	0.0104	253	33	19.1
469	0.00535	254	35	16.7
523	0.00219	254	36	22.5
572	0.00057	249	50	19.8
609	0.00024	193	24	17.6

GO09

1	2	3	4	5
0	0.14	274	43	6.6
100	0.126	273	42	3.6
200	0.105	272	43	5.8
300	0.079	277	43	6
350	0.0542	272	42	6
400	0.0305	276	48	3.9
469	0.00632	287	55	5
523	0.00032	263	26	6.1
572	0.00252	298	12	10.9
609	0.00205	32	-3	4.6

PK09

1	2	3	4	5
0	0.105	102	60	6.5
100	0.102	102	61	6.6
200	0.0942	101	60	6.9
300	0.0796	104	60	7.5
350	0.0702	100	58	8
400	0.0524	104	57	11
458	0.0269	101	55	16.5
510	0.018	100	55	22.1
568	0.00169	44	65	19.1
609	0.00062	354	19	26.8

KC01B

1	2	3	4	5
0	0.0665	67	45	2.6
100	0.0634	65	45	2.8
200	0.0519	62	45	5.5
300	0.0343	64	46	3.5
350	0.0258	64	46	4.9
400	0.0174	66	48	8.4
458	0.0089	63	44	10
510	0.00281	70	46	8.5
568	0.00087	23	31	8.8
609	0.00032	342	27	21.5

KN12

1	2	3	4	5
0	6.6E-05	293	52	7.1
100	6.1E-05	288	51	7.1
200	4.7E-05	292	53	10.5

AP08B1

1	2	3	4	5
0	0.0116	339	-64	5.6
100	0.00961	345	-63	7.4
200	0.0069	338	-63	2.9

300	3.3E-05	290	55	19.5
350	1.2E-05	294	49	24.2
400	6.2E-06	314	53	32.8
458	3.2E-06	301	42	65.2
510	1.2E-06	349	80	90

BI02

1	2	3	4	5
0	0.0828	236	55	13.6
100	0.0817	237	56	14
200	0.0806	232	54	13.4
300	0.0402	232	54	14.8
350	0.0333	237	57	15.5
400	0.0242	230	58	15.5
458	0.00803	231	55	17.9
510	0.00107	146	86	16.6
568	0.0005	338	36	18.6
609	0.00035	327	17	26.6

CA06

1	2	3	4	5
0	0.0175	288	-16	3.8
100	0.0171	283	-18	5.9
200	0.0154	292	-16	6.8
300	0.0151	292	-16	3.2
350	0.0143	287	-15	2.3
400	0.013	290	-17	4.8
469	0.0117	291	-13	8.3
523	0.00821	293	-16	10
572	0.00132	289	-12	7
609	0.00007	68	16	25.1

TM16

1	2	3	4	5
0	0.0284	25	56	10.8
100	0.0271	26	57	12
200	0.0232	26	57	15.6
300	0.0186	21	56	13.6
350	0.0142	26	52	18.8
400	0.01	32	51	22.3
458	0.00337	29	55	12
510	0.00179	28	55	14.6
568	0.00032	1	45	9.7
609	0.00012	33	37	13.6

RU12A

300	0.0018	341	-47	9.3
350	0.00094	342	-60	10.1
400	0.00062	374	-42	9.1
458	0.0004	356	-54	8.7
510	0.00024	356	-58	18.7
568	0.0001	348	-45	12
609	0.00009	351	-51	24.2

CN06

1	2	3	4	5
0	0.0512	260	31	4.9
100	0.0498	261	32	5.8
200	0.0426	261	31	4.3
300	0.0314	256	32	4.3
350	0.0261	261	32	7.8
400	0.0174	258	34	8.9
458	0.00808	258	32	8.1
510	0.00283	259	32	3.6
568	0.00097	267	31	13.8
609	0.00078	263	29	21.6

KEA

1	2	3	4	5
0	0.0824	351	46	3.7
100	0.0807	354	45	2.3
200	0.0761	356	45	2.7
300	0.0668	351	45	5.5
350	0.0613	352	43	4.4
400	0.0467	351	45	3.3
458	0.0252	345	43	3.2
510	0.00595	346	46	4.5
568	0.00065	345	22	8.9
609	0.00025	1	15	18.3

MT18

1	2	3	4	5
0	0.0103	294	10	15.9
100	0.00876	298	11	15.6
200	0.00812	298	12	13.9
300	0.00715	298	10	23.1
350	0.00603	301	13	16.3
400	0.00424	304	13	23.7
458	0.00288	310	12	26.6
510	0.00173	303	11	26.1
568	0.00027	312	11	16.9
609	0.00004	47	9	32.6

1	2	3	4	5
0	0.00023	328	62	19
100	0.0002	333	62	17.6
200	0.00016	353	56	18.7
300	4.6E-05	354	65	21.1
350	3E-05	270	65	29.9
400	2.6E-05	2	30	19.8
458	1E-05	34	14	32
510	1E-05	63	12	23.6
568	1.1E-05	350	2	16.4
609	1.1E-05	10	-7	18.9

ST09

1	2	3	4	5
0	0.0182	273	25	2.7
100	0.0182	273	23	5
200	0.017	271	22	4.5
300	0.0136	276	21	8.1
350	0.0126	267	23	8.6
400	0.0108	271	19	6.3
469	0.0075	274	22	3.4
523	0.00375	273	21	8.8
572	0.00048	291	24	5.8
609	0.00017	149	17	12.6

ST15

1	2	3	4	5
0	0.00587	197	-73	5.8
100	0.00576	202	-72	6
200	0.00536	201	-74	5.6
300	0.00402	193	-84	4.7
350	0.00316	200	-78	7.2
400	0.00234	171	-80	10.3
469	0.00085	126	-23	31.3
523	0.00082	88	45	15.8
572	0.00013	35	30	22.9
609	9.7E-05	335	-8	22.3

ST11

1	2	3	4	5
0	0.00028	196	21	9.6
100	0.00024	193	24	13.5
200	0.00026	191	23	10.2
300	0.00023	191	11	12.6
350	0.0002	183	14	6.9
400	0.00013	189	14	5.3

VE05A2

1	2	3	4	5
0	0.0201	208	-64	3.9
100	0.0186	216	-62	5.6
200	0.0137	213	-63	5.5
300	0.00884	225	-61	7.9
350	0.00586	211	-59	4.6
400	0.00342	209	-66	6.6
469	0.00188	205	-66	7.1
523	0.0001	181	-77	9.5
572	0.0001	348	-45	12
609	0.00008	243	-60	4.9

ST16

1	2	3	4	5
0	0.0644	283	-18	4.5
100	0.0636	282	-17	3.7
200	0.0583	283	-18	3.8
300	0.0474	284	-17	3.6
350	0.0401	281	-17	3.5
400	0.0324	286	-16	3.8
469	0.0167	282	-23	11.1
523	0.00238	280	-14	6.2
572	0.00025	306	-4	14.5
609	0.00011	19	-54	46.3

ST05

1	2	3	4	5
0	0.0282	310	-6	7
100	0.0282	306	-4	7.5
200	0.0273	308	-6	6
300	0.0252	307	-6	6.6
350	0.0238	304	-7	6.5
400	0.0209	301	-5	5.9
469	0.0144	297	-4	5.8
523	0.00415	303	-2	4.8
572	0.00033	316	-3	5.8
609	0.00008	152	5	17.8

ST24

1	2	3	4	5
0	0.00734	106	70	2.7
100	0.00763	105	71	1.8
200	0.00757	103	71	2.1
300	0.00681	92	77	2.8

469	4.6E-05	175	17	6.5	350	0.00595	109	73	1.5
523	1.2E-05	171	22	33.2	400	0.00465	93	72	4.8
572	2.3E-06	214	56	90	469	0.00409	102	70	3.1
					523	0.00262	88	75	9.2
					572	0.0008	90	72	3
					609	0.00022	4	34	18.2

APPENDIX B

This Appendix indicates the experiments carried out on each individual sample.

1 = Alternating field demagnetisation of natural remanent magnetisation;

2 = Alternating field demagnetisation of anhysteretic remanent magnetisation;

3 = Isothermal remanent magnetisation acquisition;

4 = Back field;

5 = Alternating field demagnetisation of isothermal remanent magnetisation;

6 = Thermal demagnetisation of isothermal remanent magnetisation;

7 = Thermal demagnetisation of natural remanent magnetisation.

	1	2	3	4	5	6	7
AG19A	•	•	•	•	•	•	
AG17			•				•
AP-08A	•			•			
AP08B1							•
AV03	•	•					
AV-07	•		•				
BA19	•		•	•			
BA20	•		•	•			
BI-07				•			
BI02			•				•
CA-02	•	•		•	•	•	
CA06			•				•
CN-09	•			•			
CN06			•				•
CO-04B	•			•			
CO01			•				•
CR-08	•		•	•			
CT35	•		•	•			
DE-17	•	•		•	•	•	
DE28			•				•
GO-04		•		•	•	•	
GO09			•				•
GR-02	•			•			
GR-04		•	•				
IN-05	•			•			
IN-08	•	•	•				
KC-12	•			•			
KC01B			•				•
KE-02	•	•		•	•		
KEA			•				•
KN05				•			
KN12							•
MO-02	•						
MO-05	•	•	•				
MT-02	•	•		•	•		
MT18							•
PE-2	•		•				
PK-06	•			•			

PK09							•
PP-01C1		•	•		•		
RU-10B				•			
RU12A			•				•
SA17	•		•	•			
SA18	•		•	•			
SE-04	•		•	•			
ST-11	•	•	•	•			
ST-15	•	•	•	•			
ST-16	•	•	•	•			
ST-24	•	•	•	•			
ST-5	•	•	•	•			
ST-9	•	•		•			
ST05-1							•
ST09-1							•
ST11-1							•
ST15-1							•
ST16-1							•
ST24-1			•				•
SY-18	•	•		•	•		
TH-04	•						
TH-05	•		•				
TI08	•		•	•			
TI16	•		•	•			
TM-04	•	•		•	•		
TM16			•				•
TS04	•		•	•			
TS05	•		•	•			
VE-04A2	•	•		•	•	•	
VE05A2							•